

Implied Modelling

Martijn van der Voort,
March 2000.

Supervisors:

Remco Bos, MeesPierson N.V.
Anna Shepeleva, MeesPierson N.V.
Prof. Dr. A.C.F. Vorst, Erasmus University Rotterdam

MeesPierson
Investment Bank

Preface

This thesis is written during my six-month internship at the derivatives research department at MeesPierson, Amsterdam. I would like to thank MeesPierson for giving me the opportunity to carry out my research here.

I would like to give special thanks to my supervisor at Erasmus University Rotterdam, Prof. Dr. A.C.F. Vorst and both supervisors at MeesPierson, Anna Shepeleva and Remco Bos. They have given me valuable comments and analysed my work thoroughly.

Finally, I would like to thank the colleagues at MeesPierson: Pieter van Gaal, François Nissen, Arjen Prinsen, Diederik Schouten, Herman van der Sluis, Yung Tjong and Maarten Wiersinga. They have made the six months a pleasurable stay.

Martijn van der Voort
Amsterdam, March 2000

Contents

	Glossary of symbols	1
1	Introduction	
	1.1 Purpose of this study	3
	1.2 Contents by chapter	4
2	Derivatives	
	2.1 Introduction	7
	2.2 Definitions	7
	2.3 Restrictions on option prices	9
3	Stochastic process of the underlying asset	
	3.1 Introduction	13
	3.2 Geometric Brownian motion	13
	3.3 Jump-diffusion model	14
	3.4 Stochastic volatility models	16
	3.5 Deterministic volatility models	16
4	Black-Scholes model	
	4.1 Introduction	17
	4.2 Black-Scholes world	17
	4.3 Black-Scholes model	18
	4.4 Hedging and the greeks	20
	4.5 Numerical pricing techniques	20
	4.6 Implied volatility	22
5	Non-constant volatility	
	5.1 Introduction	25
	5.2 Deriving the instantaneous volatility function	25

6	Implied modes	
6.1	Introduction	29
6.2	Implied binomial tree	29
6.3	Implied trinomial tree	34
6.4	Implied finite differences	37
6.5	Implied Monte Carlo simulation	48
6.6	Implied trinomial tree with stochastic volatility	50
6.7	Continuous case	57
7	Performance of the implied models	
7.1	Introduction	59
7.2	Implied binomial tree	59
7.3	Implied trinomial tree	61
7.4	Implied finite differences	63
7.5	Implied Monte Carlo simulation	66
7.6	Stochastic volatility model	68
7.7	Continuous case	69
7.8	Convergence speed	70
7.9	Summary and conclusion	71
8	Applying the implied models	
8.1	Introduction	73
8.2	Greeks of European options	73
8.3	American options	75
8.4	Barrier options	78
9	Conclusions	
9.1	Introduction	91
9.2	Conclusions	91
9.3	Further research	92
Appendix A	Stochastic calculus	93
Appendix B	Pricing barrier options	95
Appendix C	Splines	97
Appendix D	Instantaneous volatility function	105
Appendix E	Successive over-relaxation (SOR)	109
Appendix F	Stability of finite difference	111
References		113

Glossary of symbols

S	price of underlying
F	forward
r	risk-free interest rate (continuous compounded)
q	dividend yield (continuous compounded)
$C(\dots)$	price of a European call option
$P(\dots)$	price of a European put option
K	strike of an option
B	barrier
t	time parameter
T	maturity of an option
p_u, p_d, p_m	transition probabilities in bi/tri nomial tree
$\hat{\sigma}(\dots)$	implied volatility
$\sigma(\dots)$	instantaneous volatility
u, d, m	level of up/down/middle move
$N(x)$	cumulative standard normal distribution function
$n(x)$	standard normal probability density function
λ	price of Arrow-Debreu security
$\log(x)$	natural logarithm of x
e^x or $\exp(x)$	exponential function of x
PDE	partial differential equation
SDE	stochastic differential equation
W	Wiener process
$x \sim N(\mu, \sigma^2)$	x normal distributed random variable with mean μ and st.dev. σ
$\lfloor x \rfloor$	greatest integer smaller than, or equal to x

1 Introduction

1.1 Purpose of this thesis

Over the last decades, derivative instruments have gained tremendous popularity. In 1973 the Chicago Board Options Exchange (CBOE) was founded, followed by the publication of the famous article written by Black and Scholes just a few months later. Nowadays billions of dollars worth of derivatives are traded on a daily basis, on both exchanges and over-the-counter (OTC).

Although it became clear over the years that the Black-Scholes model was not able to explain the observed market values of standard options, it still is one of the most used models to price derivatives. The term implied volatility was introduced to clarify the problems resulting from the assumptions underlying the Black-Scholes model. However, it is not clear how more complex options should be priced if one wants to account for observed market values of standard options. To overcome this problem, a lot of research has been done on the assumptions underlying the Black-Scholes model. One of these assumptions involves the stochastic process for the underlying securities. Researchers have tried more complex stochastic processes to model stock price behavior. Already in 1976, Merton introduced a jump-diffusion model trying to capture jumps in stock prices, which are often observed in practice. Since 1987, stochastic volatility models made their appearance, pioneered by Hull and White (1987), Scott (1987) and Wiggins (1987). Although these models are better able to explain observed market values of options, it is extremely hard to calibrate these models to observed market values.

In 1994, the first research on implied models appeared in literature, pioneered by Derman and Kani (1994), Rubinstein (1994) and Dupire (1994). Soon other researchers followed their footsteps and introduced other implied models based on well-known numerical techniques. Very recently models that combine the implied approach with more complex stochastic models have appeared. The main goal of all these implied models is to price standard options consistent with their market values, so that they can be used to obtain prices of more exotic options and more appropriate hedge-ratios.

This thesis will discuss several of these implied models. Most attention will be focussed on simple implied models. As an example, this thesis also discusses a combination of a stochastic volatility model and an implied model. The main objectives of this study are listed below:

The objectives of this study are:

1. *Analyzing (implied) models which price (a set of) plain vanilla options consistent with their market values.*
2. *Applying these models to exotic options and investigating the impact on their prices.*

The first part of the thesis can be seen as an introduction to derivatives pricing under the Black-Scholes assumptions. The second part of the thesis deals with the first objective. The models are discussed in detail and their performance is compared. The second objective can be found at the end of this thesis where we apply the models to American options and barrier options.

1.2 Contents by chapter

This thesis starts with an introduction to different kinds of derivatives in chapter 2. The notion of simple call and put options is explained as well as more complicated options, such as barrier options. This section also introduces forward contracts, which are needed for the construction of implied models. Finally, some strategies are discussed, which lead to the derivation of some restrictions on option prices.

The third chapter deals with some characteristics of stochastic processes that can be used to model the stock price behavior. The geometric Brownian motion with drift will be discussed, on which the Black-Scholes model is based. Also a few generalizations of this stock price process will be presented. The first is the jump-diffusion model, introduced by Merton. A second type of stochastic process that will be discussed is the stochastic volatility model, proposed by Hull and White (1987) and Heston (1993). Finally, we turn to the deterministic volatility model.

The fourth chapter looks at option-pricing theory in a Black-Scholes world. After discussing the assumptions, a derivation of the Black-Scholes formulae is given. We also show a model that allows for dividends, derived by Merton. Further, the numerical techniques, on which implied models are based, will be discussed briefly. These are bi/trinomial tree models, the method of finite differences and Monte Carlo simulation. Next, the hedge-parameters will be explained. In addition, the term implied volatility is defined at the end of this chapter. Some common volatility structures are shown.

The fifth chapter considers the case of a non-constant volatility. A formula will be derived to extract the so-called instantaneous volatility function from the Black-Scholes implied volatilities. This deterministic volatility function determines a stock price process that can be used to price European options consistent with their market values.

The sixth chapter shows how the standard numerical techniques can be adapted in such a way that a set of options will be priced consistent with their market values. First, the implied binomial tree will be considered, followed by a discussion of the implied trinomial tree. After that, two alternatives for an implied finite difference model will be given. The last model that will be touched upon is a generalization of the implied trinomial tree model, which allows for stochastic volatility.

Chapter 7 discusses the performance of the numerical techniques described in chapter 6. The differences between the results of the model and market values of plain vanilla options will be compared for all models, as well as the convergence to these market values.

Chapter 8 shows the influence of the models on American and barrier options. The results of the different models will be compared. Further, there will be looked at the differences of barrier option prices generated by the Black-Scholes model and those resulting from implied models.

Chapter 9 gives a conclusion and some suggestions for further research.

2 Derivatives

2.1 Introduction

Since the main goal of this thesis is to price options consistent with market values, this first chapter will serve as an introduction to options and other derivatives. The first section starts with giving a definition of derivatives and explaining what a forward contract is. It will be explained what call and put options are. In addition, barrier options will be discussed briefly. Finally, attention will be given to some positions in options, which lead to restrictions on the prices of these derivatives.

2.2 Definitions

A good definition of a derivative can be found in Hull (1997):

A derivative is a financial instrument whose value depends on the values of other, more basic underlying variables.

There is a wide variety of possible underlying variables. For instance the price of gold, or the price of pork bellies. The underlying variable of a derivative can even be another derivative. In the remainder of this thesis, however, we will only discuss derivatives on a single underlying variable, which will be a stock, or a stock-index. There are all kinds of derivatives and probably the simplest one is a forward contract.

A forward contract is an agreement to buy or sell a certain asset at a certain time in the future, at a certain price.

The party that has agreed to buy the asset has what is called, a long position. The selling party has a short position. The delivery price of the forward contract is chosen in such a way that the value of the forward contract is zero at the time the agreement is made. In this thesis, forward contracts are only used as a tool for constructing some of the implied models.

Another well-known derivative is an option. In contrast to a forward contract, the holder of an option has no obligation to buy or sell the underlying asset. A formal definition of an option is given below:

A call (put) option is the right to buy (sell) a certain asset on or before a certain time, at a certain price.

The time when the contract ends is also known as the maturity, or the expiration date of the option. The price at which the asset may be bought (sold) is also known as the strike, or exercise price. If the asset can only be bought (sold) at expiration, the option is said to be European. If the option can be exercised at any time up to the expiration, the option is called American. These simple options of European type are also known as plain vanilla options. When we assume rational decision making, it is easy to see when the holder of a European option will exercise his right at maturity. A holder of a call option will only buy the underlying asset if the price of the asset is higher than the strike of the option. In case of a put option, the asset will only be sold if the price of the asset is lower than the strike of the option. Thus if we let S_T denote the price of the underlying asset at maturity, the value of an option at maturity will be:

$$\begin{aligned} Call_T &= \max(S_T - K, 0) \\ Put_T &= \max(K - S_T, 0) \end{aligned} \tag{2.1}$$

This value of the option at maturity is also known as the payoff of the option. If at some time $S_t > K$, a call option is said to be in-the-money, while an option is said to be out-of-the-money when $S_t < K$. When S_t equals K the option is referred to, as an at-the-money option. Further, we say that the holder of an option has a long position and the other party, the writer of the option, has a short position. The party with a short position thus has an obligation to buy or sell the underlying asset. In the remainder of this thesis, the price of a European call option will be denoted by C and a European put option by P .

Barrier options are path-dependent options that are closely related to plain vanilla options. The definition is given below:

A barrier option is an option of which the payoff depends on whether the price of the underlying asset has reached a certain value, the barrier, during the lifetime of the option

Barrier options can be divided into two types, knock-in options and knock-out options. A knock-in barrier option only comes into existence if the underlying asset has reached the barrier during the lifetime of the option. A knock-out barrier option is an option that ceases to exist as soon as the barrier is reached. Both these types can again be divided into two types, up and down barrier options. Whether a barrier is an up –or a down barrier option depends on the position of the barrier relative to the initial asset price. If the barrier is above the initial stock price, the option will be classified as an up barrier option. In the other case it would be called a down barrier option. So for instance an up-and-in barrier option with the barrier on 120 and with initial stock price of 100, will only come into existence as soon as the underlying value has reached 120. Therefore, it is easy to see that the payoff of an up-and-in call option is given by:

$$C_{ui_T} = \begin{cases} \max(S_T - K, 0) & \text{if } S_t \geq B, \text{ for some } t \in [0, T] \\ 0 & \text{else} \end{cases} \quad (2.2)$$

In case of a down-and-in option, we can replace \geq with \leq in formula (2.2). When the payoff of an out barrier option is needed, the terms $\max(S_T - K, 0)$ and 0 should be switched. From (2.1) it follows what payoff formulae should be used for put barrier options. Some barrier options specify a rebate, usually a fixed amount paid to the holder in case the barrier is reached.

2.3 Restrictions on option prices

With options, it is possible to create all kinds of (partial) linear payoff functions. For instance, one can take a long position in a European call option and a short position in a European put option with the same strike and maturity. The payoff of this portfolio, V , will then be:

$$V_T = \max(S_T - K, 0) - \max(K - S_T, 0) = \max(S_T - K, 0) + \min(S_T - K, 0) = S_T - K \quad (2.3)$$

Thus the owner of this portfolio will buy the underlying stock at maturity for a price of K . If, in addition, the owner of this portfolio shorts the stock and holds an amount of cash equal to Ke^{-rT} , it can easily be seen that the payoff will then be zero. Since this strategy has a payoff of zero, it should cost zero from the start. This gives the put-call parity:

$$C - P + Ke^{-rT} - S = 0 \quad (2.4)$$

Another interesting portfolio consists of a long position in one call, with strike K_1 and a short position in another call with strike K_2 , both with the same time-to-maturity. Now if we assume that $K_1 \leq K_2$, or $K_2 = K_1 + h$ for some $h \geq 0$. This portfolio is also known as a bull-spread. It can easily be seen that the minimum payoff of this strategy is zero and the maximum payoff is $K_2 - K_1$. Thus from the no-arbitrage assumption it follows that:

$$0 \leq C(K_1) - C(K_1 + h) \leq he^{-rT} \quad (2.5)$$

If the left inequality is violated, one can use the described portfolio and lock in a riskless profit of $C(K_1 + h) - C(K_1)$. If the other inequality is violated, one can short the portfolio and invest the proceeds in the risk-free asset. At maturity, this amount of money will be worth more than the maximum amount of money that has to be paid. If we divide inequality (2.5) by $-h$ and take the limit as h goes to zero, we get:

$$-e^{-rT} \leq \frac{\partial C}{\partial K} \leq 0 \quad (2.6)$$

When pricing options, this important restriction has to be satisfied in order to prevent arbitrage opportunities.

Another interesting combination of European call options is a butterfly spread. This spread involves three call options with different strikes and the same time to maturity. We assume we have strikes $K_1 \leq K_2 \leq K_3$. A butterfly spread consists of a long position in the options with strikes K_1 and K_3 and a short position of two options with strike K_2 . If we take $K_1 + h = K_2 = K_3 - h$, it can be seen from (2.1) that the minimum payoff from this butterfly spread is zero and the maximum payoff is h . Thus from the no-arbitrage assumption we must have:

$$0 \leq C(K_2 - h) - 2C(K_2) + C(K_2 + h) \leq he^{-rT} \quad (2.7)$$

It can be shown that arbitrage opportunities exist if one of these inequalities is violated. Now after dividing (2.7) by h^2 and taking the limit as h goes to zero, we get the following restriction:

$$\frac{\partial^2 C}{\partial K^2} \geq 0 \quad (2.8)$$

There is no upper bound that has to be satisfied, since in the limit, after dividing by h^2 , the right-hand-side of (2.8) tends to infinity.

A last portfolio consisting only of European call options that will be discussed here is a calendar spread. This involves taking a short position in a European option with a certain time to maturity and a long position in a European option with a longer time to maturity. Both options should have the same strike. If the price of the underlying asset at maturity of the first option is below or on the strike, this option will not be exercised and thus the final payoff is at least zero. If however the first option will be exercised one can short the stock and invest the proceeds in the risk-free asset. At maturity, one has to buy the stock to close the position. Because of the second option, this strategy will always have a non-negative payoff at the maturity of the second option. Thus, the calendar spread leads to the following restriction:

$$\frac{\partial C}{\partial t} \geq 0 \quad (2.9)$$

In the case of dividends, this restriction has to be adjusted a little, since the short position in the stock will also have to pay the dividend.

Finally, we look at a portfolio consisting of standard options and barrier options. All options should be of the European type. The portfolio consists of a long position in two barrier options, which are identical, except for the fact that one is a knock-out barrier and

the other a knock-in barrier. Further, a short position in a plain vanilla call option is taken. It is easy to see that the long position in the barriers is actually just a plain vanilla option. If the barrier is hit during the lifetime of the option, the knock-in barrier ends as a plain vanilla option and the knock-out is worthless. If the barrier is not hit, the knock-out will pay the same amount as the plain vanilla call and the knock-in is worthless. Thus the price of this portfolio should equal zero, since its final payoff will be zero. This results in the following equality:

$$C_{in} + C_{out} = C \quad (2.10)$$

Again, it can be shown that a violation of (2.10) will lead to arbitrage opportunities.

3 Stochastic process of the underlying asset

3.1 Introduction

Prices of derivatives depend on the value of the underlying asset. So in order to obtain prices for derivatives, we must have a model for the process of the underlying asset. This should be a stochastic process. Usually such a process consists of a deterministic part, called the drift, and a stochastic part based on a Wiener process. It is customary in financial calculus to write these stochastic processes in terms of stochastic differential equations. This chapter discusses a number of ways to model the price of the underlying asset over time. First, the geometric Brownian motion will be considered, on which the Black-Scholes model is based. Next a jump-diffusion model, introduced by Merton, and stochastic volatility processes are discussed briefly. Finally, we show a stochastic process where we have a deterministic volatility function.

3.2 Geometric Brownian motion

In order to price a derivative, Black and Scholes assumed that the price of a certain asset follows an Itô process, given by:

$$dS = \mu S dt + \sigma S dW \quad (3.1)$$

where μ denotes the drift parameter of the underlying asset and σ the volatility. W denotes a Wiener process. A definition of a Wiener process can be found in appendix A. Since a Wiener process is continuous the stock price process given by (3.1) will also be continuous. From Itô's lemma, see appendix A, it follows that the process of the natural logarithm of the stock price is given by:

$$d \log(S) = \left(\mu - \frac{1}{2} \sigma^2 \right) dt + \sigma dW \quad (3.2)$$

This is called a generalized Wiener process, or Brownian motion. Since the stock process has this property, the process is also referred to as a geometric Brownian motion. When the stock price follows a geometric Brownian motion, we have the following distribution of the log-returns of the asset over a period dt :

$$d \log(S) \sim N\left(\left(\mu - \frac{1}{2} \sigma^2\right) dt, \sigma^2 dt\right) \quad (3.3)$$

Thus, the log-returns of the stock are normally distributed, with mean $(\mu - \frac{1}{2}\sigma^2)dt$ and variance rate $\sigma^2 dt$. The following figure shows a simulated price path of the value of a stock when $\mu = 0.03$ and $\sigma = 0.3$, over 1 year. Log-returns are generated with a discretization of equation (3.2). Time is divided into 5000 equally spaced time-steps.

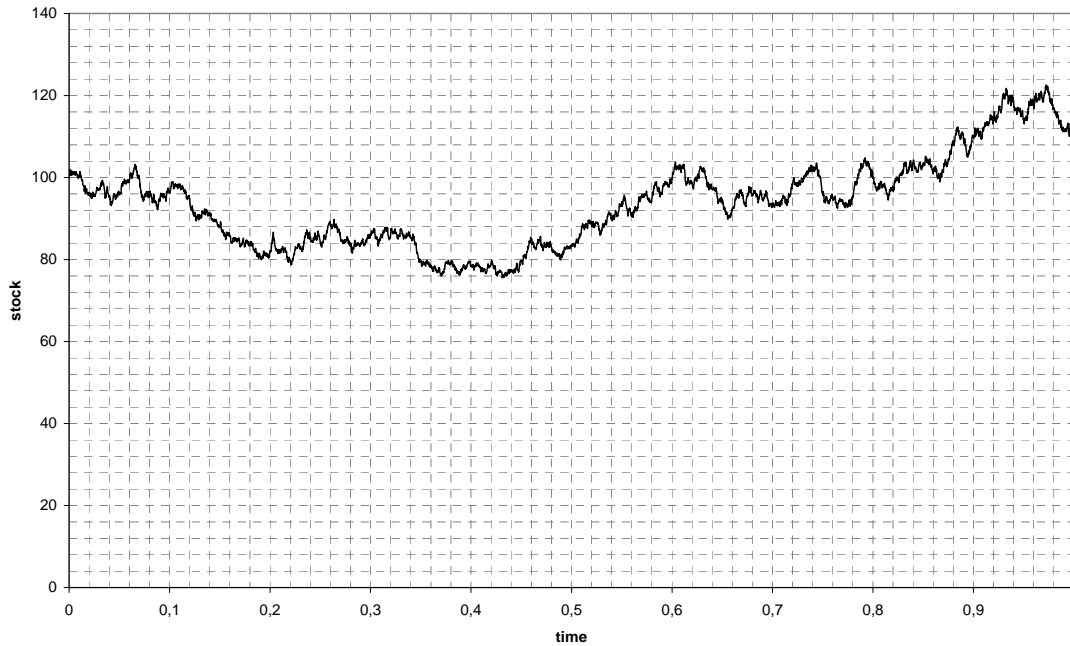


Figure 3.1: A simulated price path for the geometric Brownian motion.

In the Black-Scholes world it is assumed that both μ and σ are constant parameters. With this assumption along with the no-arbitrage principle, Black, Scholes and Merton managed to derive the well-known formulae for the price of call and put options, discussed in chapter 4. Since in practice this model is not capable of pricing options consistent with observed market values, a lot of research has been done on different stock price process, of which we will discuss two.

3.3 Jump-diffusion model

Already in 1976, three years after the Black-Scholes model, Merton used a combination of a jump process and a diffusion process to model the price of the underlying asset. He assumed the following generalisation of the Brownian motion:

$$dS = \mu S dt + \sigma S dW + (J - 1) S dq \quad (3.4)$$

where dq is a Poisson process, given by:

$$dq = \begin{cases} 0 & \text{with probability } 1 - \lambda dt \\ 1 & \text{with probability } \lambda dt \end{cases} \quad (3.5)$$

The terms of smaller order than dt are ignored. The parameter λ is called the intensity of the Poisson process and determines how often a jump on average occurs. The process of (3.4) is the same process as assumed by Black-Scholes with an occasional jump of height $(J - 1)S$. J determines the height of the jump and can be a random quantity. With the assumption of log-normally distributed jumps, Merton (1976) was able to derive a formula for options when the underlying asset follows a jump-diffusion process. Although options are not perfect hedge-able in the presence of jumps, he used diversification arguments to derive a formula. The figure below shows a simulated stock price path in the presence of jumps, when $\lambda = 15$ and $\log J \sim N(0, 0.05)$. The other parameters are set as in figure 1.

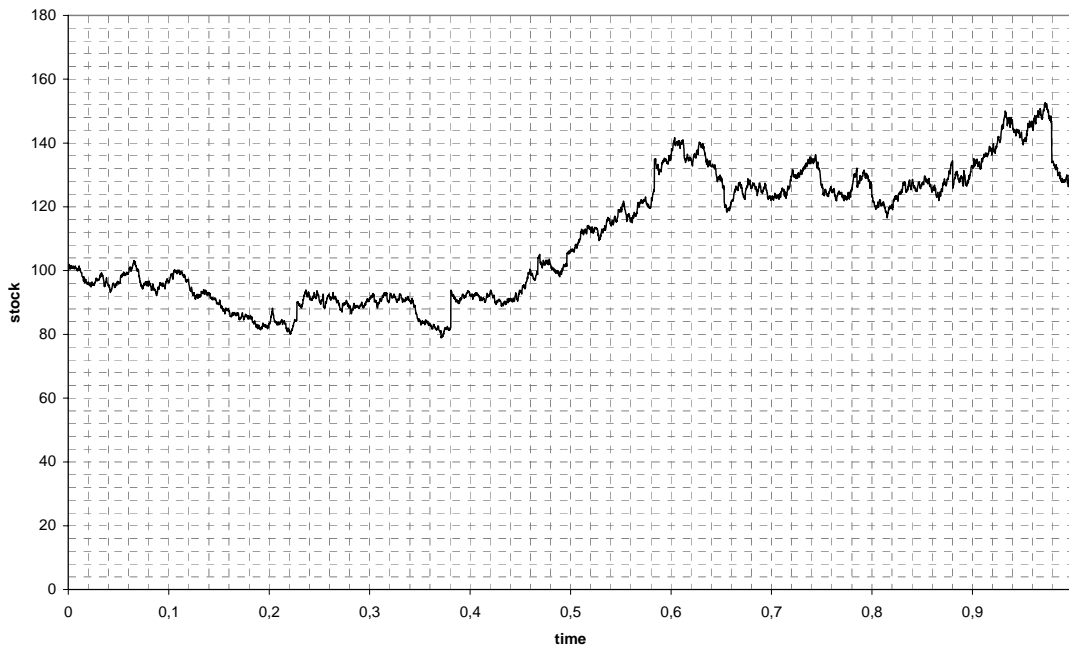


Figure 3.2: A simulated price path for jump-diffusion.

From this figure, it can be clearly seen that the stock price shows some jumps. This can also be observed in practice, for instance when important news is announced, or when a crash occurs. The model with log-normally distributed jumps used by Merton is hard to calibrate from observed market prices of options.

3.4 Stochastic volatility models

Other researchers have focussed on the relaxation of the assumption of a constant parameter σ in equation (3.1). When the assumption of a constant volatility parameter is dropped, one has to choose some function or process for the volatility. One can choose a stochastic process for the volatility parameter. Hull and White (1987) and Heston (1993) suggested a mean reverting volatility process. This mean reverting volatility process tries to capture an important phenomenon frequently encountered in practice. Sometimes the price of a stock shows little or no movement. The price of the same stock may sometimes show some hectic behaviour. This can be specified by the following equations:

$$\begin{aligned} dS &= \mu S dt + \sigma S dW_S \\ d\sigma^2 &= \alpha(\beta - \sigma^2) dt + \xi \sigma^a dW_\sigma \end{aligned} \quad (3.6)$$

Here W_S and W_σ are two, possibly correlated, Wiener processes. When parameter a is chosen to be 2, we have the Hull and White model. In case it is set to be 1 we have the Heston model. In both models, the parameter β determines the mean of the squared volatility. The parameter α can be interpreted as the speed at which the volatility process reverts to its mean. Parameter ξ can be seen as the volatility of σ . All parameters should be greater than, or equal to zero.

3.5 Deterministic volatility models

Another possibility to model the stock price process is to assume that volatility is a deterministic function of the stock price and time. This can be written as follows:

$$dS = \mu S dt + \sigma(S, t) S dW \quad (3.7)$$

The parameter $\sigma(S, t)$ is the volatility of the underlying, when its value is S at time t . It should not be confused with the implied volatility discussed later. The rest of this thesis will mainly focus on this process. Later in this thesis a formula for $\sigma(S, t)$ will be derived, such that plain vanilla options will be priced consistent with their market values when modelling the stock price process according to (3.7).

4 Black-Scholes model

4.1 introduction

This chapter will give a brief discussion of the famous Black-Scholes model. First the assumptions underlying the model will be introduced, which gives us the so-called Black-Scholes world. Further this chapter shows how a riskless position in both the option and the underlying stock can be created and how this can be used to derive the value of an option. Further, a discussion of the so-called greeks of options can be found in this chapter. These greeks are important for hedging-issues, because they describe the sensitivity of option prices w.r.t. different parameters. Next, this chapter gives an introduction to numerical techniques that can be used for valuing derivatives in a Black-Scholes world. These numerical techniques are binomial trees, trinomial trees, finite differences and Monte Carlo simulation. Finally, the term implied volatility will be explained and some volatility structures found in practice will be shown.

4.2 Black-Scholes world

Before being able to derive the price of a plain vanilla option, some assumptions have to be made. As discussed in the previous chapter, Black and Scholes assumed that the price of the underlying can be modelled with the following geometric Brownian motion:

$$dS = \mu S dt + \sigma S dW \quad (4.1)$$

Where both μ and σ are constant. Now the assumptions made by Black and Scholes can be stated as:

1. There are no arbitrage opportunities.
2. Short selling of securities with full use of proceeds is allowed.
3. There are no transaction costs or taxes. Further, all securities are divisible.
4. Security trading is continuous.
5. There are no dividends during the life of the option.
6. The risk-free interest rate, r , is constant and the same for all maturities.
7. The stock price follows a geometric Brownian motion given by (4.1).

The first restriction tells us that it is not possible to make any profit by taking a riskless position in certain financial instruments. The value of a riskless position should thus grow with the risk-free interest rate. This assumption is crucial for deriving the price of any derivative. In the remainder of this thesis we will use assumptions 1-6. The fifth assumption will be relaxed a little by assuming a constant continuous dividend-yield, as shown by Merton (1973). The seventh assumption will be dropped, later in this thesis.

4.3 Black-Scholes model

Now let C denote the value of a plain vanilla call option. Obviously the value of the option depends on its strike, the time to maturity and the underlying asset. So for a given strike, C is a function of both the underlying asset and time, thus we have from Itô's lemma:

$$dC = \frac{\partial C}{\partial S} dS + \frac{\partial C}{\partial t} dt + \frac{1}{2} \sigma^2 S^2 \frac{\partial^2 C}{\partial S^2} dt \quad (4.2)$$

Next consider a portfolio, with value V , consisting of a position in a call option and a position in the underlying asset, with weights H_c and H_s , respectively. Thus the stochastic process of this portfolio is given by:

$$dV = H_c dC + H_s dS \quad (4.3)$$

Using (4.2) this can now be written as:

$$dV = \left(\frac{\partial C}{\partial S} H_c + H_s \right) dS + \left(\frac{\partial C}{\partial t} + \frac{1}{2} \sigma^2 S^2 \frac{\partial^2 C}{\partial S^2} \right) H_c dt \quad (4.4)$$

Thus it can be seen that the change in the value of the portfolio can be made riskless by choosing $H_c = 1$ and $H_s = -\partial C / \partial S$. Since in this case the dS term is cancelled and the differential equation of (4.4) is not stochastic anymore, it thus is riskless. Now since this special portfolio is riskless its value should grow with the risk free interest, or $dV = rVdt$. This follows from the no-arbitrage assumption. Combining this with formula (4.4) yields:

$$\left(\frac{\partial C}{\partial t} + \frac{1}{2} \sigma^2 S^2 \frac{\partial^2 C}{\partial S^2} \right) dt = r \left(C - S \frac{\partial C}{\partial S} \right) dt \quad (4.5)$$

Now both sides can be divided by dt . After some rearrangements this will give the Black-Scholes equation:

$$\frac{\partial C}{\partial t} + \frac{1}{2}\sigma^2 S^2 \frac{\partial^2 C}{\partial S^2} + rS \frac{\partial C}{\partial S} - rC = 0 \quad (4.6)$$

The same relation holds for a European put option, when replacing C with P in (4.6). This partial differential equation can be solved when using the known boundary and final conditions for call and put options at maturity. Solving this equation yields the famous Black-Scholes formulae for European options:

$$\begin{aligned} C &= SN(d_+) - Ke^{-rT} N(d_-) \\ P &= Ke^{-rT} N(-d_-) - SN(-d_+) \end{aligned} \quad (4.7)$$

with:

$$d_{\pm} = \frac{\log(S/K) + rT}{\sigma\sqrt{T}} \pm \frac{1}{2}\sigma\sqrt{T} \quad (4.8)$$

Here S denotes the initial stock price, K denotes the strike price of the option, T stands for the time-to-maturity and r is the risk-free interest rate. If we allow for a continuous dividend yield, q , the short position in the stock will also have to pay dividends. Thus it is easy to see that then (4.5) becomes:

$$\left(\frac{\partial C}{\partial t} + \frac{1}{2}\sigma^2 S^2 \frac{\partial^2 C}{\partial S^2} - qS \frac{\partial C}{\partial S} \right) dt = r \left(C - S \frac{\partial C}{\partial S} \right) dt \quad (4.9)$$

This can be rearranged and solved, to yield:

$$\begin{aligned} C &= Se^{-qT} N(d_+) - Ke^{-rT} N(d_-) \\ P &= Ke^{-rT} N(-d_-) - Se^{-qT} N(-d_+) \end{aligned} \quad (4.10)$$

with:

$$d_{\pm} = \frac{\log(S/K) + (r-q)T}{\sigma\sqrt{T}} \pm \frac{1}{2}\sigma\sqrt{T} \quad (4.11)$$

These formulae were derived by Merton. He also showed that options can be priced using risk-neutrality. If V denotes the value of an option, this means that:

$$V_0 = e^{-rT} E(V_T) \quad (4.12)$$

where V_T denotes the value of the option at maturity. The expectation is taken with respect to the risk-neutral process for the stock price:

$$dS = \hat{\mu}Sdt + \sigma SdW \quad (4.13)$$

The price of an option can thus be determined as the discounted expected payoff in a risk-neutral world. When there are no dividends, one should use $\hat{\mu} = r$. In the case of a

continuous dividend-yield $\hat{\mu} = r - q$ should be used. Due to their simplicity, these formulae soon became very popular amongst financial professionals.

Using risk-neutrality arguments, it is also possible to derive prices for barrier options. These formulae can be found in appendix B. More on pricing barrier options can be found in Rich (1994) or Cheuk and Vorst (1996).

4.4 Hedging and the Greeks

As seen in the previous section one can create a riskless portfolio by taking one plain vanilla call option and a position of $-\partial C / \partial S$ in the underlying stock. When choosing this portfolio, the call option is now said to be hedged against a change in the stock price. In mathematical terms, taking a position of $\partial C / \partial S$ is just a first order approximation for the option in S . Since in practice most of the assumptions made by Black and Scholes are not valid, traders may also want to be hedged against changes of other variables. The table below lists the hedge-parameters, also known as the greeks, for some variables.

<i>Delta</i>	<i>Gamma</i>	<i>Vega</i>	<i>Theta</i>	<i>Rho</i>	<i>Epsilon</i>
$\frac{\partial C}{\partial S}$	$\frac{\partial^2 C}{\partial S^2}$	$\frac{\partial C}{\partial \sigma}$	$\frac{\partial C}{\partial T}$	$\frac{\partial C}{\partial r}$	$\frac{\partial C}{\partial q}$

These greeks are all measures of risk, except for theta. Since there is no risk involved in the passage of time, theta can not be seen as a risk measure. The parameters show what happens to the price of an option if one of the underlying variables changes. Delta hedging is often done in practice. In this case, traders adjust their position only a finite number of times, since it is impossible to hedge continuously. This is why the parameter gamma is introduced. It measures the risk of a change in the delta of the option. For the Black-Scholes formula it is easy to derive the formulae for the greeks with the use of some calculus. The formulae of these greeks for a European call option can be found in Hull (1997).

4.5 Numerical pricing techniques

Next to the closed form formula derived by Black and Scholes, there exist some numerical techniques to value European options. One advantage of most of these models is that they can easily be generalized to allow for early exercise. The models are discussed very briefly here. When discussing the implied models in chapter 6, the techniques are discussed in more detail.

Binomial and trinomial trees

Two numerical methods that can be used when valuing derivatives are the binomial and trinomial tree. The binomial tree was derived by Cox Ross and Rubinstein (1979). The trinomial tree is a simple generalization of the binomial tree. Both methods are based on a discretization of the stock price process. The time space is divided into small steps. At every time-step, the stock price can move up or down with a certain amount, when using a binomial tree. In case a trinomial tree is used, a middle movement is also possible. Figure 4.2 gives an example of such a step for both tree models. The current stock price is assumed to be 100 and can go up or down with 10% during one time-step. The trinomial tree also allows the stock price to be at the same level one time-step later.

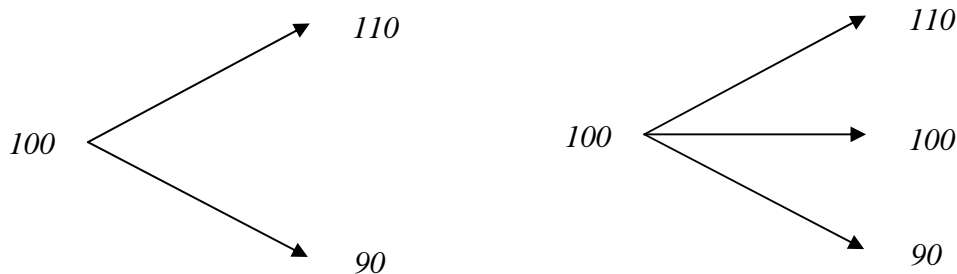


Figure 4.2: A step in binomial tree and trinomial tree

Whether the stock price goes up, down or stays the same is determined by the transition probabilities of the moves. These probabilities should be chosen such that the discrete process has the same first and second moment as the risk-neutral process. When this is done one can value a derivative by working backward through the tree. At maturity the value of a derivative is known. Next, one can determine the values of the derivative one time-step earlier by taking the discounted expectation of the value of the derivative at the current time-step. This can be done until the value of the derivative at the initial node is calculated, which gives an approximation of the derivative's current value. When calculating backwards it can be checked if early exercise is optimal given the value of the derivative. If it is, one has to replace the backward calculated value by the value that results from early exercise. This will then give an approximation for the value of an American option. Tree models can be used to value all kinds of derivatives. For instance, one can value an up-and-out barrier option by setting the values at nodes up and above the barrier to zero. When valuing barriers it is important to choose the nodes very carefully. A good way of doing this for trinomial trees can be found in Ritchken (1995) or Cheuk and Vorst (1996).

Finite difference method

Finite difference is a technique for solving partial differential equations. It is assumed that partial derivatives can be approximated numerically. This technique can for instance be applied to the Black-Scholes equation (4.6) in order to value a plain vanilla call option. First a grid should be chosen to discretize time and stock price. This is usually done using equally spaced time steps: $t \in \mathbf{T} = \{0, \Delta t, 2\Delta t, 3\Delta t, \dots, T\}$ and a number of equally spaced stock prices: $S \in \mathbf{S} = \{0, \Delta S, 2\Delta S, 3\Delta S, \dots, S_{max}\}$. T denotes the expiration date of the option. S_{max} denotes the maximum value in the grid and should be given a reasonable value, depending on time-to-maturity and volatility. With this grid one can define the option values at each node: $f_{i,j} = f(i\Delta S, j\Delta t)$. Next the partial derivatives of f can be approximated numerically, using option values at the nodes. For instance, an approximation of $\frac{\partial f}{\partial S}$ at point (i, j) can be: $\frac{f_{i+1,j} - f_{i-1,j}}{2\Delta S}$. In a similar manner, the other partial derivatives found in the differential equation can be approximated. Using some predetermined option values for the boundaries, one can then solve the values $f_{i,j}$ by working backward through the grid. At $t = T$ the option values are given by the payoff function. Values for the lower and upper bound of the stock price can be set to logical values. For instance $f_{0,j} = 0, \forall j$ is reasonable when we are valuing a call option. American options can be valued similar as in the binomial and trinomial trees. More on the finite difference method can be found in Wilmott (1998).

Monte Carlo simulation

Another way to approximate the value of a derivative is with the help of Monte Carlo simulation. This is probably the easiest way to value a derivative. One just simulates a number of stock price paths using the risk-neutral process given by (4.13). Given a certain path, the value of the derivative is easily determined. For a European option for instance, one calculates the payoff function for the final value of the simulated path. After simulating a large number of paths, one can get an approximation of the value of the derivative, as specified by (4.12), by discounting the average of all the values.

4.6 Implied volatility

The parameters in the Black-Scholes formula are all easy to observe, except for the volatility. This is the main reason the term implied volatility was introduced.

The implied volatility of an option is the volatility that, when plugged in the model, will give the market value.

The implied volatility of an option can not be found analytically and must thus be solved for numerically. Since plain vanilla options are increasing in volatility, bisection can be used. Another possibility is to use the method of Newton-Raphson. For a discussion on numerical techniques for finding a root of an equation, see for instance Press et al. (1992). When the Black-Scholes model is able to capture reality perfectly, the implied volatilities of all options with the same underlying, should be the same and constant over time. Merton has shown a way to deal with time dependence of volatility. Unfortunately, this will not suffice, because in practice implied volatilities vary with the strike and the time to maturity. The following terms are used on a regular basis:

Volatility smile/skew:

This is the dependence of the implied volatility of options on the strike, for a fixed maturity.

Volatility term structure:

This is the dependence of the implied volatility of options on the time to maturity, usually taken for at-the-money options.

Volatility surface:

This is the dependence of the implied volatility of options on both the strike and the time to maturity.

Whether the dependence of implied volatility of an option on its strike is a smile or a skew, depends on the shape of the curve. In case the implied volatility is a monotone function of strike, one speaks of a skew. When both deep in-the-money and out-of-the-money options have higher implied volatilities than at-the-money options, the term smile is used.

The usual way to define the implied volatility in practice, is by means of a volatility matrix. One dimension of the matrix is reserved for the strike price, the other dimension for the time to maturity. The table below gives an example of such a volatility matrix. It gives the implied volatilities of the S&P index, October 1995, and is taken from Andersen and Brotherton-Ratcliffe (1998).

Strike (% of Spot of the underlying)										
T	85	90	95	100	105	110	115	120	130	140
0.175	0.190	0.168	0.133	0.113	0.102	0.097	0.120	0.142	0.169	0.200
0.425	0.177	0.155	0.138	0.125	0.109	0.103	0.100	0.114	0.130	0.150
0.695	0.172	0.157	0.144	0.133	0.118	0.104	0.100	0.101	0.108	0.124
0.94	0.171	0.159	0.149	0.137	0.127	0.113	0.106	0.103	0.100	0.110
1.0	0.171	0.159	0.150	0.138	0.128	0.115	0.107	0.103	0.099	0.108
1.5	0.169	0.160	0.151	0.142	0.133	0.124	0.119	0.113	0.107	0.102
2.0	0.169	0.161	0.153	0.145	0.137	0.130	0.126	0.119	0.115	0.111
3.0	0.168	0.161	0.155	0.149	0.143	0.137	0.133	0.128	0.124	0.123
4.0	0.168	0.162	0.157	0.152	0.148	0.143	0.139	0.135	0.130	0.128
5.0	0.168	0.164	0.159	0.154	0.151	0.148	0.144	0.140	0.136	0.132

Table 4.1: An example of a volatility matrix.

To find implied volatilities for other combinations of strike and time to maturity, inter- and extrapolation techniques might be used. Appendix C shows how cubic splines can be used to interpolate and if necessary extrapolate these values. Applying this technique will give the following volatility surface:

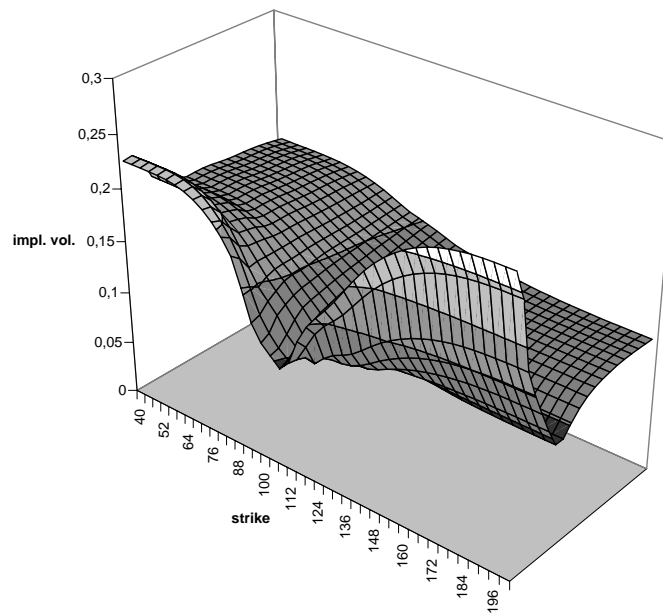


Figure 4.1: The volatility surface. The y-axis is reserved for time to maturity with the low values in front, and runs from 0 to 5 years. The x-axis has

It can be seen that the volatility smile for options with a short time to maturity is much more pronounced than the smile for options with a long time to maturity. This effect is frequently observed in practice and is also known as “the vanishing smile.”

5 Non-constant volatility

5.1 Introduction

In the previous chapter the Black-Scholes model was discussed. It was shown by Rubinstein (1985) that the model does not capture reality very well. In practice, implied volatilities are used to deal with these inconsistencies. This approach is not satisfactory since it does not give any answers for exotic options. This chapter derives a process implied by the market values of European options. The first part of this chapter shows how the risk-neutral distribution consistent with market values of European options can be derived. The second part is based on the stochastic process for the underlying asset, when the volatility is a deterministic function of both the value of the underlying and time, given by (3.7).

5.2 Deriving the instantaneous volatility function

As discussed in the previous chapter, risk-neutrality can be used to value derivatives. Thus the value of a European call option must equal the discounted expected pay-off at maturity. This can be written as follows:

$$C(S_0, T, K) = e^{-rT} \int_K^{\infty} (y - K) p(S_0, T, y) dy \quad (5.1)$$

Here, $p(\dots)$, denotes the risk-neutral transition density function. The value of this function at $S = K$ can be found by differentiating formula (5.1) twice, w.r.t. K . The first derivative of the right-hand-side can be found by using Leibniz's rule for integral differentiation:

$$e^{-rT} \left(-Kp(S_0, T, K) - \int_K^{\infty} p(S_0, T, y) dy + Kp(S_0, T, K) \right) = e^{-rT} \left(- \int_K^{\infty} p(S_0, T, y) dy \right) \quad (5.2)$$

Now the second order derivative will become $e^{-rT} p(S_0, T, K)$, again by Leibniz's rule. Thus the risk-neutral transition density function, first derived by Breeden and Litzenberger (1978), can be written as:

$$p(S_0, T, K) = e^{rT} \frac{\partial^2 C(S_0, T, K)}{\partial K^2} \quad (5.3)$$

So the risk-neutral density function, when the underlying is at level K at time T , can be obtained by taking the second order derivative of the formula for market values of call options, w.r.t. the strike price and multiply it with the appropriate discount factor. In other words, this function can be used to find the entire risk-neutral density for time T at time 0 , given the market value of European options. The figure below gives an example. The thick line gives the distribution of the stock price in a Black-Scholes world, with a volatility of 0.2 . This is thus a log-normal distribution. The dashed and the thin line give the distribution of stock prices if the market shows the following implied volatility function $\hat{\sigma} = 0.2 \pm 0.03(S_0 - K)$. For the dashed line, the plus-sign was used, while the thin line results from taking the minus-sign.

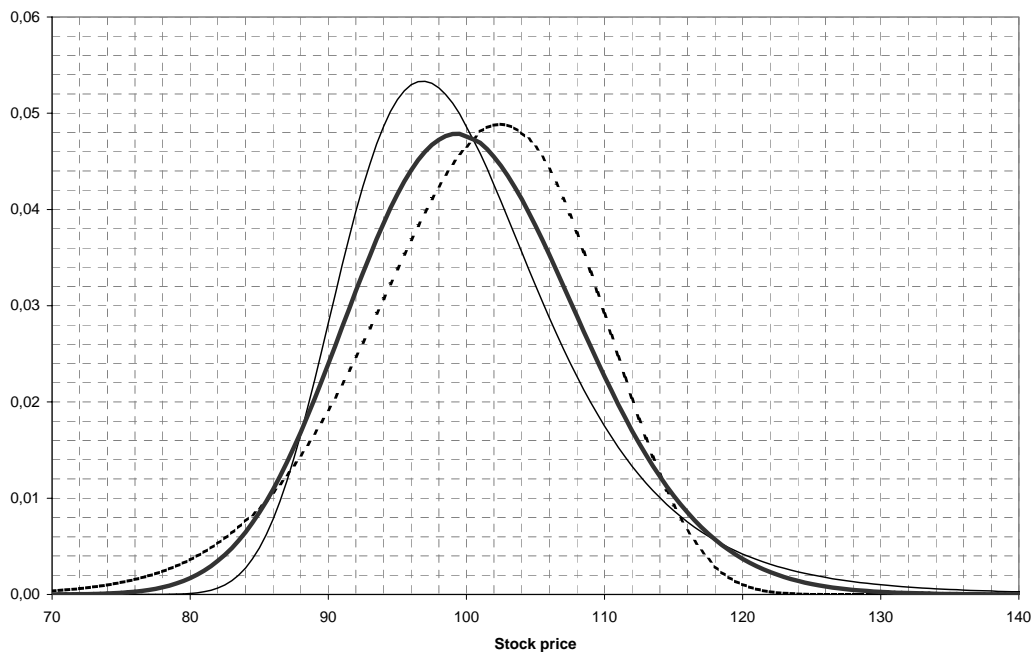


Figure 5.1: Distributions implied from market prices of plain vanilla options.

Both distributions resulting from a non-constant implied volatility function are skewed relative to the log-normal distribution. This is the reason that the dependence of volatility on the strike is sometimes referred to as the volatility skew, in case the implied volatility is a monotone function of strike. In practice a negative skew (the dashed line) appears frequently, implying a fatter tail at the low stock prices. This might mean that a higher possibility of a crash of the underlying asset value is incorporated in the market values of the options. In case the implied volatility displays more of a smile, both tails of the distribution are fatter than that of the log-normal distribution.

It can be shown that the density function $p(\dots)$ has to satisfy the Focker-Planck (or Kolmogorov forward) equation, see Øksendal (1998):

$$\frac{\partial p(S, T, K)}{\partial T} + \frac{\partial((r - q)Kp(S, T, K))}{\partial K} - \frac{1}{2} \frac{\partial^2(\sigma^2(K, T)K^2 p(S, T, K))}{\partial K^2} = 0 \quad (5.4)$$

Where $\sigma(K, T)$ is the instantaneous volatility at time T , when the value of the underlying is at K . Now from (5.3) we can determine the first term of (5.4):

$$\frac{\partial p}{\partial T} = re^{rT} \frac{\partial^2 C}{\partial K^2} + e^{rT} \frac{\partial(\partial^2 C / \partial K^2)}{\partial T} = e^{rT} \left(r \frac{\partial^2 C}{\partial K^2} + \frac{\partial(\partial^2 C / \partial K^2)}{\partial T} \right) \quad (5.5)$$

Next (5.4) can be rewritten as:

$$\frac{\partial^2}{\partial K^2} \left(\frac{\partial C}{\partial T} \right) + r \frac{\partial^2 C}{\partial K^2} + (r - q) \left(\frac{\partial(K(\partial^2 C / \partial K^2))}{\partial K} \right) = \frac{1}{2} \frac{\partial^2(\sigma^2(K, T)K^2(\partial^2 C / \partial K^2))}{\partial K^2} \quad (5.6)$$

This equation can then be integrated twice with respect to K to yield:

$$\frac{\partial C}{\partial T} + rC + (r - q) \left(K \frac{\partial C}{\partial K} - C \right) = \frac{1}{2} \sigma^2(K, T)K^2 \frac{\partial^2 C}{\partial K^2} + A(T)K + B(T) \quad (5.7)$$

The price of the call option, C , goes to zero for large K . The term $K \partial C / \partial K$ can also be ignored when K goes to infinity, for the following reason. Suppose $K \partial C / \partial K$ tends to a nonzero limit as K goes to infinity. If we define $R = 1 / K$ this can be written as:

$$\lim_{K \rightarrow \infty} K \frac{\partial C}{\partial K} = - \lim_{R \downarrow 0} R \frac{\partial C}{\partial R} = O(1) \quad (5.8)$$

For small R we would then have:

$$\frac{\partial C}{\partial R} = O\left(-\frac{1}{R}\right) \quad (5.9)$$

which can be integrated, to find that $C = O(-\log R)$ as $R \downarrow 0$. This is inconsistent with C being finite. Thus the term $K \partial C / \partial K$ goes to zero for large K . Same arguments can be used to show that other terms involving C will go to zero as K approaches infinity. This means that the terms on the right-hand-side, $A(T)$ and $B(T)$ must be equal to zero. Now the instantaneous volatility $\sigma^2(K, T)$ can be solved from (5.7):

$$\sigma^2(K, T) = 2 \frac{\frac{\partial C}{\partial T} + qC + K(r - q) \frac{\partial C}{\partial K}}{K^2 \left(\frac{\partial^2 C}{\partial K^2} \right)} \quad (5.10)$$

This equation can also be written in terms of the observed implied volatilities. In order to do this, we have to replace the derivatives. One must not forget that the implied volatilities depend on the strike and the maturity, or $\hat{\sigma} = \hat{\sigma}(K, T)$ so the chain rule must be used. Appendix D shows that (5.10) can be written as:

$$\sigma^2(K, T) = \frac{2 \frac{\partial \hat{\sigma}}{\partial T} + \frac{\hat{\sigma}}{T} + 2K(r - q) \frac{\partial \hat{\sigma}}{\partial K}}{K^2 \left(\frac{\partial^2 \hat{\sigma}}{\partial K^2} - d_+ \sqrt{T} \left(\frac{\partial \hat{\sigma}}{\partial K} \right)^2 + \frac{1}{\hat{\sigma}} \left(\frac{1}{K\sqrt{T}} + d_+ \frac{\partial \hat{\sigma}}{\partial K} \right)^2 \right)} \quad (5.11)$$

Using the following process to model stock prices:

$$dS = \mu S dt + \sigma(S, t) dW, \quad (5.12)$$

where $\sigma(S, t)$, which is calculated from (5.11), will yield option prices consistent with their market values. The implied models discussed in the next chapter all satisfy the relation in (5.11) in the limit.

6 Implied models

6.1 Introduction

This chapter shows how implied models can be built. The first section discusses the implied binomial tree of Derman and Kani (1994). Later in this section, some modifications to this model suggested by Barle and Cakici (1998) are considered. The second section discusses the implied trinomial tree of Derman, Kani and Chriss (1996). The third section will then focus on two possible alternatives for an implied finite difference model, proposed by Andersen and Brotherton-Ratcliffe (1998). The fourth section will show how Monte Carlo simulation can be used in the presence of a volatility structure. A last model that will be discussed is that of Neuberger and Britten-Jones (2000). This model allows for a stochastic process, which will then be adjusted to fit market prices of options. Finally, we will discuss how implied trees can be used in combination with the instantaneous volatility.

6.2 Implied binomial tree

The model of Derman and Kani

When building an implied binomial tree as proposed by Derman and Kani (1994), one must work through the tree from time 0 to time T , recursively. At every time-step the nodes and their corresponding transition probabilities are chosen in such a way, that one European call option is priced consistent with the market and the expected stock price equals its forward price. Assume that the tree is already constructed up to the n -th time period. Now let $S_{n,i}$ denote the stock price corresponding with node i at timestep n , $n = 0, \dots, N$, where N is the total number of steps in the tree and i runs from 0 at the bottom to n at the top of the tree. The forward price, denoted by $F_{n,i}$, should equal $e^{(r-q)\Delta t} S_{n,i}$, where r and q denote the continuous risk-free interest rate and dividend yield, respectively. This follows from the no-arbitrage principle. To assure risk-neutrality in the tree, the forward price is required to satisfy the following condition:

$$F_{n,i} = p_{n,i} S_{n+1,i+1} + (1 - p_{n,i}) S_{n+1,i} \quad (6.1)$$

Let $C(K, t_{n+1})$ denote the market value of a European call option maturing at time t_{n+1} , with a strike price of K . This option is based on the underlying security whose spot price

S is fixed at the root of the tree, $S_{0,0}$. In the tree constructed so far, the option will be priced using the following formula:

$$C_{tree}(K, t_{n+1}) = \sum_{i=0}^{n+1} \lambda_{n+1,i} \max(S_{n+1,i} - K, 0) \quad (6.2)$$

Where $\lambda_{n,i}$ is known as the Arrow-Debreu price at node i of the n -th timestep, which is defined as the value of a security that pays 1 if $S_{n,i}$ is reached at time t_n and 0 for all other values of S at time t_n . In a binomial tree, λ_{n+1} can be calculated using the following formula:

$$\lambda_{n+1,i} e^{r\Delta t} = \begin{cases} p_{n,n} \lambda_{n,n} & \text{for } i = n+1 \\ p_{n,i-1} \lambda_{n,i-1} + (1 - p_{n,i}) \lambda_{n,i} & \text{for } 1 \leq i \leq n \\ (1 - p_{n,0}) \lambda_{n,0} & \text{for } i = 0 \end{cases} \quad (6.3)$$

When determining $S_{n+1,i+1}$, Derman and Kani choose the strike of the option to be $S_{n,i}$, as shown in figure 6.1.

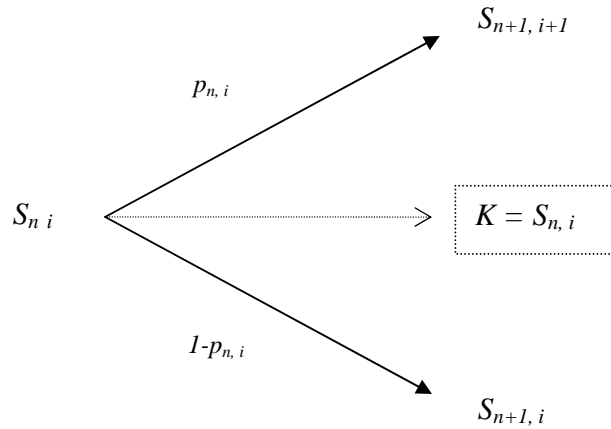


Figure 6.1: Setting the strike equal to $S_{n,i}$.

Setting the market value of the option equal to the right-hand-side of equation (6.2) and using expressions (6.3) and (6.1) yields:

$$e^{r\Delta t} C(S_{n,i}, t_{n+1}) = p_{n,i} \lambda_{n,i} (S_{n+1,i+1} - S_{n,i}) + \sum_{j=i+1}^n \lambda_{n,j} (F_{n,j} - S_{n,i}) \quad (6.4)$$

When combining this equality with equation (6.1), $S_{n+1,i+1}$ and $p_{n,i}$ can be solved for, resulting in the following expressions:

$$S_{n+1,i+1} = \frac{S_{n+1,i} \Delta C_i - \lambda_{n,i} S_{n,i} (F_{n,i} - S_{n+1,i})}{\Delta C_i - \lambda_{n,i} (F_{n,i} - S_{n+1,i})} \quad (6.5)$$

$$p_{n,i} = \frac{F_{n,i} - S_{n+1,i}}{S_{n+1,i+1} - S_{n+1,i}} \quad (6.6)$$

where:

$$\Delta C_i = e^{r\Delta t} C(S_{n,i}, t_{n+1}) - \sum_{j=i+1}^n \lambda_{n,j} (F_{n,j} - S_{n,i}) \quad (6.7)$$

Formula (6.5) and (6.6) can now be used iteratively to find all the nodes and the corresponding transition probabilities above the centre of the tree for time t_{n+1} . In a similar way the nodes and transition probabilities below the centre of the tree can be derived, using put options instead of call options to make the algorithm faster. Deriving the equations in a similar manner as discussed above gives the following solution for $S_{n+1,i}$:

$$S_{n+1,i} = \frac{S_{n+1,i+1} \Delta P_i + \lambda_{n,i} S_{n,i} (F_{n,i} - S_{n+1,i+1})}{P_i + \lambda_{n,i} (F_{n,i} - S_{n+1,i+1})} \quad (6.8)$$

with:

$$\Delta P_i = e^{r\Delta t} P(S_{n,i}, t_{n+1}) - \sum_{j=1}^{i-1} \lambda_{n,j} (S_{n,i} - F_{n,j}) \quad (6.9)$$

The corresponding transition probabilities can be found by using (6.6). It is possible that negative probabilities are encountered. From the equation, it can be seen that the following relation must hold for nonnegative transition probabilities:

$$F_i \leq S_{n+1,i+1} \leq F_{i+1} \quad (6.10)$$

If the left part of the inequality is violated, $p_{n,i}$ will be greater than 1, and thus $1 - p_{n,i}$ will be negative. If the right part of the inequality is not satisfied, $p_{n,i+1}$ will become negative. If this inequality is violated, $S_{n+1,i}$ should be set to an other value. One possibility is to set $S_{n+1,i+1}$ equal to $0.5F_{n,i} + 0.5F_{n,i+1}$. Now, all that is left, is to choose a value for $S_{n+1,i}$ at the centre of the tree before formulas (6.5) to (6.8) can be applied to find the entire set of nodes at time t_{n+1} . When $n+1$ is even, an easy choice for the central node will be the spot price of the underlying:

$$S_{n+1, \frac{1}{2}(n+1)} = S_{0,0} \quad (6.11)$$

When $n+1$ is odd there are two central nodes at time t_{n+1} . An obvious way to choose the central nodes will be in such a way that the logarithmic spacing between the nodes and the spot price will be the same, or:

$$S_{n+1,1+\frac{1}{2}n} S_{n+1,\frac{1}{2}n} = S_{0,0}^2 \quad (6.12)$$

Substituting this relation into equation (6.5) and noticing that $S_{0,0} = S_{n,i}$, $S_{n+1,i}$ can now be solved for:

$$S_{n+1,i} = S_{n,i} \frac{\lambda_{n,i} F_{n,i} - \Delta C_i}{\lambda_{n,i} S_{n,i} + \Delta C_i} \quad (6.13)$$

Modifications to the model

As discussed above, for nonnegative transition probabilities, inequality (6.10) should be satisfied. However when using the algorithm of Derman and Kani it is possible that the calculated value of $S_{n+1,i+1}$ falls between $S_{n,i+1}$ and $F_{n,i+1}$. This causes a small error when calculating $S_{n+1,i+2}$, since $S_{n+1,i+1}$ is greater than $S_{n,i+1}$, the strike of the option, which is not assumed in the algorithm. For this reason Barle and Cakici (1998) propose to use the forward price, $F_{n,i}$, rather than $S_{n,i}$ as the strike of the option needed for equation (6.4). Figure 6.2 depicts this situation:

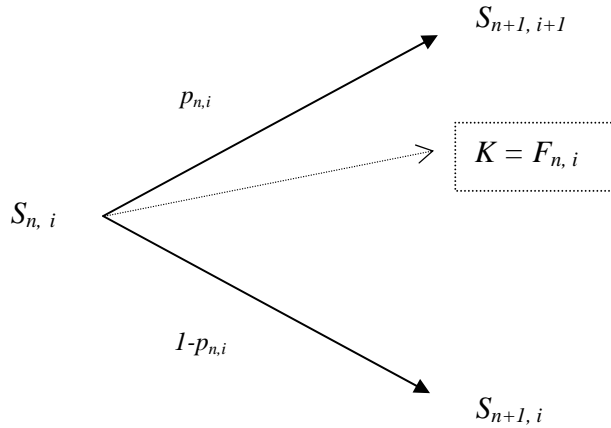


Figure 6.2: setting the strike equal to $F_{n,i}$

Using $F_{n,i}$ for the strike price of the option has the advantage that $S_{n+1,i+1}$ will never be greater than the strike in the next step: $F_{n,i+1}$, since inequality (6.10) has to be satisfied. Changing the strike price to $F_{n,i}$ will result in a change in formula (6.5):

$$S_{n+1,i+1} = \frac{S_{n+1,i} \Delta C_i - \lambda_{n,i} F_{n,i} (F_{n,i} - S_{n+1,i})}{\Delta C_i - \lambda_{n,i} (F_{n,i} - S_{n+1,i})} \quad (6.14)$$

where ΔC_i is now defined as:

$$\Delta C_i = e^{r\Delta t} C(F_{n,i}, t_{n+1}) - \sum_{j=i+1}^n \lambda_{n,j} (F_{n,j} - F_{n,i}) \quad (6.15)$$

Similar adjustments must be made to equations (6.8) and (6.9), for the nodes below the center of the implied tree. The only thing that's left to be done, is to check if $S_{n+1,i+1}$ is in between $F_{n,i}$ and $F_{n,i+1}$. If this is not the case, one must override $S_{n+1,i+1}$.

A second modification proposed by Barle and Cakici to the model of Derman and Kani is to use the forward price when setting the middle node (or nodes, if $n+1$ is odd) of the tree. This modification will change formulas (6.11), (6.12) and (6.13) to become:

$$S_{n+1, \frac{1}{2}(n+1)} = F_{n, \frac{1}{2}n} \quad (6.16)$$

$$S_{n+1, l+\frac{1}{2}n} S_{n+1, \frac{1}{2}n} = F_{n, \frac{1}{2}n}^2 \quad (6.17)$$

$$S_{n+1,i} = F_{n,i} \frac{\lambda_{n,i} F_{n,i} - \Delta C_i}{\lambda_{n,i} F_{n,i} + \Delta C_i} \quad (6.18)$$

When $r - q = 0$ the modified model will be exactly the same as the original model of Derman and Kani, since then $F_{n,i} = S_{n,i}$. In their article Barle and Cakici show that their adjustments can improve the model significantly. Especially in the case of a high interest rate, improvements are very clear. To demonstrate this, the following figure is presented. In this figure one can see the linear, downward sloping, volatility function. Options have a time to maturity of 1 year. Interest rate was set at 10% per annum. The underlying asset has an initial value of 100 and does not pay dividends. Both the original implied tree and the modified implied tree with 50 steps were used to value options with different strikes. From these prices the implied volatility was calculated and compared with the input volatility skew. The results are given in the figure below:



Figure 6.3: Implied volatilities of options priced with the model

It can be seen that the modified model works better than the original Derman and Kani model. This is caused by the high interest rate. Taking even larger values for the interest rates will worsen the results of the Derman Kani model even more. More examples can be found in Barle and Cakici (1998). Therefore, it is obvious that the modified model is preferred to the original one.

6.3 Implied trinomial tree

Soon after developing an implied binomial tree model, Derman, Kani and Chriss came up with a similar approach for the construction of an implied trinomial tree. This section describes how one can build an implied trinomial tree given a certain volatility structure.

The model of Derman Kani and Chriss

As with implied binomial trees, an implied trinomial tree is designed to price certain options consistent with their market prices. Once again one starts from the root of the tree and works through the tree, until time T is reached. Assume that the tree is already build up to the n -th level, or time t_n , where n can range from 0 to N . At this level the tree has $2n + 1$ nodes, $S_{n,i}$, where $i = 0, \dots, 2n$. Next assume the existence of options with strikes equal to this nodes and time to maturity t_{n+1} . We now want to choose the parameters of the tree in such a way that the tree values these options consistent with the market. Since

we can choose $2(n+1)+1$ nodes and $2(2n+1)$ transition probabilities (one up- and one down transition probability at each node) we have $6n+5$ degrees of freedom. From the options we have $2n+1$ restrictions. Demanding risk-neutrality will give us another $2n+1$ restrictions. This leaves us with $2(n+1)+1$ degrees of freedom, which is exactly the amount, given by the freedom to choose the node values. So an easy way to eliminate these degrees of freedom, is to choose the statespace in advance. This is the main difference between implied binomial and implied trinomial trees. So when arrived at step n , we have $2n+1$ forward restrictions:

$$F_{n,i} = Pu_{n,i}S_{n+1,i+2} + (1 - Pu_{n,i} - Pd_{n,i})S_{n+1,i+1} + Pd_{n,i}S_{n+1,i} \quad (6.19)$$

Where $F_{n,i}$ is again defined as $e^{(r-q)At}S_{n,i}$. Now the option with a strike $K = S_{n+1,i+1}$, is considered. This strike corresponds with the price of the underlying after a middle move. In the implied tree constructed so far, this option will be priced using the following formula:

$$C_{tree}(K, t_{n+1}) = \sum_{i=0}^{2n+3} \lambda_{n+1,i} \max(S_{n+1,i} - K, 0) \quad (6.20)$$

The Arrow-Debreu securities $\lambda_{n,i}$ can be calculated in a similar way as was done in the previous section. This will give the following formula:

$$\lambda_{n+1,i}e^{rAt} = \begin{cases} Pu_{n,2n}\lambda_{n,2n} & \text{for } i = 2(n+1) \\ Pu_{n,2n-1}\lambda_{n,2n-1} + Pm_{n,2n}\lambda_{n,2n} & \text{for } i = 2n+1 \\ Pu_{n,i-2}\lambda_{n,i-2} + Pm_{n,i-1}\lambda_{n,i-1} + Pd_{n,i}\lambda_{n,i} & \text{for } 2 \leq i \leq 2n \\ Pd_{n,1}\lambda_{n,1} + Pm_{n,0}\lambda_{n,0} & \text{for } i = 1 \\ Pd_{n,0}\lambda_{n,0} & \text{for } i = 0 \end{cases} \quad (6.21)$$

Where $Pm_{n,i}$ denotes the middle transition probability, so $Pm_{n,i} = 1 - Pu_{n,i} - Pd_{n,i}$. Next equations (6.19), (6.20) and (6.21) can be combined to get:

$$e^{rAt}C(S_{n+1,i+1}, t_{n+1}) = Pu_{n,i}\lambda_{n,i}(S_{n+1,i+2} - S_{n+1,i+1}) + \sum_{j=i+1}^{2n} \lambda_{n,j}(F_{n,j} - S_{n+1,i+1}) \quad (6.22)$$

Now we can set this option price, evaluated by the tree, equal to the market value of this option and solve for $Pu_{n,i}$. This yields:

$$Pu_{n,i} = \frac{e^{rAt}C(S_{n+1,i+1}, t_{n+1}) - \sum_{j=i+1}^{2n} \lambda_{n,j}(F_{n,j} - S_{n+1,i+1})}{\lambda_{n,i}(S_{n+1,i+2} - S_{n+1,i+1})} \quad (6.23)$$

With the risk-neutrality condition (6.19) we can solve for $Pd_{n,i}$:

$$Pd_{n,i} = \frac{F_{n,i} - Pu_{n,i}(S_{n+1,i+2} - S_{n+1,i+1}) - S_{n+1,i+1}}{S_{n+1,i} - S_{n+1,i+1}} \quad (6.24)$$

To increase computational speed, we can use put options to determine the node transition probabilities below the centre of the tree in a similar way:

$$Pd_{n,i} = \frac{e^{r\Delta t} P(S_{n+1,i+1}, t_{n+1}) - \sum_{j=1}^{i-1} \lambda_{n,j} (S_{n+1,i+1} - F_{n,j})}{\lambda_{n,i} (S_{n+1,i+1} - S_{n+1,i})} \quad (6.25)$$

and

$$Pu_{n,i} = \frac{F_{n,i} + Pd_{n,i}(S_{n+1,i} - S_{n+1,i+1}) - S_{n+1,i+1}}{S_{n+1,i+2} - S_{n+1,i+1}} \quad (6.26)$$

After determining the transition probabilities with formulae (6.23)-(6.26), the Arrow-Debreu security for time t_{n+1} can be calculated with the use of (6.21). After this, the procedure repeats.

One should be careful when negative transition probabilities occur. In this case Derman and Kani propose to use the following formulae to override these negative probabilities:

$$\begin{aligned} \text{if } S_{n+1,i+1} < F_{n,i} < S_{n+1,i+2} \\ Pu_{n,i} &= \frac{1}{2} \left[\frac{F_{n,i} - S_{n+1,i+1}}{S_{n+1,i+2} - S_{n+1,i+1}} + \frac{F_{n,i} - S_{n+1,i}}{S_{n+1,i+2} - S_{n+1,i}} \right] \\ Pd_{n,i} &= \frac{1}{2} \left[\frac{S_{n+1,i+2} - F_{n,i}}{S_{n+1,i+2} - S_{n+1,i}} \right] \end{aligned} \quad (6.27)$$

$$\begin{aligned} \text{if } S_{n+1,i} < F_{n,i} < S_{n+1,i+1} \\ Pd_{n,i} &= \frac{1}{2} \left[\frac{S_{n+1,i+2} - F_{n,i}}{S_{n+1,i+2} - S_{n+1,i}} + \frac{S_{n+1,i+1} - F_{n,i}}{S_{n+1,i+1} - S_{n+1,i}} \right] \\ Pu_{n,i} &= \frac{1}{2} \left[\frac{F_{n,i} - S_{n+1,i}}{S_{n+1,i+2} - S_{n+1,i}} \right] \end{aligned}$$

This will give positive transition probabilities that satisfy the risk-neutrality condition given in (6.19) but the option is not priced consistent with the market. To overcome this

problem, the statespace of the tree should be chosen wisely. Taking too small steps ΔS will cause the model to underprice the options compared with their market values. While taking too large steps will yield prices, which are too high. Another way to replace negative probabilities is given below:

$$\begin{aligned}
& \text{if } S_{n+1,i+1} < F_{n,i} < S_{n+1,i+2} & \text{if } S_{n+1,i} < F_{n,i} < S_{n+1,i+1} \\
& \text{if } Pu_{n,i} < 0 \text{ and / or } Pd_{n,i} < 0 & \text{if } Pu_{n,i} < 0 \text{ and / or } Pd_{n,i} < 0 \\
& Pu_{n,i} = \frac{F_{n,i} - S_{n+1,i+1}}{S_{n+1,i+2} - S_{n+1,i+1}} & Pd_{n,i} = \frac{S_{n+1,i+1} - F_{n,i}}{S_{n+1,i+1} - S_{n+1,i}} \\
& Pd_{n,i} = 0 & Pu_{n,i} = 0 \\
& \text{if } Pu_{n,i} + Pd_{n,i} > 1 & \text{if } Pu_{n,i} + Pd_{n,i} > 1 \\
& Pu_{n,i} = \frac{F_{n,i} - S_{n+1,i}}{S_{n+1,i+2} - S_{n+1,i}} & Pu_{n,i} = \frac{F_{n,i} - S_{n+1,i}}{S_{n+1,i+2} - S_{n+1,i}} \\
& Pd_{n,i} = 1 - Pu_{n,i} & Pd_{n,i} = 1 - Pu_{n,i}
\end{aligned} \tag{6.28}$$

This results from the following reasoning: In the tree the volatility over one time-step is bounded both from above and below. If the volatility in one node falls outside the boundaries, which is possible in case of negative transition probabilities, the probabilities are adjusted in such a way that the volatility is at the boundary. This can easily be achieved by fixing one of the transition probabilities at zero and solving the other transition probabilities from the forward restriction. Since the maximum volatility at a node can be found by setting the middle transition probability at zero. The minimum volatility can be found by setting the up and down transition probabilities as low as possible.

6.4 Implied finite differences

Another way to incorporate a volatility surface in a model is to use the method of finite differences. In this section two alternative methods will be discussed. Both methods involve choosing values for the volatility for every node in the finite difference grid. The first method uses the instantaneous volatility function to get the values for the volatilities at every node. The second method that will be discussed here was introduced by Andersen and Brotherton-Ratcliffe (1998). They propose an implied model based on finite difference where the volatilities are chosen in such a way that the model prices European options consistent with the market. This means that the volatilities at every node have to be solved for. This section will first focus on the finite difference method, followed by the two alternative ways to choose the local volatilities.

Finite difference method

With the help of arbitrage arguments Merton (1973) has shown that the value of a contingent claim at any time before T , $V(S,t)$, satisfies a partial differential equation (PDE). The original derivation of Merton assumes a volatility independent of S and t , however the formula is easy to generalize for non-constant volatilities:

$$\frac{\partial V(S,t)}{\partial t} + \frac{1}{2}\sigma^2(S,t)S^2 \frac{\partial^2 V(S,t)}{\partial S^2} + (r-q)S \frac{\partial V(S,t)}{\partial S} = rV(S,t) \quad (6.29)$$

Where $\sigma(S,t)$ is the instantaneous volatility when the underlying is at value S at time t . If $g(S_T)$ denotes the pay-off function, the above PDE has the following final condition:

$$V(S_T, T) = g(S_T) \quad (6.30)$$

This PDE can be solved numerically with the finite difference method. To achieve this, a grid has to be constructed along which option values will be determined at each point of the grid. The easiest way of doing this is to take a fixed time-step Δ_t and a fixed step for S , Δ_S . However to increase efficiency it is better to use $x = \ln S$ and create a grid using a fixed step Δ_x . If we let $H(x,t) = V(S,t)$, the PDE given in (6.29) after this transformation will become:

$$\frac{\partial H(x,t)}{\partial t} + \frac{1}{2}v(x,t) \frac{\partial^2 H(x,t)}{\partial x^2} + b(x,t) \frac{\partial H(x,t)}{\partial x} = rH(x,t) \quad (6.31)$$

where:

$$b(x,t) = r - q - \frac{1}{2}v(x,t), \quad v(x,t) = \sigma^2(S,t) = \sigma^2(e^x, t)$$

To make the model price European options consistent with their market values, one should choose values for $v(x,t)$ and thus $b(x,t)$. For the moment, we replace the parameters $v(x,t)$ and $b(x,t)$ by $\hat{v}(x,t)$ and $\hat{b}(x,t)$, respectively. Later in this chapter two alternative ways to determine $\hat{v}(x,t)$ and $\hat{b}(x,t)$, will be given. Next the grid can be created using uniform spacing in the x and t directions. $M+2$ nodes along the t -axis and $N+2$ nodes along the x -axis are used to get:

$$x_i = x_0 + i\Delta_x = x_0 + i \frac{x_{N+1} - x_0}{N+1} \quad i = 0, \dots, N+1 \quad (6.32)$$

$$t_j = t_0 + j\Delta_t = t_0 + j \frac{T}{M+1} \quad j = 0, \dots, M+1 \quad (6.33)$$

The indices $i = 0$, $i = N + 1$, $j = 0$ and $j = M + 1$ are used for the limits of the grid. At these nodes, values for the contingent claim have to be prescribed by some boundary condition. The values for x_0 and x_{N+1} should be set sufficiently low and high, respectively to ensure that most of the significant x space is captured by the grid. Further it is assumed that the spot value of the underlying is positioned on a point in the grid, or when using S_{ini} for the initial value of the underlying:

$$x_\beta = \ln S_{ini},$$

for some integer $\beta \in [1, N]$. One could for example choose S_{ini} to be in the middle of the grid, and take $\beta = \left\lfloor \frac{N+1}{2} \right\rfloor$. Next x_0 and Δ_x can then be chosen as:

$$x_0 = \ln(Q S_{ini}) \qquad \Delta_x = \frac{\ln S_{ini} - x_0}{\beta},$$

Q is some number between zero and one. If for example $Q = \frac{1}{4}$ is chosen, the grid will range from $S_0 = \frac{1}{4} S_{ini}$ to about $S_{N+1} = 4 S_{ini}$.

At this point the PDE can be solved backward. Therefore, values for the partial derivatives in (6.31) have to be given. These partial derivatives can be approximated numerically with values of the contingent claim, at particular nodes in the grid. Good approximations for the terms of (6.31) at node (x_i, t_j) are given in the following formulae:

$$\frac{\partial H}{\partial t} \approx \frac{H(x_i, t_{j+1}) - H(x_i, t_j)}{\Delta_t}, \tag{6.34a}$$

$$\frac{\partial H}{\partial x} \approx (1 - \Theta) \frac{H(x_{i+1}, t_j) - H(x_{i-1}, t_j)}{2\Delta_x} + \Theta \frac{H(x_{i+1}, t_{j+1}) - H(x_{i-1}, t_{j+1})}{2\Delta_x}, \tag{6.34b}$$

$$\begin{aligned} \frac{\partial^2 H}{\partial x^2} \approx & (1 - \Theta) \frac{H(x_{i+1}, t_j) - 2H(x_i, t_j) + H(x_{i-1}, t_j)}{\Delta_x^2} + \\ & \Theta \frac{H(x_{i+1}, t_{j+1}) - 2H(x_i, t_{j+1}) + H(x_{i-1}, t_{j+1})}{\Delta_x^2} \end{aligned} \tag{6.34c}$$

for $i = 1, \dots, N$ and $j = 0, \dots, M$. The parameter $\Theta \in [0, 1]$ is used to determine the time at which the approximations of the partial derivatives w.r.t. x are evaluated. If Θ is set to zero, the resulting finite difference method is called fully implicit. When $\Theta = 1$, the discretization scheme is also known as the explicit finite difference method, which is closely related to the trinomial tree. Finally, when $\Theta = \frac{1}{2}$, the method is known as the

Crank-Nicholson discretization scheme. Of course other values for Θ are also possible but are little used in practice. Equipped with these approximations for the derivatives and substituting $\hat{v}(x,t)$, $\hat{b}(x,t)$ for $v(x,t)$ and $b(x,t)$, respectively, the PDE in (6.31) can, after some manipulations, be written as follows:

$$\left((1+r\Delta_t)\mathbf{I} - (1-\Theta)\mathbf{M}_j \right) \mathbf{H}_j = (\Theta \mathbf{M}_j + \mathbf{I}) \mathbf{H}_{j+1} + \mathbf{B}_j \quad j = 0, \dots, M \quad (6.35)$$

where \mathbf{I} is the $N \times N$ identity matrix. \mathbf{H}_j is the $N \times 1$ vector of contingent claim values at time t_j . The $N \times 1$ vector \mathbf{B}_j contains the prescribed contingent claim values along the x boundary of the grid:

$$\mathbf{B}_j = \begin{bmatrix} l_{1,j} \left((1-\Theta)H_{0,j} + \Theta H_{0,j+1} \right) \\ 0 \\ \vdots \\ 0 \\ u_{N,j} \left((1-\Theta)H_{N+1,j} + \Theta H_{N+1,j+1} \right) \end{bmatrix}$$

\mathbf{M}_j can be written as the following $N \times N$ matrix:

$$\mathbf{M}_j = \begin{bmatrix} c_{1,j} & u_{1,j} & 0 & 0 & 0 & \dots & 0 \\ l_{2,j} & c_{2,j} & u_{2,j} & 0 & 0 & \dots & 0 \\ 0 & \cdot & \cdot & \cdot & 0 & \vdots & \vdots \\ \vdots & 0 & \cdot & \cdot & \cdot & \cdot & 0 \\ \vdots & \vdots & 0 & \dots & l_{N-1,j} & c_{N-1,j} & u_{N-1,j} \\ 0 & 0 & 0 & \dots & 0 & l_{N,j} & c_{N,j} \end{bmatrix}$$

Where we have:

$$c_{i,j} = -\alpha \hat{v}_{i,j}, \quad u_{i,j} = \frac{1}{2} \alpha \left(\hat{v}_{i,j} + \Delta_x \hat{b}_{i,j} \right),$$

$$d_{i,j} = \frac{1}{2} \alpha \left(\hat{v}_{i,j} - \Delta_x \hat{b}_{i,j} \right), \quad \alpha = \frac{\Delta_t}{\Delta_x^2}$$

The boundary values for H , needed to construct the vector \mathbf{B}_j , are often easy to choose. For example when pricing a European call option with strike K , the values $H_{0,j}$ can be set to 0 for all j , since the probability of ending in the money is extremely small when x_0 is chosen sufficiently low. One should be careful when the strike is close to zero. The values for $H_{N+1,j}$ can be set to $E(S_{N+1,T} - K) = S_{N+1}e^{-q(T-t_j)} - Ke^{-r(T-t_j)}$, since the probability of ending out of the money is very small when x_{N+1} is chosen high enough. Once the values of $\hat{v}(x,t)$ and $\hat{b}(x,t)$ and the boundary values of H are chosen, the value of the contingent claim can be solved numerically. Starting at time T , we have the boundary condition $\mathbf{H}_T = \mathbf{H}_{M+1} = g(\mathbf{S}_T)$, a vector of the known pay-off values at maturity. Next \mathbf{H}_M can be found by pre-multiplying the right-hand-side, with the inverse of the tridiagonal matrix $(I + r\Delta_t)\mathbf{I} - (I - \Theta)\mathbf{M}_M$. This step can be repeated until finally \mathbf{H}_0 is solved. The value of the contingent claim at time t_0 can now be found by taking the β -th element of vector \mathbf{H}_0 . Although this algorithm involves inverting $N \times N$ matrices M times, it is actually quite fast. Since the matrices on the left-hand-side are tridiagonal, the solution to (6.35) can be coded efficiently, of $O(N)$. A discussion of an algorithm to solve a system of linear equations, when a tridiagonal matrix is used, can be found in Cheney and Kincaid (1994), or Press et al. (1992).

Instantaneous volatility approach

Now that the finite difference method is discussed, values for $\hat{v}(x,t)$ and $\hat{b}(x,t)$ should be found in order to be able to use the algorithm. One possible candidate for $\hat{v}(x,t)$ is the instantaneous volatility, which can be seen as the volatility at time T , given that the price of the underlying is at K . The formula for this instantaneous volatility was derived in chapter 5:

$$\sigma(K,T) = \sqrt{\frac{2\frac{\partial\hat{\sigma}}{\partial T} + \frac{\hat{\sigma}}{T} + 2K(r-q)\frac{\partial\hat{\sigma}}{\partial K}}{K^2\left(\frac{\partial^2\hat{\sigma}}{\partial K^2} - d_+\sqrt{T}\left(\frac{\partial\hat{\sigma}}{\partial K}\right)^2 + \frac{1}{\hat{\sigma}}\left(\frac{1}{K\sqrt{T}} + d_+\frac{\partial\hat{\sigma}}{\partial K}\right)^2\right)}} \quad (6.36)$$

Where $\hat{\sigma} = \hat{\sigma}(K,T)$ denotes the implied volatility of a European call option on the same underlying, with strike K and time-to-maturity T , observed at time t_0 . This instantaneous value for the volatility can be used for every point in the finite-difference grid:

$$\hat{v}(x,t) = \sigma^2(e^x, t) \qquad \hat{b}(x,t) = r - q - \frac{1}{2}\hat{v}(x,t), \quad (6.37)$$

Next the finite difference algorithm can be applied to value all kinds of contingent claims on S using the given volatility structure. If the function $\hat{\sigma} = \hat{\sigma}(K, T)$ is not given explicitly, one can use interpolation techniques on a set of given implied volatilities.

Method of Andersen and Brotherton-Ratcliffe

As discussed in the previous section $\hat{v}(x, t)$ can be set to the instantaneous volatility. And $\hat{b}(x, t)$ follows directly from that choice. However in doing so, the coefficients would then be based on a continuous time setting, which causes the discretization-scheme to yield correct prices only in the limit. Therefore, $\hat{v}(x, t)$ and $\hat{b}(x, t)$ shall be solved for in such a way that the discretization scheme of the PDE will return correct market prices for stock forwards and a set of European options. First r will be replaced by its discrete version:

$$\hat{r} = \frac{1}{\Delta_t} (e^{r\Delta_t} - 1)$$

In the next section $\hat{b}(x, t)$ will be solved for, followed by a solution for $\hat{v}(x, t)$. One important fact that has been exploited, is that the constructed finite difference grid can also be used for pricing forward contracts and Arrow-Debreu securities, since they are both contingent claims on the underlying and thus should satisfy the PDE given in (6.31).

Forcing risk-neutrality

In order to get risk-neutral value from the finite difference method, the forward has to be priced correctly when the method is used. Here it will be discussed how $b(x, t)$ should be chosen in order to get correct prices for the forward. To find $\hat{b}(x, t)$ we look at a contract at time t_j that pays out $g(S_{t_{j+1}}) = S_{t_{j+1}}$ at time t_{j+1} . The value of this contract at node (x_i, t_j) follows from risk-neutral valuation:

$$H_{i,j} = S_i e^{-q(t_{j+1}-t_j)}$$

$H_{i,j+1}$ is of course equal to S_{i+1} . Since this contract is also a contingent claim on S , it has to satisfy the PDE given in (6.31). So values for H can now be substituted in (6.35). This yields the following equality that has to be satisfied

$$\begin{aligned} & S_i \left[1 - e^{-q\Delta_t} (1 + r\Delta_t) - \alpha \hat{v}_{i,j} \left((1 - \Theta) e^{-q\Delta_t} + \Theta \right) \right] + (S_{i+1} + S_{i-1}) \left[\frac{1}{2} \alpha \hat{v}_{i,j} \left((1 - \Theta) e^{-q\Delta_t} + \Theta \right) \right] \\ & + (S_{i+1} - S_{i-1}) \left[\frac{1}{2} \alpha \Delta_x \hat{b}_{i,j} \left((1 - \Theta) e^{-q\Delta_t} + \Theta \right) \right] = 0 \quad i = 1, \dots, N, \quad j = 0, \dots, M \end{aligned} \quad (6.38)$$

Now, since

$$S_{i+l} + S_{i-l} = S_i e^{A_x} + S_i e^{-A_x} = 2S_i \cosh \Delta_x, \quad S_{i+l} - S_{i-l} = S_i e^{A_x} - S_i e^{-A_x} = 2S_i \sinh \Delta_x \quad (6.39)$$

Formula (6.38) can also be written as:

$$\frac{1 - e^{-q\Delta_t} (1 + r\Delta_t)}{(1 - \Theta)e^{-q\Delta_t} + \Theta} + \alpha \hat{v}_{i,j} (\cosh \Delta_x - 1) + \alpha \hat{b}_{i,j} \Delta_x \sinh \Delta_x = 0 \quad (6.40)$$

Using the fact that:

$$\tanh \frac{1}{2} \Delta_x = \frac{\cosh \Delta_x - 1}{\sinh \Delta_x},$$

equation (6.40) can be solved to yield:

$$\hat{b}_{i,j} = \frac{\Delta_x}{\Delta_t \sinh \Delta_x} \left(\frac{e^{r\Delta_t} - e^{q\Delta_t}}{(1 - \Theta) + \Theta e^{q\Delta_t}} \right) - \frac{\hat{v}_{i,j}}{\Delta_x} \tanh \frac{\Delta_x}{2} \quad (6.41)$$

Now that a solution for $b_{i,j}$ is found, we find out what happens as Δ_x and Δ_t go to zero.

first we take the limit of $\hat{b}_{i,j}$ as Δ_x goes to zero:

$$\lim_{\Delta_x \rightarrow 0} \hat{b}_{i,j} = \frac{1}{\Delta_t} \left(\frac{e^{r\Delta_t} - e^{q\Delta_t}}{(1 - \Theta) + \Theta e^{q\Delta_t}} \right) \lim_{\Delta_x \rightarrow 0} \frac{\Delta_x}{\sinh \Delta_x} - \hat{v}_{i,j} \lim_{\Delta_x \rightarrow 0} \frac{\tanh \frac{\Delta_x}{2}}{\Delta_x}$$

The first limit of the right-hand-side is:

$$\lim_{\Delta_x \rightarrow 0} \frac{\Delta_x}{\sinh \Delta_x} = 1$$

Next we evaluate the second limit of the equation:

$$\lim_{\Delta_x \rightarrow 0} \frac{\tanh \frac{\Delta_x}{2}}{\Delta_x} = \frac{1}{2}$$

Therefore, we have the following relation:

$$\lim_{\Delta_x \rightarrow 0} \hat{b}_{i,j} = \frac{1}{\Delta_t} \left(\frac{e^{r\Delta_t} - e^{q\Delta_t}}{(1 - \Theta) + \Theta e^{q\Delta_t}} \right) - \frac{1}{2} \hat{v}_{i,j}$$

Next, we take the limit of the expression above as Δ_t goes to zero:

$$\lim_{\Delta_x \rightarrow 0, \Delta_t \rightarrow 0} \hat{b}_{i,j} = \frac{e^{r\Delta_t} - e^{q\Delta_t}}{\Delta_t} - \frac{1}{2} \hat{v}_{i,j} = re^{r\Delta_t} - qe^{q\Delta_t} - \frac{1}{2} \hat{v}_{i,j} = r - q - \frac{1}{2} \hat{v}_{i,j}$$

Where the rule of l'hospital was used again. This expression is the same as derived above for the continuous time, as it should be. Now, once the values of the local volatilities are chosen, the values for $\hat{b}_{i,j}$ follow immediately and the finite difference algorithm can be applied.

Fitting European call options

Now that we have determined $\hat{b}_{i,j}$ the next step will be to solve for $v_{i,j}$. Therefore we assume the existence of observable market prices for European call options, with strike prices and time-to-maturities consistent with all the nodes in the grid. The solution for the local volatilities is derived in two steps. First European call prices at any particular time can be translated to Arrow-Debreu prices at that time. After that the discretization scheme of Arrow-Debreu securities can be used to solve the local volatilities for all the nodes.

Let $C_{i,j}$ denote a European call option with strike price $S_i = e^{x_i}$ and time to maturity $t_j = j\Delta_t$, where i ranges from 1 to N and j ranges from 1 to $M+1$. Let $A_{ini}^{i,j}$ denote the value of an Arrow-Debreu security, so $A_{ini}^{i,j}$ denotes the time 0 price of a security that pays 1 if $S_i = e^{x_i}$ is reached at time t_j . For this reason, Arrow-Debreu securities are also contingent claims on the same underlying. Using arbitrage arguments, it is easy to show that the values of Arrow-Debreu securities satisfy the following constraints:

$$\sum_{i=0}^{N+1} A_{ini}^{i,j} = e^{-rt_j}, \tag{6.42}$$

$$\sum_{i=0}^{N+1} A_{ini}^{i,j} S_{i,j} = S_{ini} e^{-qt_j} \tag{6.43}$$

The first summation can be seen as the value of a contract that pays 1 at time t_j , no matter what the value of the underlying will be at that time. It thus follows that the value should be e^{-rt_j} . The summation in (6.43) can be seen as the value of a contract that pays out the stock value at time t_j . It thus follows that this value must be equal to $S_{ini} e^{-qt_j}$. Further, when $j = 0$, $A_{ini}^{i,j}$ is of course 1 if $i = \beta$ and 0 else. It can be seen that the value of a call option will be priced by the finite difference method with the following formula:

$$C_{i,j} = \sum_{k=i+1}^{N+1} A_{ini}^{k,j} (S_k - S_i) \quad i = 1, \dots, N, \quad j = 0, \dots, M + 1. \tag{6.44}$$

Formula (6.44) is quite similar to formulas for options used when building implied tree models. When using formulas (6.42) and (6.43) in combination with (6.44) it can be

shown that for $i = N+1$ and for $i = 0$, the following values for the options will have to be taken:

$$C_{N+1,j} = 0 \quad j = 0, \dots, M+1$$

$$C_{0,j} = S_{ini} e^{-qt_j} - S_0 e^{-rt_j} \quad j = 0, \dots, M+1$$

Formula (6.44) can be solved for $A_{ini}^{i,j}$. This yields the following relation:

$$A_{ini}^{i,j} = \frac{(S_i - S_{i-1})C_{i+1,j} - (S_{i+1} - S_{i-1})C_{i,j} + (S_{i+1} - S_i)C_{i-1,j}}{(S_{i+1} - S_i)(S_i - S_{i-1})} \quad (6.45)$$

Next, let $A_{i,j}^{k,l}$ (where $l \geq j$) denote the value of an Arrow-Debreu security, observed at node (i, j) that pays 1 if and only if node (k, l) is reached. As already mentioned, Arrow-Debreu securities are contingent claims on S , so formula (6.35) can again be used.

$$(e^{r\Delta} \mathbf{I} - (I - \Theta)\mathbf{M}_j) \mathbf{A}_j^{k,j+1} = (\Theta \mathbf{M}_j + \mathbf{I}) \mathbf{A}_{j+1}^{k,j+1} + \mathbf{B}_j^k \quad j = 0, \dots, M, \quad k = 1, \dots, N \quad (6.46)$$

where we have:

$$\mathbf{A}_j^{k,j+1} \equiv \begin{bmatrix} \mathbf{A}_{1,j}^{k,j+1} \\ \vdots \\ \mathbf{A}_{N,j}^{k,j+1} \end{bmatrix}, \quad \mathbf{B}_j^k = \begin{bmatrix} l_{1,j} \left((I - \Theta) \mathbf{A}_{0,j}^{k,j+1} + \Theta \mathbf{A}_{0,j+1}^{k,j+1} \right) \\ 0 \\ \vdots \\ 0 \\ u_{N,j} \left((I - \Theta) \mathbf{A}_{N+1,j}^{k,j+1} + \Theta \mathbf{A}_{N+1,j+1}^{k,j+1} \right) \end{bmatrix}$$

The vector $\mathbf{A}_{j+1}^{k,j+1}$ is of course a vector with 1 on the k -th place and 0 for all other places. When we assume the boundaries are absorbing, then it follows that $A_{0,j}^{k,l} = e^{-r(t_l - t_j)}$ for $k = 0$ and $A_{0,j}^{k,l} = 0$ for all other k . The same relation holds for $A_{N+1,j}^{k,l}$. When using this assumption of absorbing boundaries, it follows that $\mathbf{B}_j^k = \mathbf{0}$ for $k = 1, \dots, N$. Since (6.46) holds for $k = 1, \dots, N$, equation (6.46) can also be written with the use of matrices $\mathbf{A}_j^{j+1} = [\mathbf{A}_j^{1,j+1}, \dots, \mathbf{A}_j^{N,j+1}]$, $\mathbf{A}_{j+1}^{j+1} = [\mathbf{A}_{j+1}^{1,j+1}, \dots, \mathbf{A}_{j+1}^{N,j+1}]$ and $\mathbf{B}_j = [\mathbf{B}_j^1, \dots, \mathbf{B}_j^N]$, instead of $\mathbf{A}_j^{k,j+1}$, $\mathbf{A}_{j+1}^{k,j+1}$ and \mathbf{B}_j^k , respectively. Where the second matrix is of course the $N \times N$ identity matrix and \mathbf{B}_j the zero matrix. With this notation, equation (6.46) can be written as the following equation, assuming $\Theta \neq I$.

$$\mathbf{A}_j^{j+1} = \frac{-\Theta}{1-\Theta} \mathbf{I} + \left(e^{r\Delta} \mathbf{I} - (1-\Theta) \mathbf{M}_j \right)^{-1} \left(\mathbf{I} \frac{\Theta e^{r\Delta} + (1-\Theta)}{1-\Theta} \right) \quad (6.47)$$

From the assumption of absorbing boundaries it follows that the next relation for the Arrow-Debreu prices must hold:

$$\left(\mathbf{A}_{ini}^{j+1} \right)^T = \left(\mathbf{A}_{ini}^j \right)^T \mathbf{A}_j^{j+1} \quad (6.48)$$

where \mathbf{A}_{ini}^j is a vector containing the Arrow-Debreu security prices, observed at time zero.

Now equation (6.47) can be written in terms of $\left(\mathbf{A}_{ini}^{j+1} \right)^T$, by simply pre-multiplying both sides of the equation with $\left(\mathbf{A}_{ini}^j \right)^T$. Since equation (6.45) shows how to compute the vector $\left(\mathbf{A}_{ini}^j \right)^T$ for all j , all the terms of the equation are known, except for the matrix \mathbf{M}_j , which depends on the unknown node volatilities. To solve these node volatilities \mathbf{M}_j can be written as:

$$\left(\mathbf{M}_j \right)^T = \begin{bmatrix} -\alpha \hat{v}_{1,j} & U \hat{v}_{2,j} & 0 & 0 & \dots & 0 \\ L \hat{v}_{1,j} & -\alpha \hat{v}_{2,j} & U \hat{v}_{3,j} & 0 & \dots & 0 \\ 0 & L \hat{v}_{2,j} & -\alpha \hat{v}_{3,j} & U \hat{v}_{4,j} & \dots & 0 \\ \vdots & \vdots & \vdots & \vdots & \vdots & 0 \\ 0 & 0 & \dots & L \hat{v}_{N-2,j} & -\alpha \hat{v}_{N-1,j} & U \hat{v}_{N,j} \\ 0 & 0 & 0 & 0 & L \hat{v}_{N-1,j} & -\alpha \hat{v}_{N,j} \end{bmatrix} + \begin{bmatrix} 0 & -\lambda & 0 & 0 & \dots & 0 \\ \lambda & 0 & -\lambda & 0 & \dots & 0 \\ 0 & \lambda & 0 & -\lambda & \dots & 0 \\ \vdots & \vdots & \vdots & \vdots & \vdots & 0 \\ 0 & 0 & \dots & \lambda & 0 & -\lambda \\ 0 & 0 & \dots & 0 & \lambda & 0 \end{bmatrix} = \mathbf{V}_j + \Lambda$$

Where

$$U = \frac{1}{2} \alpha \left(1 + \tanh \frac{1}{2} \Delta_x \right) \quad L = \frac{1}{2} \alpha \left(1 - \tanh \frac{1}{2} \Delta_x \right)$$

$$\lambda = \frac{1}{2 \sinh \Delta_x} \left(\frac{e^{r\Delta} - e^{q\Delta}}{(1-\Theta) + \Theta e^{q\Delta}} \right)$$

When this equation for M_j is combined with equation (6.47) written in terms of $(A_{ini}^{j+1})^T$, the following relation can be found after some manipulations:

$$\Psi_j \hat{v}_j = (e^{r\Delta t} A_{ini}^{j+1} - A_{ini}^j) - \Lambda_j \bar{A}_{ini}^j \quad (6.49)$$

where:

$$\bar{A}_{ini}^j = (1 - \Theta) A_{ini}^{j+1} + \Theta A_{ini}^j$$

and

$$\Psi_j = \begin{bmatrix} -\alpha \bar{A}_{ini}^{1,j} & U \bar{A}_{ini}^{2,j} & 0 & 0 & \dots & 0 \\ L \bar{A}_{ini}^{1,j} & -\alpha \bar{A}_{ini}^{2,j} & U \bar{A}_{ini}^{3,j} & 0 & \dots & 0 \\ 0 & L \bar{A}_{ini}^{2,j} & -\alpha \bar{A}_{ini}^{3,j} & U \bar{A}_{ini}^{4,j} & \dots & 0 \\ 0 & 0 & \vdots & \vdots & \vdots & 0 \\ \vdots & \vdots & \vdots & L \bar{A}_{ini}^{N-2,j} & -\alpha \bar{A}_{ini}^{N-1,j} & U \bar{A}_{ini}^{N,j} \\ 0 & 0 & \dots & 0 & L \bar{A}_{ini}^{N-1,j} & -\alpha \bar{A}_{ini}^{N,j} \end{bmatrix}$$

Now the local volatilities can be found, by solving equation (6.49). Notice that the matrix, Ψ_j from equation (6.49), is also tridiagonal, making a numerical procedure to solve the equation very fast. Some problems may arise when trying to solve this system for low values of j , i.e. when calculating the local volatilities for nodes close to time zero. This problem can be overcome by truncating the grid to the statistically significant part. For example, one can use only nodes $\beta - q, \dots, \beta + q$ for some integer q , which should depend on the time-step. The local volatilities for the other nodes can be set to some properly chosen value, for instance the instantaneous volatility at those points. It may be preferred to use successive over-relaxation, SOR, to solve for the v_j 's. Appendix E gives a discussion on SOR. With this method it is possible to restrict the values for v_j to fall in some interval. In this way negative values for the volatilities will never arise. However the answer does not exactly satisfy (6.49). Andersen and Brotherton-Ratcliffe propose to minimise the square of the right-hand-side of (6.49) using Lemke's method, with the restriction that v falls within a certain range.

So before being able to use the method of finite differences with local volatilities, one first has to calculate the Arrow-Debreu prices for every time-step j , given the market prices of European call options on every node in the grid. Given these values of the Arrow-Debreu securities, Ψ_j and the right-hand-side of (6.49) can be created for all j . Finally the vector \hat{v}_j can be solved from the equation. This vector \hat{v}_j contains the local volatilities for all nodes at time t_j . When the local volatilities are solved for, the values for \hat{b}_j follow from formula (6.41) and the method of finite differences can next be applied to value all kinds of contingent claims, consistent with the given volatility surface.

Stability

Appendix F gives a von Neumann stability analysis for this finite difference method. It is shown that the method is unconditionally stable when the vectors \hat{v}_j contain only non-negative values and $\Theta \leq \frac{1}{2}$.

6.5 Implied Monte Carlo simulation

The theory of derivative valuation is based on the random walk assumption of asset prices. In chapter 4, it was shown that derivatives can be valued, using the expected payoff of the derivative under a risk-neutral process of the underlying. This means that one can use the Monte Carlo simulation techniques to value derivatives. This section shows how the price process of an asset can be simulated in the presence of a volatility structure and how we can get the value of an option from a number of simulations.

Simulating a price path

In chapter 3 we have seen the stochastic process for the underlying asset that can be used when volatility is assumed to be a function of the price of the underlying asset and time. In a risk-neutral world this process looks as follows:

$$dS = (r - q)Sdt + \sigma(S, t)SdW \quad (6.50)$$

where $\sigma(S, t)$ is the instantaneous volatility, at time t when the underlying is at S . The formula that derives this instantaneous volatility from market prices of European call options was given in chapter 5. Applying Ito's lemma to $\ln(S_t)$, we get:

$$d \ln(S) = \left(r - q - \frac{1}{2} \sigma^2(S, t) \right) dt + \sigma(S, t) dW \quad (6.51)$$

Now, under the assumption that $\sigma(S, t)$ is constant over a small time-step Δt , the expression above can be integrated exactly to give:

$$S_{t+\Delta t} = S_t \exp \left\{ \left(r - q - \frac{1}{2} \sigma^2(S_t, t) \right) \Delta t + \sigma(S_t, t) \sqrt{\Delta t} \phi \right\} \quad (6.52)$$

where ϕ is drawn from a standardized normal distribution. When working with a constant volatility, the term Δt can be set to any value without creating errors. In this case however, we work with the instantaneous volatility so (6.52) is only true in the limit

as Δt goes to zero. With this formula we can now simulate an entire price path, given the initial value of the asset. The algorithm looks as follows, starting from $t = 0$ and $S_t = S_0$:

- calculate $\sigma(S, t)$ (6.53)
- generate a random variable ϕ from a standardized normal distribution
- calculate $S_{t+\Delta t}$ from (6.52)
- set t to $t + \Delta t$

These steps are repeated until finally S_T is calculated, where T denotes the maturity of the derivative that needs to be valued. After simulating a price path, the value of a European derivative is easily calculated. One just needs the payoff function to determine the value of the derivative given this price path. For instance when valuing a plain vanilla call option we have:

$$C_{\text{payoff}}(S) = \max(S_T - K, 0) \tag{6.54}$$

where $C_{\text{payoff}}(S)$ is the value of the option at time T , given that the process of the underlying is S . K denotes the strike of the option. Another example is an up-and-in barrier option, with barrier B :

$$C_{\text{ui payoff}}(S) = \begin{cases} \max(S_T - K, 0) & \text{if } S_t \geq B, \text{ for some } t \in [0, T] \\ 0 & \text{else} \end{cases} \tag{6.55}$$

Now from risk-neutral valuation we have for European type derivatives:

$$V(S) = e^{-rT} E(V_{\text{payoff}}(S)) \tag{6.56}$$

where V is the value of the underlying at time $t = 0$ and V_{payoff} the value, or payoff, of the derivative at time T , given price path S . From this it follows that one can approximate the value of the derivative by simply averaging the values corresponding to a number of simulated paths and multiplying this with the appropriate discount factor, i.e.:

$$V \approx e^{-rT} \frac{1}{n} \sum_{i=1}^n V_{\text{payoff}}(S^i) \tag{6.57}$$

where price paths $S^i, i = 1, \dots, n$, can be simulated using the algorithm in (6.53). Unfortunately a lot of price path simulations are needed to get good results. There are some techniques to speed up convergence, such as the antithetic variable technique. With this technique one samples two price paths, one based on ϕ and one based on $-\phi$. This works because of the symmetry in the normal distribution. More on speeding up convergence can be found in Press et al. (1992).

6.6 Implied Trinomial tree with stochastic volatility

This section discusses the algorithm derived by Britten-Jones and Neuberger. They relax the assumption of a deterministic volatility and show how an arbitrary volatility process can be adjusted to fit the market values of European options exactly. The first part shows a condition that characterises all arbitrage free price processes, consistent with the market values of European option prices. In the second part the algorithm is discussed for the case of zero interest rate and no dividend yield. Next it will be discussed how non-zero interest rates and dividend yields can be incorporated in the model. After that it will be shown that the Derman, Kani and Chriss implied trinomial tree model is a special case of the model discussed here. Finally some restrictions will be derived, which are necessary to avoid negative transition probabilities.

Conditional volatility

First a time-price grid is constructed, in much the same way as is done in a trinomial tree. Let T denote the maximum value of time that is used in the grid. Assume there are N steps in the time direction, so with $\Delta t = \frac{T}{N}$ we have $t \in \mathbf{T} = \{0, \Delta t, 2\Delta t, 3\Delta t, \dots, T\}$. Further let S_0 denote the initial price of the underlying. Let \mathbf{K} denote the set of possible values of the underlying asset, at any time. Define \mathbf{K} as the set: $\mathbf{K} = \{K : K = S_0 u^i, i = -M, \dots, 0, \dots, M\}$, where $u > 1$. Further assume that the price of the underlying asset can move from some $K \in \mathbf{K}$ to Ku , K , or K/u , this grid can thus be seen as a trinomial tree. Assume also that a complete set of European option prices $C(t, K)$, with time to maturity $t \in \mathbf{T}$ and strike $K \in \mathbf{K}$ are given. As mentioned before, this may require interpolation and extrapolation techniques. For now it is assumed that interest rates and dividend yields are equal to zero. Later in this section, it is shown how non-zero interest rates and dividend yields can be dealt with.

Now since the price of a European call option must equal the expected value of its payoff, we have:

$$C(t, K) = E[\max(S_t - K, 0)] \quad (6.58)$$

As was shown in chapter 5, the risk-neutral probability can be found by taking the second derivative of the call option, with respect to the strike. The discrete counterpart of this, is given in the following formula:

$$\pi(t, K) \equiv Pr\{S_t = K\} = E[\mathbf{1}_{S_t=K}] = \frac{C(t, Ku) - (1+u)C(t, K) + uC(t, K/u)}{K(u-1)} \quad (6.59)$$

Where $\mathbf{1}$ is the indicator function. The validity of (6.59) can be seen by observing the option position given in the numerator of (6.59). This position pays off $K(u-1)$ if $S_t = K$ and pays off zero for all $S_t \neq K$, from (6.58) it then follows. It is a special case

of formula (6.45), where no particular spacing between the nodes is assumed. Since it is assumed that both interest rates and dividend yields are zero, $\pi(t, K)$ is in this case equal to the price of the Arrow-Debreu security at that node. To derive the conditional probability of an up-move, consider the following position:

- long I European call option with strike K and expiration $t + \Delta t$
- short I European call option with strike K and expiration t

At time t , if $S_t > K$ the short call will be exercised. If this happens, short the stock and invest the proceeds in the riskless asset. At time $t + \Delta t$ the position is closed. Now it can be seen that this strategy only has a non-zero payoff, when $S_t = K$ and $S_{t+\Delta t} = Ku$. In this situation the payoff at $t + \Delta t$ will be $Ku - K$. In all other situations the payoff will be zero. This follows from the fact that we have assumed that the underlying asset can only move up or down one level, or stays the same from time t to $t + \Delta t$. Now since the cost of this position should equal the expected payoff of the strategy, the following relation can be derived:

$$Pr\{S_{t+\Delta t} = Ku \text{ and } S_t = K\}(Ku - K) = C(t + \Delta t, K) - C(t, K) \quad (6.60)$$

Now, the law of conditional probability implies that:

$$Pr\{S_{t+\Delta t} = Ku / S_t = K\} = \frac{Pr\{S_{t+\Delta t} = Ku \text{ and } S_t = K\}}{Pr\{S_t = K\}} \quad (6.61)$$

Substituting for both terms of the right-hand-side with formulae (6.59) and (6.60) it follows that:

$$Pr\{S_{t+\Delta t} = Ku / S_t = K\} = \frac{C(t + \Delta t, K) - C(t, K)}{C(t, Ku) - (I + u)C(t, K) + uC(t, K/u)} \quad (6.62)$$

Next, for brevity we introduce $\lambda(t, K)$:

$$\lambda(t, K) \equiv \frac{I}{\Delta t} \frac{C(t + \Delta t, K) - C(t, K)}{C(t, Ku) - (I + u)C(t, K) + uC(t, K/u)} \quad (6.63)$$

With the risk-neutrality condition and the fact that the conditional probabilities must sum to one, the conditional probabilities of a down move and no change, follow:

$$Pr\{S_{t+\Delta t} = \hat{K} / S_t = K\} = \begin{cases} \Delta t \lambda(t, K) & \text{if } \hat{K} = Ku \\ 1 - (I + u)\Delta t \lambda(t, K) & \text{if } \hat{K} = K \\ u\Delta t \lambda(t, K) & \text{if } \hat{K} = K/u \end{cases} \quad (6.64)$$

Equipped with this formula, it is easily seen that the formula for the expectation of squared returns, conditional on the price of the underlying and time is given by:

$$E \left[\left(\frac{S_{t+\Delta t} - S_t}{S_t} \right)^2 \mid S_t = K \right] = \Delta t \lambda(t, K) (u - 1) \left(u - \frac{1}{u}\right) \quad (6.65)$$

It is interesting to see that in the right-hand-side of (6.65) we have after some manipulations:

$$\lambda(t, K) (u - 1) \left(u - \frac{1}{u}\right) \approx \frac{2 \frac{\partial C}{\partial t}}{K^2 \frac{\partial^2 C}{\partial K^2}} \quad (6.66)$$

With equality in the limit, as both Δt and $u - 1$ go to zero from above. The right-hand-side of (6.66) is the formula for the instantaneous volatility, when the interest rate and dividend yield are both equal to zero.

Next, it can be shown inductively that any process that satisfies (6.65) will correctly price all European options $C(t, K)$ with $t \in T$ and $K \in K$. To prove this, consider any process that satisfies (6.65). Denote the price of European call options under this process as $\tilde{C}(t, K)$. Obviously $\tilde{C}(0, K)$ must equal $C(0, K)$, since they both equal the payoff, which is given at time 0. Now suppose that the process prices all European options correctly up to time t , or $\tilde{C}(t, K) = C(t, K)$, it follows that:

$$\tilde{C}(t + \Delta t, K) = \tilde{C}(t, K) + Pr\{S_{t+\Delta t} = Ku \mid S_t = K\} Pr\{S_t = K\} (Ku - K) \quad (6.67)$$

Substituting the values in formulae (6.59) and (6.61) yields:

$$\tilde{C}(t + \Delta t, K) = \tilde{C}(t, K) + C(t + \Delta t, K) - C(t, K) = C(t + \Delta t, K) \quad (6.68)$$

This can be easily seen, by noticing that the product of the two probabilities in (6.67) is given by the probability in (6.60). The next section shows how a given base model of volatility can be adjusted to fit the pre-specified set of European option prices exactly, by using condition (6.65).

The model

To be able to incorporate different base models of volatility a discrete framework for the volatility is needed. We therefore use Markovian volatility processes. Suppose there are L volatility states $\mathbf{Z} = \{1, 2, \dots, L\}$. Next let $P = \{p_{ij}\}$ denote the $L \times L$ matrix with transition probabilities, where:

$$p_{ij} \equiv \Pr\{Z_{t+\Delta t} = i | Z_t = j\} \quad (6.69)$$

Further let $v(\mathbf{Z})$, $\mathbf{Z} \in \mathbf{Z}$ denote the different volatility states. Now P and $v(\dots)$ can be chosen to get the desired base model of volatility. When $L = 1$, we end up with a deterministic model for volatility. Next it is assumed that

$$\Pr\{S_{t+\Delta t} = Ku | S_t = K, Z_t = z\} = q(t, K)v(z)\Delta t \quad (6.70)$$

where $q(t, K)$ is some adjustment that will be calibrated to fit initial option prices. It can be shown that equation (6.65) is satisfied if adjustments satisfy the following condition:

$$\lambda(t, K)\pi(t, K) = q(t, K) \sum_{z=1}^L v(z)\pi(t, K, z) \quad (6.71)$$

Where $\pi(t, K, z) \equiv \Pr\{S_t = K \text{ and } Z_t = z\}$. Since it is assumed that the underlying asset can only go up, down or stay the same during one time period, it follows that $\pi(t, K, z) = 0$, for all $K = S_0 u^i$, with $|i| > t / \Delta t$. In order to solve for the values of $q(t, K)$, a two-step algorithm that moves forward to the tree can be used. Suppose that $\pi(t, K, z)$ and $q(t, K)$ are already determined for all price levels K and volatility states z up to time t . Calculate:

$$\pi(t + \Delta t, K, z) = \sum_{j=1}^L p_{zj} (A_j + B_j + C_j) \quad (6.72)$$

with:

$$\begin{aligned} A_j &\equiv [\Delta t q(t, K/u)v(j)]\pi(t, K/u, j) \\ B_j &\equiv [u\Delta t q(t, Ku)v(j)]\pi(t, Ku, j) \\ C_j &\equiv [1 - (1+u)\Delta t q(t, K)v(j)]\pi(t, K, j) \end{aligned} \quad (6.73)$$

This step follows from the Kolmogorov-Forward equation, which in the discrete case states that in order to reach node $(t + \Delta t, K)$ the path must go through one of the tree predecessors: $(t, K/u)$, (t, K) or (t, Ku) . The terms in brackets denote the up, down and middle transition probabilities for A, B and C, respectively. The formula is similar to formula (6.21). Next in the second step, $q(t, K)$ can be determined from formula (6.71):

$$q(t + \Delta t, K) = \frac{\lambda(t + \Delta t, K)\pi(t + \Delta t, K)}{\sum_{z=1}^L v(z)\pi(t + \Delta t, K, z)} \quad (6.74)$$

Where formulae (6.59) and (6.63) should be used for the terms in the numerator. The two steps can then be repeated. To initiate the algorithm one has to choose an initial volatility state, z_0 , and set $\pi(0, S_0, z_0) = 1$ and $q(0, S_0) = \lambda(0, S_0) / v(z_0)$. When this calibration algorithm is done, one can value all kinds of derivatives with this model, based on the following formula:

$$V(t - \Delta t, K, z) = \sum_{j=1}^L p_{jz} (D_j + E_j + F_j), \quad (6.75)$$

with:

$$\begin{aligned} D_j &\equiv [\Delta t q(t - \Delta t, K) v(z)] V(t, Ku, j) \\ E_j &\equiv [u \Delta t q(t - \Delta t, K) v(z)] V(t, K/u, j) \\ F_j &\equiv [1 - (1 + u) \Delta t q(t - \Delta t, K) v(z)] V(t, K, j) \end{aligned} \quad (6.76)$$

Where $V(t, K, z)$ is the value of the derivative, at node (t, K) for the volatility state z . For path-dependent derivatives such as American and barrier options, the usual restrictions should be used when calculating backwards through the grid.

When interest rates and dividend yields are non-zero

The algorithm explained in the previous section only works in the absence of interest rates and dividend yields. In this case the underlying asset follows a price process, which is a martingale. Now by standard pricing theory, see Harrison and Pliska (1981), we can write:

$$\frac{\tilde{C}(t, \tilde{K})}{e^{(r-q)t}} = e^{-rt} E[\max(S_t - K, 0)], \quad K = \frac{\tilde{K}}{e^{(r-q)t}}, \quad S_t = \frac{\tilde{S}_t}{e^{(r-q)t}} \quad (6.77)$$

Where the terms $\tilde{C}(\dots)$, \tilde{S}_t and \tilde{K} , denote prices in the presence of interest rates and dividend yields. This follows from the fact that the stock price divided by its forward follows a martingale process. The expectation term is just the price of the call option we need for the algorithm. The adjustments that have to be made are now easy to derive:

$$C(t, K) = \tilde{C}(t, \tilde{K}) e^{qt}, \quad \text{with } \tilde{K} = K e^{(r-q)t} \text{ and } \tilde{S} = S e^{(r-q)t} \quad (6.78)$$

With this formula the algorithm can now be used to construct the implied tree.

Relation with the Derman, Kani and Chriss model

To see that the Derman, Kani and Chriss (DKC) implied trinomial tree model can be seen as a special case of the model discussed here (NBJ), we consider a zero interest rate and no dividend yield. The DKC model assumes that volatility is not stochastic, this can be implemented in the NBJ model by taking L equal to 1 . The matrix of transition probabilities will then automatically be 1×1 with value 1 . Further it is of course assumed that both models use the same nodes. In the DKC model the transition probabilities for an up move can be calculated with the following formula for nodes above the centre of the tree:

$$Pu_{n,i} = \frac{e^{r\Delta t} C(S_{n+1,i+1}, t_{n+1}) - \sum_{j=i+1}^n \lambda_{n,j} (F_{n,j} - S_{n+1,i+1})}{\lambda_{n,i} (S_{n+1,i+2} - S_{n+1,i+1})} \quad (6.79)$$

Where in contrast to DKC, the index for the height in the tree, at time-step n , runs from $-n$ to n . Now, using the notation of NBJ, and the assumptions of zero interest rates and no dividend yield, this formula can be written as:

$$Pr\{S_{t+\Delta t} = Ku / S_t = K\} = \frac{C(t + \Delta t, K) - \sum_{j=i+1}^n \pi(t, S_0 u^j) (S_0 u^j - K)}{\pi(t, K) (Ku - K)}, \quad (6.80)$$

where $t = n\Delta t$ and $K = S_0 u^i$. The sum can be seen as the value of a call option with expiration t and strike K , given by the model built so far. Since the model was calibrated in the previous step to correctly price this call consistent with the market, it should be $C(t, K)$. Combining this with (6.59), we get:

$$Pr\{S_{t+\Delta t} = Ku / S_t = K\} = \frac{C(t + \Delta t, K) - C(t, K)}{C(t, Ku) - (1 + u)C(t, K) + uC(t, K/u)} \quad (6.81)$$

which equals (6.62). One should be careful for the nodes at the top and bottom of the tree at time $t + \Delta t$. For instance at the top of the tree the sum in (6.80) will equal zero, which of course is not equal to $C(t, K)$. If $C(t, K)$ is set zero at the highest node at time t and we set $C(t, K) = C(t, Ku) + (Ku - K)$ for the lowest node at time t , the equality between the up transition probabilities of both models will still hold. Further, in the DKC model we have the formula for the probability of a down move:

$$Pd_{n,i} = \frac{F_{n,i} - p_{n,i} (S_{n+1,i+2} - S_{n+1,i+1}) - S_{n+1,i+1}}{S_{n+1,i} - S_{n+1,i+1}} \quad (6.82)$$

which can be seen to equal $uPu_{n,i}$. Which is also true in the BJN model, as can be seen in (6.64). For the transition probabilities below and including the centre of the tree, the put-

call parity: $C - P = S - K$ can be used. It can also be shown that in the case of dividend yields and non-zero interest rates the DKC model equals the BJN model when the tree is chosen to grow along the forward rate. It should be noted that in the DKC model one must override the transition probabilities calculated by (6.79) and (6.82) whenever they are negative. If this happens, the model does not price that option consistent with the market. In this case the sum in (6.80) will not equal the market price of the option, $C(t, K)$. This will lead to a difference in both models. It thus can be expected that in case of differences, the method of DKC performs better, since it does not rely on a good calibration in the previous step.

Choosing a volatility process

As an example of a stochastic volatility process, we look at the Heston (1993) model, which was already discussed in chapter 3:

$$\begin{aligned} dS &= \mu S dt + \sigma S dW_s \\ d\sigma^2 &= \alpha(\beta - \sigma^2) dt + \xi \sigma dW_\sigma \end{aligned} \tag{6.83}$$

Where the Wiener processes have a correlation of ρ . We assume the following parameter values: $\alpha = 1$, $\beta = (0.25)^2$, $\xi = 0.6$ and $\rho = 0$. Thus the volatility is mean reverting with a mean of 25%. When using a tree with $\Delta t = 0.01$, this process can be approximated using the following transition-probability matrix:

t/t+h	1	0,81	0,64	0,49	0,36	0,25	0,16	0,09	0,04
1	0,974591	0,022826	0,002583	0	0	0	0	0	0
0,81	0,004426	0,965317	0,030257	0	0	0	0	0	0
0,64	0	0,008642	0,958311	0,033046	0	0	0	0	0
0,49	0	0	0,014077	0,948256	0,037666	0	0	0	0
0,36	0	0	0	0,02148	0,933147	0,045373	0	0	0
0,25	0	0	0	0	0,032242	0,909127	0,05863	0	0
0,16	0	0	0	0	0	0,049128	0,868368	0,082504	0
0,09	0	0	0	0	0	0	0,077848	0,796255	0,125897
0,04	0	0	0	0	0	0	0,004289	0,077855	0,917856

Table 6.1: An example of a transition-probability matrix.

Here the values along the sides denote the possible volatility states. This matrix is chosen such that it fits the first two moments of the volatility process:

$$\begin{aligned} E(\Delta\sigma^2) &= E(\sigma_{t+\Delta t}^2 - \sigma_t^2) = \alpha(\beta - \sigma_t^2)\Delta t \\ E((\Delta\sigma^2)^2) &= E((\sigma_{t+\Delta t}^2 - \sigma_t^2)^2) = \xi^2 \sigma_t^2 \Delta t \end{aligned} \tag{6.84}$$

When Δt changes, one can adjust the values off the diagonal with the same factor as the time change. The diagonal values can then be set by the restriction that the probabilities must sum to 1. It follows that Δt can not be too high, or else negative probabilities will arise. In case one wants a nonzero correlation, three different transition probability

matrices have to be used. One for every possible move of the stock price over a time-step. Other stochastic models can also be approximated by carefully choosing a transition-probability matrix. Britten-Jones and Neuberger show how Wiggins (1987) model can be approximated.

6.7 Continuous case

When the number of steps in an implied trinomial tree gets very large, it might be preferred to use the instantaneous volatility to determine the probabilities. In the implied tree the volatility over one time-step can be calculated using the following formula:

$$F_{n,i}^2 \sigma^2 \Delta t = Pu_{n,i} (S_{n+1,i+2} - F_{n,i})^2 + Pm_{n,i} (S_{n+1,i+1} - F_{n,i})^2 + Pd_{n,i} (S_{n+1,i} - F_{n,i})^2 \quad (6.85)$$

where $Pm_{n,i} = 1 - Pu_{n,i} - Pd_{n,i}$. Using the instantaneous volatility in (6.85) combined with the forward relation, one can solve for the transition probabilities. This yields:

$$\begin{aligned} Pd_{n,i} &= \frac{F_{n,i} - S_{n+1,i+1} - (F_{n,i}^2 \sigma_{n,i}^2 \Delta t) \xi}{S_{n+1,i} - S_{n+1,i+1} - ((S_{n+1,i} - F_{n,i})^2 - (S_{n+1,i+1} - F_{n,i})^2) \xi} \\ Pu_{n,i} &= \frac{F_{n,i} - S_{n+1,i+1} - Pd_{n,i} (S_{n+1,i} - S_{n+1,i+1})}{S_{n+1,i+2} - S_{n+1,i+1}} \end{aligned} \quad (6.86)$$

where,

$$\xi = \left(\frac{S_{n+1,i+2} - S_{n+1,i+1}}{(S_{n+1,i+2} - F_{n,i})^2 - (S_{n+1,i+1} - F_{n,i})^2} \right) \quad \sigma_{n,i}^2 = \sigma^2(S_{n,i}, n\Delta t)$$

In the implied tree of Britten-Jones and Neuberger, this can be incorporated by choosing the adjustment factor equal to:

$$q(t + \Delta t, K) = \frac{Pu_{n,i} \sum_{z=1}^L \pi(t + \Delta t, K, z)}{\Delta t \sum_{z=1}^L v(z) \pi(t + \Delta t, K, z)} \quad (6.87)$$

Where $Pu_{n,i}$ is given by (6.86). Using these formulae, one does not have to construct the tree starting from the root. One can just begin at the end of the tree and calculate backwards using the probabilities given in (6.86). In case negative probabilities arise one can use the methods described in (6.27) and (6.28) to adjust them. Another advantage is that the programming of this method does not require storage of the transition probabilities, making it possible to construct trees with a large number of steps. In the implied trinomial tree of Derman, Kani and Chriss, for instance, using a 1000-step tree

would require storage of about half a million up transition probabilities and the same amount of down transition probabilities.

7 Performance of the implied models

7.1 Introduction

Five different implied models were discussed in the previous chapter. Before applying these models to different kinds of exotic options, in this chapter we will look at the performance of these models. Given the volatility matrix shown in chapter 4 we investigate to what extent these models can price European options consistent with the observed market values. Further we look at the speed with which the prices generated by the model converge to the market values. Based on the performance of the models, we will select with which to price the exotic derivatives in the following chapter. Throughout this chapter we will assume a spot price of the underlying of 100 and a risk-free interest rate and dividend yield of 5% and 3%, respectively. For the market values we use the volatility matrix shown in table 4.1, combined with cubic splines for interpolation and extrapolation as discussed in appendix C.

7.2 Implied binomial tree

In theory the implied binomial tree should price a set of options consistent with their market values. The number of options used to calibrate the model increases with the number of steps in the tree. So one can expect that a standard option with any given strike and time to maturity will be priced more consistent with its market value, when the number of steps used in the tree is high. However, when constructing an implied binomial tree one has to adjust for negative transition probabilities. This will affect the performance of the model. One way to check the performance of the implied models, is to compare the market values of options, which are used as input for the model with the option values according to the model. We use the model of Derman and Kani (1994) with the modifications suggested by Barle and Cakici (1998).

Market values of European options corresponding with the volatility matrix are given in the shaded cells of table 7.1. The prices generated by the model with 500 steps can be found in the cells below them. From this table it can be seen that the implied binomial tree has some difficulties pricing options consistent with their market values. It seems that this model values options too low. The largest differences (in percentages) can be found for out-of-the-money options. Using the model without the modifications suggested by Barle and Cakici (1998) will worsen the results even more.

t/strike	85	90	95	100	105	110	115	120	130	140
0,175	15,2654	10,4337	5,76567	2,05143	0,321329	0,017254	0,005403	0,002379	0,000243	7,65E-05
	15,2661	10,4335	5,75849	2,05256	0,211562	0,000569	3,54E-08	1,46E-13	2,13E-28	1,5E-48
0,425	15,8392	11,2381	7,03704	3,63052	1,27316	0,319943	0,056263	0,026122	0,003684	0,001176
	15,829	11,2294	7,05565	3,55341	0,980781	0,054197	6,16E-05	2,12E-09	5,28E-22	1,68E-39
0,695	16,516	12,197	8,28259	5,00966	2,41468	0,826052	0,249063	0,076066	0,008686	0,002947
	16,4009	12,062	8,10066	4,69688	1,9762	0,399964	0,009087	4,19E-06	9,94E-17	5,74E-32
0,94	17,1425	13,0256	9,32216	6,05618	3,50818	1,58424	0,623565	0,223836	0,020523	0,004998
	17,1131	12,9999	9,21442	5,78802	2,78862	0,830727	0,066364	0,000165	7,04E-14	6,83E-28
1	17,2957	13,2085	9,56074	6,30172	3,73359	1,78437	0,727431	0,266349	0,025468	0,005979
	17,2424	13,2019	9,52508	6,30339	3,62219	1,62328	0,55003	0,175167	0,016925	0,002705
1,5	18,4433	14,6369	11,1416	8,03592	5,39933	3,29924	1,91737	0,976988	0,214528	0,03216
	18,0802	14,1995	10,5997	7,32864	4,41925	2,15699	0,684128	0,061318	2,41E-08	1,99E-19
2	19,5032	15,8879	12,5455	9,5289	6,89175	4,73355	3,16767	1,88205	0,672753	0,194748
	19,1228	15,5099	12,1826	9,16289	6,46246	4,18224	2,46585	1,3074	0,295504	0,061299
3	21,2567	17,9116	14,8357	12,0151	9,47596	7,24087	5,44982	3,91413	2,01034	1,01878
	21,0329	17,7682	14,7037	11,8391	9,17083	6,71774	4,64343	2,99067	0,962198	0,192082
4	22,7053	19,596	16,7262	14,0645	11,6942	9,49325	7,60685	5,96693	3,58363	2,13184
	21,5856	18,5198	15,6428	12,9513	10,4417	8,11237	6,03024	4,25994	1,68177	0,360329
5	23,8921	21,058	18,3282	15,7657	13,5273	11,4879	9,57122	7,8526	5,29193	3,40811
	22,711	19,8063	17,0484	14,4306	11,9469	9,60242	7,41277	5,48627	2,4712	0,658526

Table 7.1: Input values compared with output values for the implied binomial model.

Another way to investigate the performance of the implied binomial tree is to look at the convergence of the prices to the market values, as the number of steps increases. With a given number of steps the model prices European options with strikes ranging from 40 to 200, with a spacing of 0.5. Time-to-maturities are ranging from 0.1 to 4.6, with spacing 0.5. This yields a total of 3210 options. For every option the difference with the market value is calculated. With this dataset we can calculate the mean absolute difference, the mean difference, the variance of the errors and the maximum and minimum differences. The figure below shows the results for the implied binomial tree with the modifications:

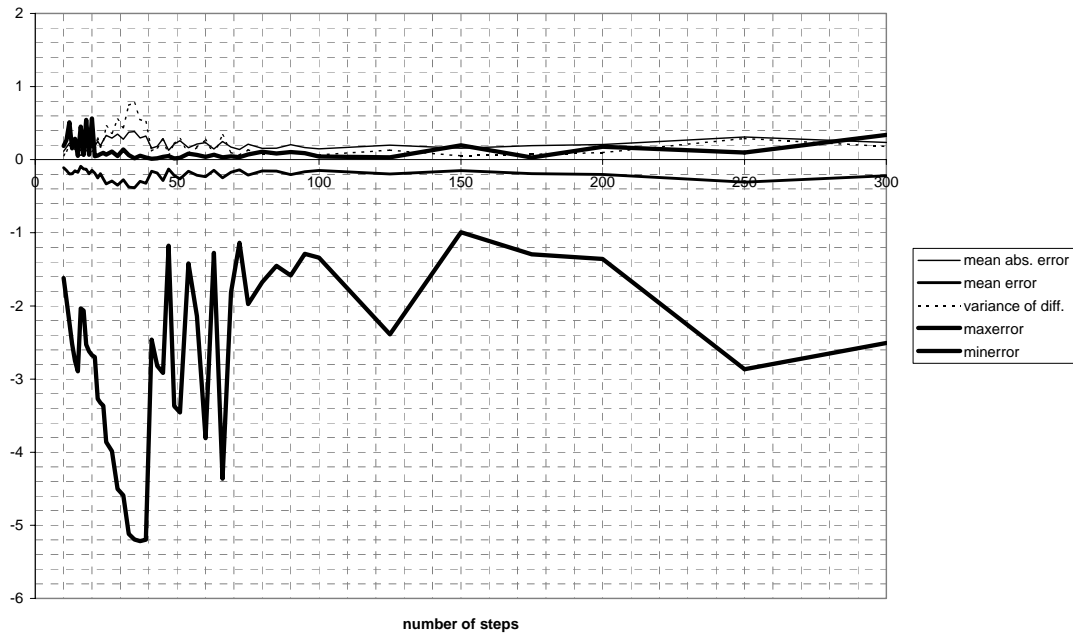


Figure 7.1: Convergence of performance measures of the implied binomial tree.

From this figure it can be seen that the performance of the model does not seem to improve when the number of steps is increased. The mean error lies somewhere around -0.2 , indicating that the model gives too low prices relative to the market values. This was also the case in table 7.1.

7.3 Implied trinomial tree

Using the same arguments as in the previous section, one can expect that any European option will be priced consistent with its market value, as the number of steps used in the implied trinomial tree is high. However, negative transition probabilities have to be adjusted again. While discussing the implied trinomial tree in chapter 6, we have seen that there are more ways to adjust for negative transition probabilities. The two methods given in the previous chapter, (6.27) and (6.28) will be compared in this section. First we look at the prices generated by the models compared with the market values. Again we use a 500-step tree. The shaded cells contain the market values of the options. The cells directly below them result from using the implied trinomial tree with (6.27). Every third row results from using (6.28) to adjust negative transition probabilities.

t/strike	85	90	95	100	105	110	115	120	130	140
0,175	15,2654	10,4337	5,76567	2,05143	0,321329	0,017254	0,005403	0,002379	0,000243	7,65E-05
	15,2277	10,3525	5,75704	2,05143	0,323018	0,01744	0,002381	0,000281	2,26E-06	9,67E-09
	15,2542	10,4107	5,76648	2,05325	0,322928	0,017475	0,003728	0,000899	4,11E-05	1,44E-06
0,425	15,8392	11,2381	7,03704	3,63052	1,27316	0,319943	0,056263	0,026122	0,003684	0,001176
	15,689	11,1491	7,03708	3,63052	1,27757	0,32024	0,056564	0,023852	0,003693	0,000413
	15,8227	11,2389	7,03826	3,63175	1,27817	0,320759	0,056389	0,025623	0,003703	0,001176
0,695	16,516	12,197	8,28259	5,00966	2,41468	0,826052	0,249063	0,076066	0,008686	0,002947
	16,3064	12,0713	8,27246	5,00966	2,4181	0,829747	0,24944	0,076731	0,008704	0,002526
	16,5097	12,1981	8,28285	5,01222	2,41843	0,831027	0,251076	0,076119	0,008756	0,00295
0,94	17,1425	13,0256	9,32216	6,05618	3,50818	1,58424	0,623565	0,223836	0,020523	0,004998
	16,8883	12,8568	9,22764	6,05618	3,51076	1,59012	0,625634	0,225217	0,020662	0,005001
	17,1431	13,0279	9,32381	6,06038	3,51004	1,58547	0,625313	0,224154	0,020825	0,005008
1	17,2957	13,2085	9,56074	6,30172	3,73359	1,78437	0,727431	0,266349	0,025468	0,005979
	17,0306	13,0401	9,44627	6,30172	3,73638	1,79227	0,732222	0,268111	0,025852	0,00598
	17,2948	13,2101	9,56196	6,30544	3,73653	1,79074	0,731701	0,268664	0,025866	0,005993
1,5	18,4433	14,6369	11,1416	8,03592	5,39933	3,29924	1,91737	0,976988	0,214528	0,03216
	18,1525	14,4402	11,0628	8,03592	5,40401	3,30137	1,91985	0,982188	0,215232	0,032778
	18,4434	14,6381	11,1426	8,03869	5,40384	3,30648	1,91746	0,97916	0,215087	0,03268
2	19,5032	15,8879	12,5455	9,5289	6,89175	4,73355	3,16767	1,88205	0,672753	0,194748
	19,1613	15,6463	12,425	9,50848	6,89357	4,73404	3,16865	1,89361	0,675394	0,19615
	19,5043	15,8895	12,5481	9,53371	6,8976	4,74487	3,16908	1,88302	0,673018	0,196538
3	21,2567	17,9116	14,8357	12,0151	9,47596	7,24087	5,44982	3,91413	2,01034	1,01878
	20,8906	17,6758	14,7016	11,9691	9,48107	7,24494	5,45224	3,9267	2,01671	1,02246
	21,2582	17,9164	14,8388	12,017	9,48104	7,24825	5,45137	3,92525	2,0165	1,02179
4	22,7053	19,596	16,7262	14,0645	11,6942	9,49325	7,60685	5,96693	3,58363	2,13184
	22,3169	19,3401	16,5689	14,0016	11,649	9,50223	7,6116	5,97247	3,59198	2,13204
	22,7056	19,6006	16,7281	14,0735	11,6963	9,5033	7,61276	5,97859	3,58808	2,13835
5	23,8921	21,058	18,3282	15,7657	13,5273	11,4879	9,57122	7,8526	5,29193	3,40811
	23,5242	20,7549	18,1647	15,7518	13,5287	11,4904	9,57857	7,86537	5,2987	3,41768
	23,8947	21,0596	18,3287	15,7662	13,5284	11,4903	9,5785	7,86567	5,29873	3,41774

Table 7.2: Input values compared with output values for the two alternative implied trinomial models.

From this table it can be seen that the implied trinomial model does a good job pricing options consistent with their market values. It is also clear from table 7.2 that negative transition probabilities can best be adjusted using (6.28). Applying (6.27) gives bad results for in-the-money options. For out-of-the-money options the differences between the two alternatives are very small.

We next look at the convergence of the implied trinomial tree. The same approach as given in the previous section is used to obtain some measures of the performance. When using the method proposed by Derman, Kani and Chriss (1996) to adjust negative transition probabilities, (6.27), the following figure results:

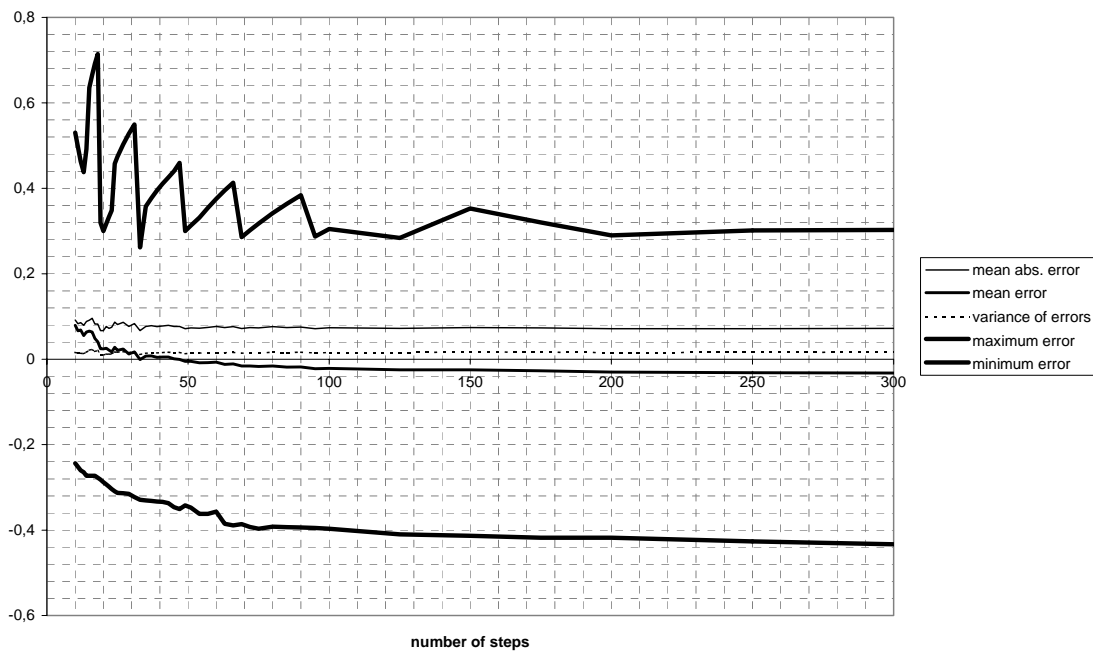


Figure 7.2: Convergence of performance measures of the implied trinomial tree, using (6.27).

This figure shows some improvement over the implied binomial tree. The mean error converges to about -0.04 , meaning that the implied trinomial tree prices options too low, with respect to their market values. On average the options priced with this model differ 0.08 from their market values. Further it is clear from figure 7.2 that the performance measures do not converge to zero. When using the other method, given in the previous section, to adjust negative probabilities the figure looks as follows:

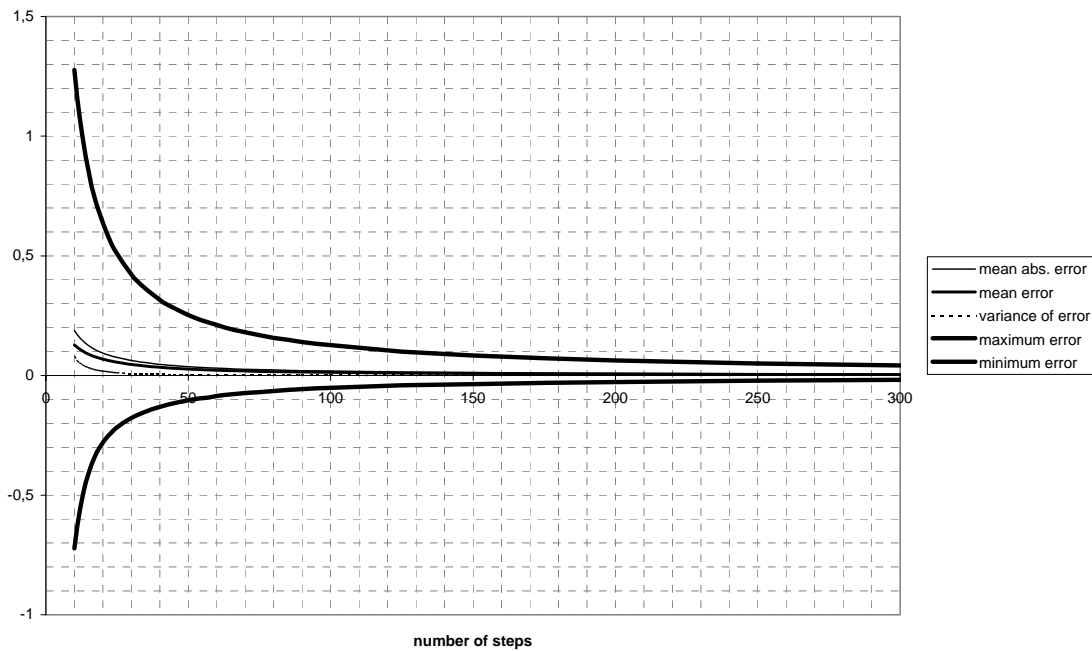


Figure 7.3: Convergence of performance measures of the implied trinomial tree, using (6.28)

This figure shows that the model has much better convergence properties when (6.28) is used instead of (6.27). All measures seem to converge to zero smoothly, as the number of steps used in the model increases. From figures 7.2 and 7.3 and table 7.2 it is clear that (6.28) is definitely preferred over (6.27).

7.4 Implied Finite differences

The previous chapter has discussed two alternatives for an implied finite difference scheme. One involves using the instantaneous volatility function, while the other approach suggested by Andersen and Brotherton-Ratcliffe (1998) was based on fitting market values of European options directly. As the number of grid-points increases, the two alternatives should give similar results. Here, we have used the Cranck-Nicholson scheme, or $\theta = \frac{1}{2}$, with a square 500×500 grid. In table 7.3, the results from both methods are compared with the input values of the options. The shaded cells are used for the market values of the options. Every second row gives the results from applying finite difference in combination with the forward volatility. Every third row gives the results when the method of Andersen and Brotherton-Ratcliffe (1998) is used.

t/strike	85	90	95	100	105	110	115	120	130	140
0,175	15,2654	10,4337	5,76567	2,05143	0,321329	0,017254	0,005403	0,002379	0,000243	7,65E-05
	15,2655	10,4335	5,76381	2,04679	0,323084	0,017731	0,00054	2,09E-06	3,63E-07	1,97E-07
	15,2619	10,4292	5,7601	2,04484	0,318791	0,012393	0,000511	7,96E-09	3,48E-09	2,47E-09
0,425	15,8392	11,2381	7,03704	3,63052	1,27316	0,319943	0,056263	0,026122	0,003684	0,001176
	15,8389	11,2377	7,03472	3,62811	1,27416	0,320175	0,054683	0,012254	0,002586	0,000644
	15,826	11,2232	7,01977	3,6116	1,25724	0,301075	0,037394	0,00918	0,000262	2,25E-06
0,695	16,516	12,197	8,28259	5,00966	2,41468	0,826052	0,249063	0,076066	0,008686	0,002947
	16,5156	12,1963	8,28068	5,00818	2,41414	0,825565	0,246447	0,071243	0,005776	0,001849
	16,5025	12,1816	8,26461	4,98986	2,3959	0,806331	0,229771	0,060338	0,003047	0,000637
0,94	17,1425	13,0256	9,32216	6,05618	3,50818	1,58424	0,623565	0,223836	0,020523	0,004998
	17,1421	13,0252	9,32052	6,0527	3,50579	1,58154	0,621377	0,220602	0,017399	0,003454
	17,1315	13,0131	9,30717	6,0396	3,49151	1,56836	0,608616	0,21146	0,015329	0,003133
1	17,2957	13,2085	9,56074	6,30172	3,73359	1,78437	0,727431	0,266349	0,025468	0,005979
	17,2952	13,2083	9,55921	6,29793	3,73121	1,78143	0,725248	0,263391	0,022403	0,004363
	17,2853	13,1969	9,54659	6,28606	3,71799	1,76934	0,713567	0,254813	0,020628	0,004369
1,5	18,4433	14,6369	11,1416	8,03592	5,39933	3,29924	1,91737	0,976988	0,214528	0,03216
	18,4427	14,6359	11,1397	8,03245	5,3961	3,29541	1,91316	0,973613	0,211703	0,030412
	18,4384	14,6309	11,134	8,02725	5,39115	3,29154	1,91008	0,971891	0,212624	0,033251
2	19,5032	15,8879	12,5455	9,5289	6,89175	4,73355	3,16767	1,88205	0,672753	0,194748
	19,5018	15,8861	12,5423	9,52487	6,88781	4,72872	3,163	1,87886	0,669801	0,192635
	19,5047	15,8889	12,5454	9,52818	6,89168	4,73382	3,16746	1,8842	0,675788	0,199668
3	21,2567	17,9116	14,8357	12,0151	9,47596	7,24087	5,44982	3,91413	2,01034	1,01878
	21,2548	17,9093	14,8324	12,0105	9,47096	7,23549	5,44448	3,90927	2,00659	1,01607
	21,2731	17,9288	14,8528	12,0324	9,494	7,2595	5,46803	3,93359	2,02933	1,03764
4	22,7053	19,596	16,7262	14,0645	11,6942	9,49325	7,60685	5,96693	3,58363	2,13184
	22,7025	19,5926	16,7217	14,0584	11,6877	9,48616	7,60011	5,96078	3,57831	2,12798
	22,7307	19,6231	16,7539	14,0929	11,7234	9,52344	7,63714	5,99784	3,61407	2,16137
5	23,8921	21,058	18,3282	15,7657	13,5273	11,4879	9,57122	7,8526	5,29193	3,40811
	23,8886	21,0535	18,3228	15,759	13,5208	11,4808	9,56431	7,84626	5,28564	3,40339
	23,9198	21,0872	18,3586	15,7972	13,56	11,5211	9,60522	7,88753	5,32615	3,44189

Table 7.3: Input values compared with output values for the two implied finite difference models.

From this table it follows that both methods are well capable of pricing the given European options consistent with their market values. It can be seen that using the instantaneous volatility can be preferred in this case, since its results better match the market values in most cases. When a small number of grid points is taken, the method of Andersen and Brotherton-Ratcliffe performs better. For example, when table 7.3 is created for a 50x50 grid, the method of Brotherton-Ratcliffe outperforms the instantaneous volatility method in most cases. This can also be seen from the convergence plots of both methods, shown later in this section.

When looking at the convergence of the model as the number of grid points increases, we get the following figure for the finite difference method based on the instantaneous volatility.

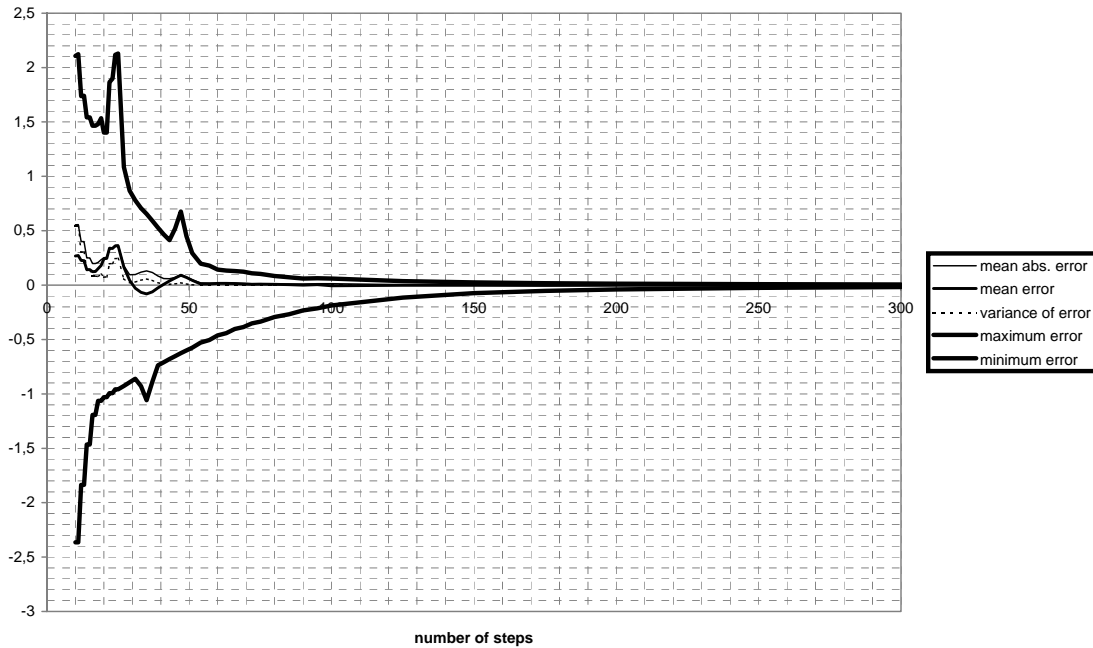


Figure 7.4: Convergence of the finite difference method with instantaneous volatility.

Again we have used a square grid. From this figure it follows that option-prices given by this method, converge to the market values. When using a 500×500 grid all measures are smaller than 0.005 in absolute terms. Despite the fact that option values converge to their market values, this method does not converge very smoothly. Some spikes can be observed in both the minimum and the maximum errors. This behaviour seems to disappear when the number of steps gets larger.

When using the method suggested by Andersen and Brotherton-Ratcliffe we get the following figure for the convergence of the differences between model values and market values.

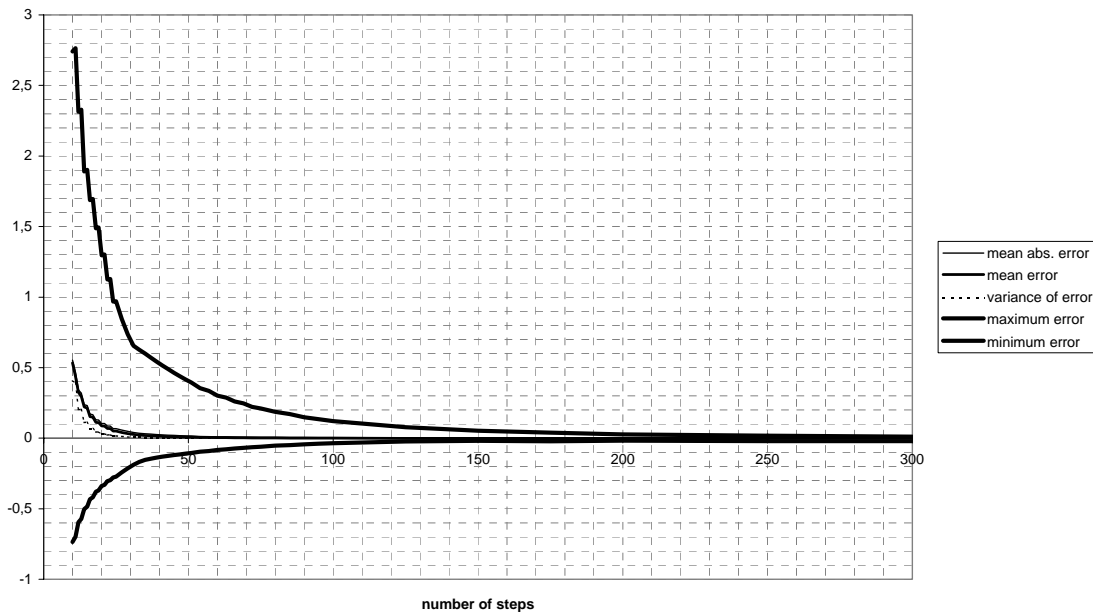


Figure 7.5: Convergence of the finite differences with the method of Andersen and Brotherton-Ratcliffe.

This also shows a good convergence, which is much smoother than before. The mean absolute error, the mean error and the variance of the errors go to zero very fast. However, when taking even larger numbers of grid-points this method seems to diverge somewhat.

7.5 Implied Monte Carlo simulation

The fourth model discussed in the previous chapter was Monte Carlo simulation. This section uses the antithetic variable technique, to reduce variance. Table 7.4 shows the results from applying the model to the European options. Once again, the shaded cells give the market values of the options. The values in every second row give the results from the Monte Carlo simulation using 1000 simulations consisting of 1000 time-steps. Options with the same time to maturity were priced using the same simulated price paths, in order to avoid long computation time. This may explain that the options with a two year time-to-maturity are all priced to low compared to the market values, while the three year options are all priced to high.

t/strike	85	90	95	100	105	110	115	120	130	140
0,175	15,2654	10,4337	5,76567	2,05143	0,321329	0,017254	0,005403	0,002379	0,000243	7,65E-05
	15,2523	10,4375	5,7842	2,07877	0,351152	0,022092	0,00607	0,003592	0	0
0,425	15,8392	11,2381	7,03704	3,63052	1,27316	0,319943	0,056263	0,026122	0,003684	0,001176
	15,8701	11,2517	6,99673	3,59009	1,2233	0,305333	0,062219	0,030032	0,000764	0
0,695	16,516	12,197	8,28259	5,00966	2,41468	0,826052	0,249063	0,076066	0,008686	0,002947
	16,5695	12,2906	8,3584	5,02114	2,40494	0,855548	0,262803	0,072293	0,007716	0
0,94	17,1425	13,0256	9,32216	6,05618	3,50818	1,58424	0,623565	0,223836	0,020523	0,004998
	17,1294	13,0317	9,34311	6,05379	3,49939	1,58957	0,613306	0,231477	0,024365	0,005132
1	17,2957	13,2085	9,56074	6,30172	3,73359	1,78437	0,727431	0,266349	0,025468	0,005979
	17,3008	13,1999	9,53495	6,276	3,68502	1,7319	0,696013	0,242637	0,020293	0
1,5	18,4433	14,6369	11,1416	8,03592	5,39933	3,29924	1,91737	0,976988	0,214528	0,03216
	18,3843	14,5793	11,0821	7,98386	5,38084	3,28208	1,88214	0,938294	0,204811	0,037755
2	19,5032	15,8879	12,5455	9,5289	6,89175	4,73355	3,16767	1,88205	0,672753	0,194748
	19,3045	15,6705	12,3033	9,24524	6,6037	4,49063	2,96323	1,71893	0,582894	0,166121
3	21,2567	17,9116	14,8357	12,0151	9,47596	7,24087	5,44982	3,91413	2,01034	1,01878
	21,7038	18,3786	15,3223	12,5065	9,94212	7,69887	5,9306	4,39609	2,42237	1,3731
4	22,7053	19,596	16,7262	14,0645	11,6942	9,49325	7,60685	5,96693	3,58363	2,13184
	22,8286	19,7446	16,8964	14,2498	11,8928	9,6952	7,79735	6,12895	3,7052	2,25134
5	23,8921	21,058	18,3282	15,7657	13,5273	11,4879	9,57122	7,8526	5,29193	3,40811
	23,7919	20,9946	18,3086	15,7893	13,575	11,5462	9,64134	7,92619	5,32236	3,38234

Table 7.4: Input values compared with output values for Monte Carlo simulation.

From this table it can also be seen that some options have been given a value of zero with the Monte Carlo simulation method. This means that none of the 1000 simulated price paths has ended above the strike price of that option. Logically this occurs for deep out of the money options with a short time-to-maturity. To obtain good values for these kind of options a lot more simulations have to be made. Overall it can be seen that this method gives reasonable values when a lot of simulations are used.

Figure 7.6 shows the convergence properties of the Monte Carlo simulation. The same approach as in the previous sections was used.

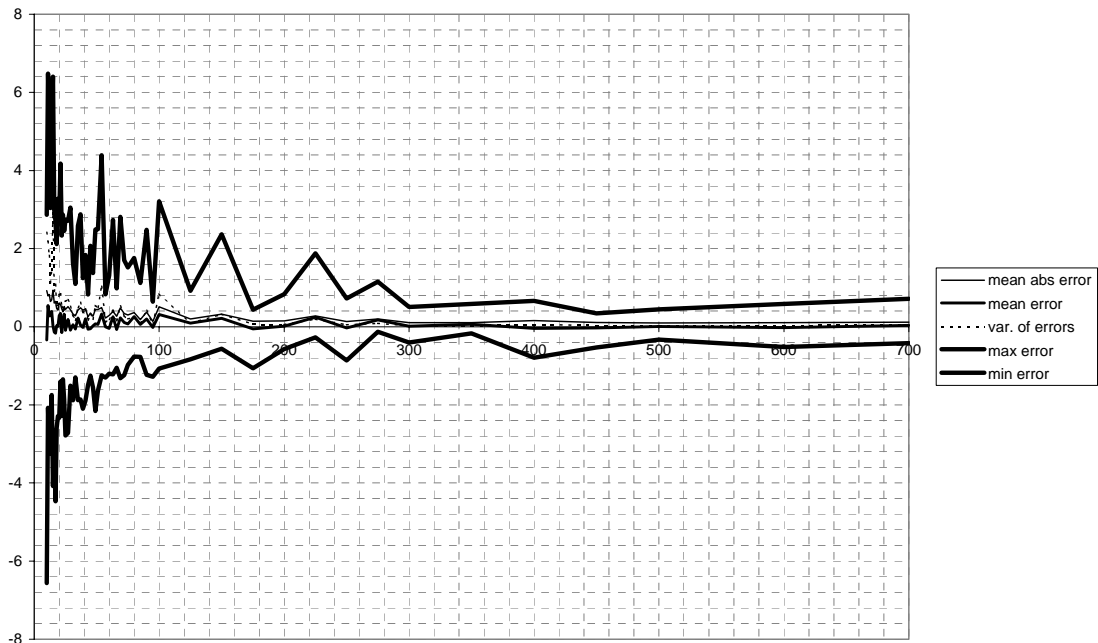


Figure 7.5: Convergence of Monte Carlo simulation to market values.

This figure shows that the model does converge, but very slowly. The maximum and minimum errors are still quite large for 700 simulated paths consisting of 700 time-steps. Further it can be seen that the convergence is not smooth, but that can be expected from Monte Carlo simulation.

7.6 Stochastic volatility model

The last model discussed in the previous chapter was the implied tree, which allows for a stochastic volatility process. Since the chosen model of volatility has no influence on the price of European options given by the model, the results below are generated using a one state volatility process as our base model of volatility. As discussed in Chapter 6, this model should yield similar results as the implied trinomial tree of Derman, Kani and Chriss (DKC). This is reflected in the table below. A 500-tree is constructed, with which options are priced and compared to their market values. In the algorithm, negative transition probabilities are adjusted, using (6.28).

t/strike	85	90	95	100	105	110	115	120	130	140
0,175	15,2654	10,4337	5,76567	2,05143	0,321329	0,017254	0,005403	0,002379	0,000243	7,65E-05
	15,2542	10,4107	5,76649	2,05327	0,322931	0,017475	0,003728	0,000899	4,11E-05	1,44E-06
0,425	15,8392	11,2381	7,03704	3,63052	1,27316	0,319943	0,056263	0,026122	0,003684	0,001176
	15,8058	11,2117	7,0383	3,63186	1,27819	0,320765	0,054757	0,02251	0,002921	0,000543
0,695	16,516	12,197	8,28259	5,00966	2,41468	0,826052	0,249063	0,076066	0,008686	0,002947
	16,4758	12,1702	8,28296	5,01252	2,41849	0,831051	0,249966	0,072656	0,0079	0,002314
0,94	17,1425	13,0256	9,32216	6,05618	3,50818	1,58424	0,623565	0,223836	0,020523	0,004998
	17,1024	13,0001	9,32207	6,06092	3,51017	1,58553	0,62464	0,220846	0,019882	0,00437
1	17,2957	13,2085	9,56074	6,30172	3,73359	1,78437	0,727431	0,266349	0,025468	0,005979
	17,2555	13,1823	9,5572	6,30605	3,73668	1,79081	0,731151	0,265454	0,02491	0,005358
1,5	18,4433	14,6369	11,1416	8,03592	5,39933	3,29924	1,91737	0,976988	0,214528	0,03216
	18,4029	14,6111	11,1325	8,04001	5,40416	3,30668	1,91757	0,976354	0,213915	0,032048
2	19,5032	15,8879	12,5455	9,5289	6,89175	4,73355	3,16767	1,88205	0,672753	0,194748
	19,4649	15,8607	12,5335	9,53572	6,89815	4,74525	3,16933	1,88083	0,671593	0,195924
3	21,2567	17,9116	14,8357	12,0151	9,47596	7,24087	5,44982	3,91413	2,01034	1,01878
	21,2231	17,8834	14,8177	12,0192	9,48248	7,24912	5,45202	3,92516	2,0145	1,02128
4	22,7053	19,596	16,7262	14,0645	11,6942	9,49325	7,60685	5,96693	3,58363	2,13184
	22,6745	19,5639	16,7044	14,0675	11,6999	9,50482	7,61398	5,97955	3,58557	2,13792
5	23,8921	21,058	18,3282	15,7657	13,5273	11,4879	9,57122	7,8526	5,29193	3,40811
	23,8686	21,0252	18,303	15,752	13,535	11,4928	9,58041	7,86724	5,297	3,41732

Table 7.5: Input values compared with output values for the Britten-Jones and Neuberger trinomial tree.

This table shows good results for the model. However, it can be seen that the results are not as good as the DKC implied trinomial tree. This must have been caused by the difference in both models, discussed in section 6.6¹. Figure 7.6 shows the convergence plot for this model.

¹ In section 6.6 it was already argued that the DKC algorithm would yield better results because it does not rely on perfect calibration results in a previous step.

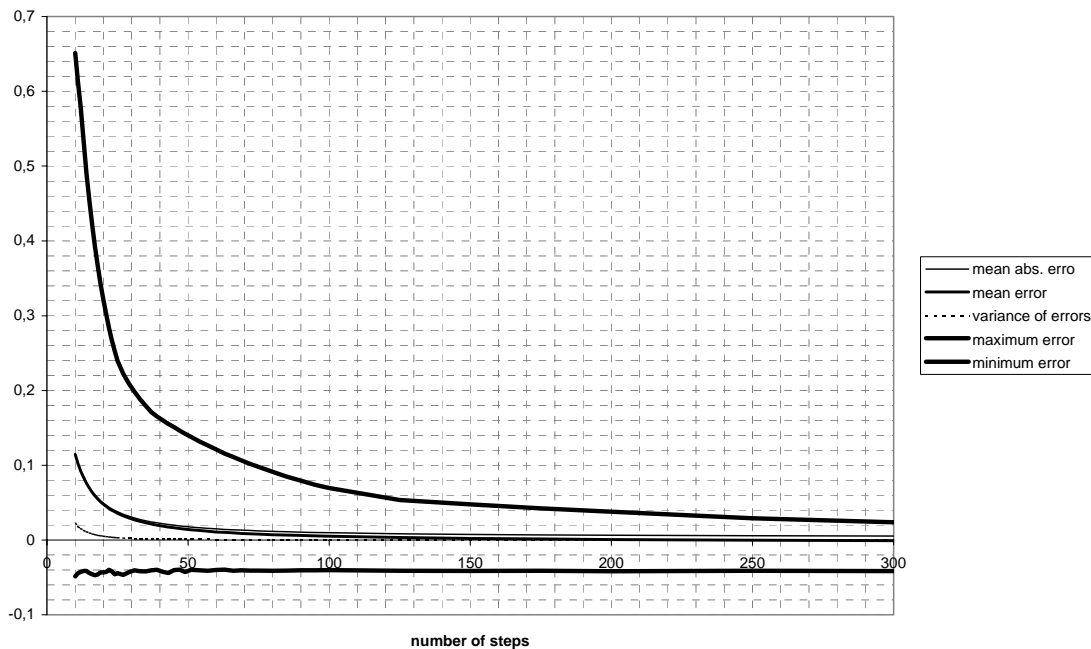


Figure 7.6: Convergence of the BJN implied trinomial tree to market values.

This shows a smooth convergence for almost all measures. The minimum error shows some erratic behaviour. It also does not seem to converge to zero, but rather to -0.04 . This might indicate that the statespace is chosen too narrow, or u too small.

7.7 Continuous case

At the end of chapter 6 a method was given, to determine the transition probabilities in implied trinomial trees directly from the instantaneous volatility. This method also gives a close fit when we use a tree consisting of 500 steps. Differences with the market values are all smaller than 0.05. The figure below shows the convergence of this method. It shows that it does not converge as fast as the implied models that fit market values of options directly. However, when one wants to use a large number of steps, this model can be used. Further, it can be seen that the minimum error does not seem to converge to zero. Setting u to a larger value will lead to a better convergence to zero. However, with a larger u the convergence gets slower. This is also the case for the implied trinomial tree and the stochastic implied tree, discussed earlier. One has to make a choice what u to use. This may depend on the number of steps one is willing to use.

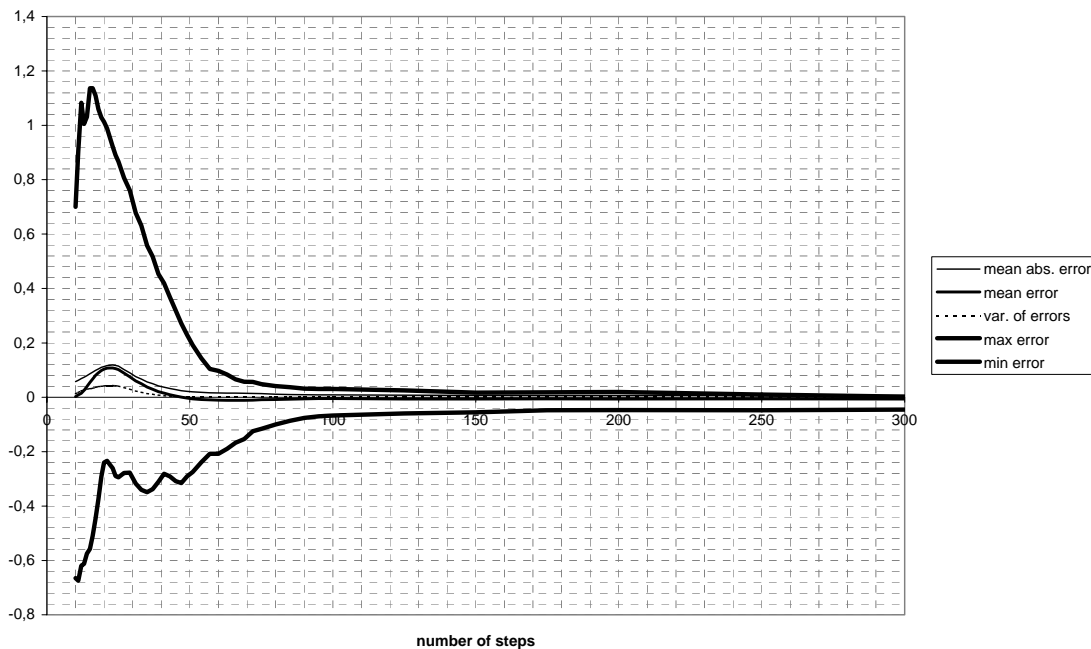


Figure 7.7: Convergence of the implied trinomial tree, using the instantaneous volatility.

7.8 Convergence speed

For use in practice, it is interesting to know how fast the implied models are. To measure the speed, one can look at the order of the model when building it. When considering the implied binomial tree, we must calculate option prices that result from the tree constructed so far. To calculate these options a sum must be evaluated in (6.4) and (6.9). However, when working out this sum, one can use the result from the previous option calculation. It follows that the calculation of every option can be done $O(1)$. Since at every step one must calculate a number of options equal to that time-step, it follows that the implied binomial tree is $O(n^2)$. When considering the implied trinomial tree, same arguments can be used to show that it is also $O(n^2)$. When using finite differences combined with the instantaneous volatility, at every step one must calculate n instantaneous volatilities. Next a tridiagonal system must be solved. It was discussed that this can be done $O(n)$. Thus this model is also $O(n^2)$. When using the method described by Andersen and Brotherton-Ratcliffe, volatilities should be solved by the system given by (6.49). Again, this is a tridiagonal system and thus this method is $O(n^2)$. When using the Monte Carlo simulation with n paths consisting of n time-steps, it is easy to see that it will be $O(n^2)$. The model of Britten-Jones and Neuberger is closely related to the implied trinomial tree. However, when the number of volatility states increases, more calculations have to be done. From (6.72) it follows that the method is $O(m^2 n^2)$, where m denotes the number of volatility states. When the implied trinomial tree uses the instantaneous

volatility instead of directly fitting the options, the order of the model remains unchanged.

In the following figure we show the time (in seconds) it takes to build implied models. For the implied trinomial tree, we show only the model with adjustments according to (6.28). The BJN tree is as fast as the DKC tree, when one volatility state is used. All programs were written in C++ on a Pentium 200.

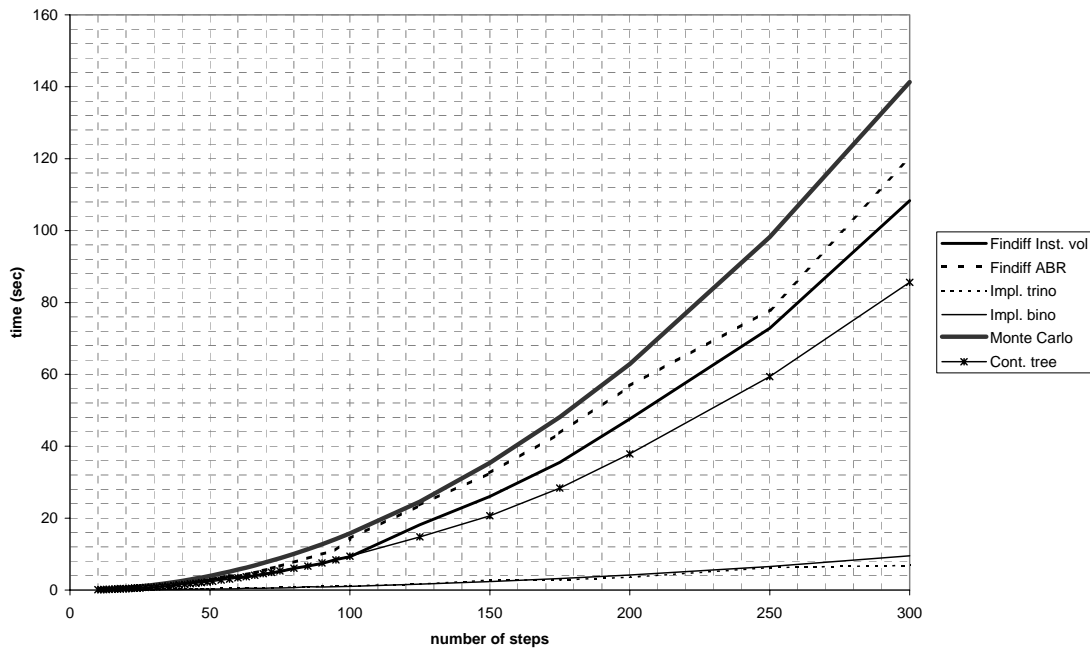


Figure 7.8: Time it takes to build the implied models as a function of the number of steps used.

It shows that the implied binomial and trinomial models are very fast. A tree of 300 steps can be built in the same time as a 100x100 grid for finite differences. It can be seen that the models, that use the instantaneous volatility, are slower than the models that fit the European options directly. The same figure can be made setting out the log of time, against the log of the number of steps. This shows relations that are more or less linear, all with a slope close to 2. This shows that the models are indeed $O(n^2)$.

7.9 Summary and conclusions

From the analysis in this chapter we have learned that the implied binomial tree has a bad performance. It is not capable of pricing European options consistent with their market values. Another fact that became clear is that the performance does not improve much when the number of steps increases. The implied trinomial tree performs much better. Using (6.28) to adjust negative transition probabilities gives the best results. The

algorithm of Britten-Jones and Neuberger also shows a good performance, since this model is closely related to the implied trinomial trees. The same argument holds for the implied trinomial tree based on the instantaneous volatility. For the implied finite difference method it was seen that both alternatives show a good performance. The method of Andersen and Brotherton-Ratcliffe shows better convergence properties. To summarise the results, the following figure shows the mean absolute error for all models as a function of the number of steps used. In this figure, trinomial 1 and 2 denote the implied trinomial tree with adjustments given by (6.27) and by (6.28), respectively. The method of finite differences combined with the instantaneous volatility function is denoted by Fin. Diff 1, while the method of Andersen and Brotherton-Ratcliffe is denoted by Fin. Diff 2. The figure shows again the bad results for implied Monte Carlo simulation (MC) and the implied binomial tree. It also shows that the implied trinomial tree combined with (6.27) does not give a very good performance.

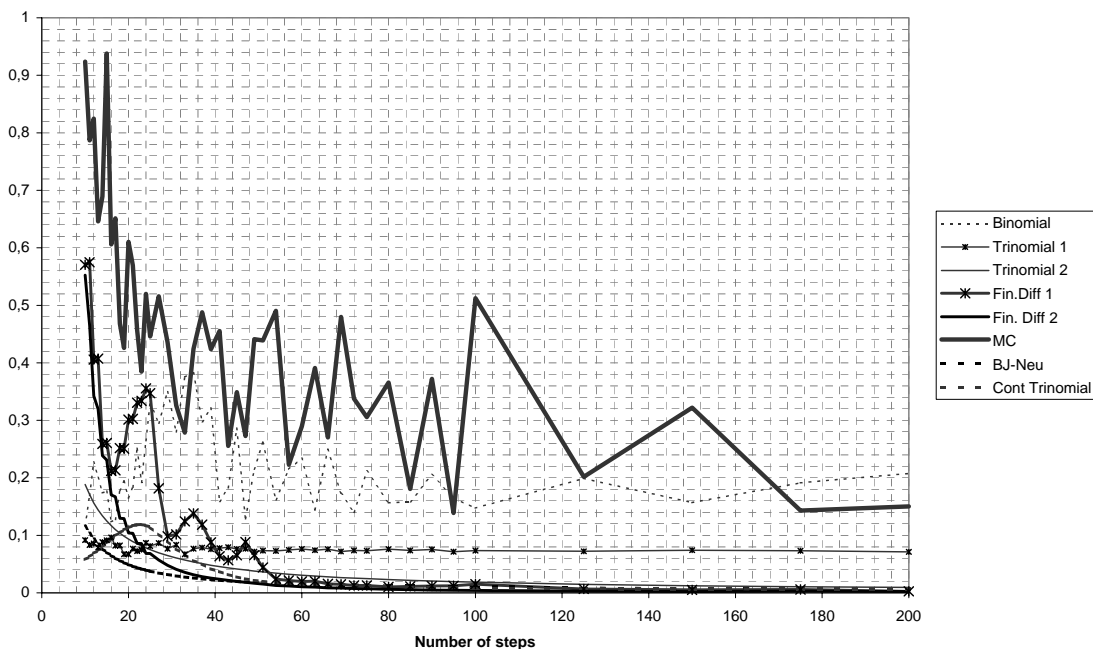


Figure 7.7: Convergence of the mean absolute error for all implied models.

Based on the conclusions in this chapter, in the rest of this thesis we will no longer focus on the implied binomial tree and Monte Carlo simulation. The trinomial tree will, from now on, only be used in combination with (6.28). Since the finite difference model combined with the instantaneous volatility gives better results for a large number of steps and the fact that it is faster than the method of Andersen and Brotherton-Ratcliffe, we will work with the former. The remainder of this thesis will focus on deterministic volatility and thus the model of BJN will not be considered further.

8 Applying the implied models

8.1 Introduction

Now that we have seen that implied models can do a good job pricing standard options consistent with their market values, we look at options that are more complex. First, we start by investigating the greeks for standard European options. Then we will apply the different models to American options. The results will be compared with that of a normal trinomial tree. After this, the models will be applied to barrier options. These results will be compared with the formulae that can be derived using risk-neutral analysis. These formulae are given in appendix B and are used with the implied volatility of the European option with the same strike and the same maturity.

8.2 Greeks of European options

In the previous chapter, it became clear that some of the implied models show very good results. Here, we look at the greeks of European options that result from using implied models and compare them to the analytic formulae. To calculate hedge-parameters with implied models, we use the method described in Pelsser and Vorst (1994). To determine rho and epsilon, the implied models have to be built two times. Since the implied volatility is a function of both the underlying asset and time-to-maturity we can expect that applying the implied models yield differences compared to the analytical formulae when determining the delta, gamma and theta. For rho and epsilon, we expect that the results are equal. It is not clear, how vega should be determined, since volatility is an entire structure. Thus, a way to express the risk involved in changes in the volatility structure has to be found.

In the following table, we show the delta for European call options. The parameters are set to the same values as in chapter 7¹. The volatility structure is defined by the volatility matrix shown in table 4.1. The values in the shaded cells are found analytically. The analytical values for the greeks of an option are determined by assuming a constant volatility equal to its implied volatility. This is also known as the sticky-strike rule, a term introduced by Derman (1999). Other implied methods with a good performance give similar results and are not shown here.

¹ $S_0 = 100$, $r = 5\%$ and $q = 3\%$. Options have strike and time-to-maturity corresponding with the elements of the volatility matrix.

t/strike	85	90	95	100	105	110	115	120	130	140
0,175	0,978202	0,938476	0,839962	0,536064	0,14837	0,012407	0,003561	0,001431	0,000143	4,08E-05
	0,971541	0,915387	0,791443	0,489249	0,127972	0,010719	0,00265	0,000703	3,78E-05	1,51E-06
0,425	0,926309	0,869313	0,751383	0,550589	0,293781	0,102651	0,023502	0,010541	0,001553	0,000469
	0,88642	0,80473	0,669764	0,466426	0,239964	0,084545	0,022094	0,011354	0,001998	0,000671
0,695	0,884905	0,818379	0,711776	0,559935	0,372152	0,181406	0,069578	0,024589	0,003249	0,001052
	0,824103	0,736931	0,615816	0,458245	0,288035	0,139025	0,056337	0,022451	0,003939	0,001489
0,94	0,855837	0,788687	0,691605	0,56617	0,415891	0,2527	0,126542	0,054632	0,006685	0,001672
	0,784761	0,697995	0,585453	0,455711	0,315198	0,184175	0,094333	0,043034	0,007	0,002226
1	0,849642	0,783423	0,687988	0,567415	0,423184	0,267001	0,139028	0,061817	0,007986	0,001952
	0,776718	0,691437	0,580439	0,455277	0,320412	0,193789	0,102217	0,047847	0,008008	0,002517
1,5	0,811968	0,750329	0,671735	0,575853	0,465079	0,345713	0,237259	0,144519	0,041926	0,008036
	0,72978	0,650469	0,558735	0,457077	0,351256	0,249953	0,165783	0,099191	0,030026	0,006975
2	0,784669	0,728974	0,661104	0,581064	0,49023	0,392949	0,300335	0,210173	0,093451	0,033092
	0,698791	0,626755	0,546852	0,46117	0,373109	0,288098	0,212224	0,1439	0,062774	0,022275
3	0,748181	0,701937	0,647452	0,585968	0,518326	0,445976	0,373458	0,301277	0,184529	0,106732
	0,660773	0,601402	0,537006	0,469649	0,401245	0,333987	0,271092	0,21291	0,126759	0,072097
4	0,721249	0,681647	0,636278	0,586246	0,532181	0,475075	0,416604	0,357982	0,251767	0,169492
	0,636596	0,585877	0,532013	0,476449	0,420237	0,3646	0,311439	0,261468	0,177832	0,117514
5	0,699209	0,663921	0,625605	0,583706	0,538542	0,491708	0,443234	0,39387	0,302354	0,220937
	0,620128	0,574647	0,528195	0,48091	0,433243	0,386077	0,339755	0,295522	0,219364	0,155987

Table 8.1: Delta calculated analytically compared with the delta resulting from applying the implied trinomial tree

This table shows some differences. In most cases, the implied model gives smaller values for the delta. Further research has shown that delta is lower when implied volatility is a decreasing function of strike and higher when it is an increasing function of strike. When implied volatility is a function of time only, the results from the implied model are equal to the analytical case. The delta for put options can be determined in a similar way. Subtracting the delta for a put option from the delta of the corresponding call option will result in e^{-qT} . This follows from the put-call parity. It has been checked that this is indeed the case. Using the same argument, it can be shown that European call and put options must have the same gamma. The table below shows this gamma for the analytical case and the implied trinomial tree.

t/strike	85	90	95	100	105	110	115	120	130	140
0,175	0,005183	0,016102	0,042718	0,083631	0,054154	0,007918	0,002126	0,000786	7,83E-05	2,03E-05
	0,010908	0,030175	0,060148	0,080639	0,040159	0,005542	0,001602	0,000471	2,98E-05	1,36E-06
0,425	0,010431	0,019493	0,034037	0,047863	0,048128	0,026547	0,008494	0,003749	0,000594	0,000171
	0,023724	0,036891	0,048894	0,051549	0,040341	0,020261	0,007735	0,004425	0,000938	0,000333
0,695	0,011674	0,01853	0,027133	0,034686	0,037903	0,030177	0,015953	0,006822	0,00109	0,000341
	0,0251	0,033058	0,038851	0,039589	0,034748	0,023705	0,012809	0,00653	0,001595	0,000662
0,94	0,011709	0,017045	0,022983	0,028589	0,030984	0,028779	0,02003	0,011015	0,001924	0,000504
	0,023688	0,029337	0,032876	0,033685	0,030155	0,023862	0,015859	0,009105	0,002346	0,000902
1	0,011649	0,016708	0,022182	0,027432	0,029861	0,028164	0,020505	0,01176	0,002203	0,000573
	0,023285	0,028565	0,031691	0,032528	0,029422	0,023667	0,016218	0,009572	0,002548	0,000985
1,5	0,010801	0,01426	0,017899	0,021211	0,023416	0,023585	0,020764	0,01619	0,006772	0,001752
	0,020151	0,023446	0,025572	0,026114	0,024825	0,021815	0,017311	0,012547	0,00536	0,001815
2	0,009851	0,012434	0,015086	0,017533	0,019358	0,019994	0,018872	0,016706	0,010105	0,00465
	0,017421	0,01986	0,021498	0,022121	0,021619	0,019883	0,016965	0,013699	0,007667	0,003453
3	0,008281	0,009998	0,011681	0,013236	0,014509	0,015366	0,01541	0,014922	0,011982	0,008418
	0,01389	0,015512	0,016611	0,017181	0,017171	0,016599	0,015327	0,013744	0,010039	0,006644
4	0,007088	0,008341	0,00955	0,010679	0,011573	0,012321	0,012694	0,01272	0,011559	0,009435
	0,011469	0,012666	0,013524	0,014052	0,014168	0,014028	0,013512	0,012722	0,010511	0,008049
5	0,00617	0,007103	0,00805	0,00896	0,009658	0,01021	0,010654	0,010908	0,010497	0,009396
	0,009726	0,010618	0,011388	0,011955	0,012133	0,012085	0,011906	0,011546	0,010177	0,008453

Table 8.2: Gamma calculated analytically compared with the gamma from the implied trinomial tree

It can be seen in table 8.2 that the gamma is higher in most cases, when using the implied model. This means that the delta changes faster when the underlying asset changes for the implied models. Thus, a trader may want to update his position more often when delta hedging. Table 8.3 shows the theta of European call options, calculated in the tree. It is the negative equivalent of the theta defined in chapter 4.

t/strike	85	90	95	100	105	110	115	120	130	140
0,175	-2,12871	-3,62762	-5,16963	-6,30402	-3,0976	-0,396436	-0,15988	-0,082017	-0,011446	-0,004142
	-2,19714	-4,12498	-6,90818	-8,40556	-3,98941	-0,53748	-0,154413	-0,045207	-0,002848	-0,000129
0,425	-2,69473	-3,5182	-4,39197	-4,65637	-3,38309	-1,59745	-0,468921	-0,26337	-0,053077	-0,020111
	-3,19428	-4,48923	-5,55069	-5,56338	-4,18237	-2,0442	-0,762872	-0,434045	-0,091199	-0,032283
0,695	-2,67076	-3,31051	-3,82274	-3,93549	-3,26262	-1,95337	-0,924395	-0,393354	-0,069607	-0,028152
	-3,16336	-3,94762	-4,4424	-4,36049	-3,69842	-2,44899	-1,29519	-0,649927	-0,155919	-0,064408
0,94	-2,56641	-3,08063	-3,46851	-3,51116	-3,15487	-2,26361	-1,34713	-0,682369	-0,108513	-0,03358
	-2,92095	-3,48065	-3,77144	-3,75118	-3,26874	-2,51572	-1,63702	-0,923951	-0,231396	-0,088069
1	-2,53759	-3,01832	-3,39361	-3,43066	-3,10557	-2,30714	-1,41545	-0,734131	-0,122634	-0,037003
	-2,85971	-3,38628	-3,63889	-3,63	-3,19921	-2,50639	-1,68096	-0,974966	-0,251934	-0,096284
1,5	-2,24414	-2,59408	-2,82719	-2,88768	-2,72983	-2,33982	-1,8488	-1,2738	-0,460828	-0,105603
	-2,41539	-2,7546	-2,94456	-2,94733	-2,7475	-2,36918	-1,85011	-1,31939	-0,548693	-0,181149
2	-2,00089	-2,27513	-2,46088	-2,52834	-2,45328	-2,23877	-1,94044	-1,50908	-0,821473	-0,342955
	-2,04531	-2,30959	-2,46982	-2,50755	-2,41665	-2,19256	-1,84756	-1,47063	-0,806292	-0,356141
3	-1,60207	-1,80421	-1,95647	-2,04023	-2,0466	-1,97122	-1,8374	-1,62931	-1,18966	-0,799325
	-1,55167	-1,75128	-1,87894	-1,93861	-1,92784	-1,85173	-1,69738	-1,50982	-1,08768	-0,711715
4	-1,30753	-1,47803	-1,61332	-1,7028	-1,74745	-1,73538	-1,67888	-1,57677	-1,3011	-1,0053
	-1,20488	-1,3703	-1,48615	-1,55705	-1,57436	-1,55982	-1,50001	-1,40835	-1,1547	-0,877299
5	-1,07448	-1,23016	-1,35248	-1,44157	-1,50207	-1,52718	-1,51277	-1,46396	-1,31091	-1,09006
	-0,949643	-1,08353	-1,19893	-1,28534	-1,31861	-1,32176	-1,30816	-1,27187	-1,12058	-0,92745

Table 8.3: Theta calculated analytically compared with the gamma from the implied trinomial tree

The thetas of the short-term options are higher, in absolute terms, for the implied model. For long-term options, the thetas are lower. As expected the rho and epsilon of implied models are almost equal to the analytical values. Tables are thus not listed here.

To get a measure of the risk involved in a change of the volatility structure, one can determine vega by lifting the entire volatility structure with a small amount. Doing this will, of course, give the same value for vega as in the analytical case.

8.3 American options

Unfortunately, there is no formula for the price of an American option. However, as discussed in chapter 4, American options are easy to price using numerical methods. At every step, one has to check whether early exercise is optimal. In this section, we will use a standard trinomial tree to obtain an approximation for the value of American options. For the volatility needed to value the American option, we take the implied volatility of the corresponding European option. Table 8.4 gives the value of American call options priced with a standard trinomial tree in the dark cells. Every second row gives the corresponding result when applying the implied trinomial tree. Every third row gives the

result of the finite difference method combined with the instantaneous volatility. Both tree models consist of 500 steps, while the finite difference grid is 200x200. Again, we assume an interest rate of 5% and a dividend yield of 3% per annum. For the market values of European options, we again use the volatility matrix from chapter 4, combined with cubic splines for interpolation and extrapolation.

In contrast to the previous chapter, we do not expect that the values generated by the implied models are equal to those generated by a standard tree. We do expect that both implied models yield similar results. That this is indeed the case, can be checked in table 8.4. The table shows that there are some small differences in the values of American call options valued with implied models and those valued with a constant volatility model. Especially for long term and in-the-money options, the differences are clear. This can be expected, since out-of-the money options behave more like European options. Further, it is clear that the difference between a European and an American call option is small when time-to-maturity is short. This explains small differences for short-term options.

t/strike	85	90	95	100	105	110	115	120	130	140
0,175	15,2653	10,4337	5,76588	2,05118	0,32139	0,017163	0,005364	0,002352	0,000237	7,42E-05
	15,2542	10,4107	5,76648	2,05325	0,322928	0,017475	0,003728	0,000899	4,11E-05	1,44E-06
	15,2654	10,4326	5,75955	2,02211	0,316342	0,021665	0,001706	0,000116	3,11E-05	1,61E-05
0,425	15,8389	11,2384	7,03722	3,63011	1,27337	0,319858	0,056098	0,025993	0,00364	0,001157
	15,8227	11,2389	7,03826	3,63175	1,27817	0,320759	0,056389	0,025623	0,003703	0,001176
	15,8373	11,2367	7,03012	3,61914	1,259	0,324294	0,06274	0,017596	0,003604	0,000939
0,695	16,5162	12,1976	8,28351	5,00914	2,4148	0,826207	0,248626	0,075873	0,008581	0,002898
	16,5098	12,1981	8,28285	5,01223	2,41843	0,831027	0,251076	0,076119	0,008756	0,00295
	16,5143	12,1957	8,27868	5,00328	2,40339	0,826396	0,256972	0,08006	0,008471	0,002747
0,94	17,1439	13,0261	9,32326	6,0556	3,50796	1,58476	0,623371	0,223605	0,020381	0,004937
	17,1431	13,0279	9,32381	6,06038	3,51004	1,58547	0,625313	0,224154	0,020825	0,005008
	17,141	13,0261	9,31818	6,04375	3,50811	1,5765	0,630629	0,229588	0,021571	0,004962
1	17,2963	13,2091	9,56087	6,30113	3,73411	1,7845	0,727329	0,266118	0,025305	0,005913
	17,2948	13,2102	9,56196	6,30544	3,73653	1,79074	0,731701	0,268664	0,025866	0,005993
	17,2944	13,2097	9,55696	6,28867	3,73318	1,77694	0,734388	0,272642	0,026903	0,00605
1,5	18,4484	14,6401	11,1419	8,03536	5,40077	3,29961	1,9169	0,977051	0,214102	0,031879
	18,4436	14,6381	11,1426	8,0387	5,40384	3,30648	1,91746	0,97916	0,215087	0,03268
	18,4425	14,6363	11,1389	8,02719	5,39358	3,29036	1,915	0,979963	0,217387	0,033345
2	19,5205	15,8961	12,5493	9,52899	6,89398	4,73457	3,16651	1,88232	0,672168	0,194195
	19,5054	15,8898	12,5482	9,53372	6,8976	4,74487	3,16908	1,88302	0,673018	0,196538
	19,5017	15,8866	12,5411	9,52102	6,88332	4,71852	3,15914	1,88364	0,67412	0,195038
3	21,3196	17,9464	14,8549	12,0223	9,48202	7,2431	5,45101	3,91541	2,01004	1,01788
	21,2715	17,9224	14,8416	12,0183	9,48164	7,24853	5,4515	3,92531	2,01651	1,02179
	21,267	17,9152	14,8326	12,0048	9,4638	7,22278	5,43621	3,90591	2,00657	1,01599
4	22,8538	19,6861	16,7793	14,0937	11,7112	9,50186	7,61067	5,9684	3,58239	2,13232
	22,7544	19,6282	16,7437	14,0824	11,7014	9,50618	7,6144	5,97953	3,58839	2,13846
	22,7488	19,618	16,7323	14,0573	11,6862	9,4754	7,59138	5,95417	3,57384	2,12478
5	24,1603	21,239	18,448	15,8381	13,5778	11,5188	9,59107	7,86537	5,29748	3,41007
	24,0086	21,1303	18,3725	15,7933	13,5452	11,5008	9,58504	7,86979	5,30037	3,4184
	23,9971	21,1178	18,3588	15,774	13,5286	11,4821	9,56237	7,84346	5,27958	3,39741

Figure 8.4: Values of American call options.

The same analysis has been repeated for different volatility structures. Both an upward and downward sloping skew, as well as an upward and downward sloping term-structure of volatility was considered. The formulae of these volatility structures are given by:

$$\begin{aligned} \hat{\sigma}(K, T) &= 0.2 \pm 0.001(S_0 - K) \\ \hat{\sigma}(K, T) &= 0.2 \pm 0.005T \end{aligned} \tag{8.1}$$

In all four cases, the differences between prices given by a standard tree and the values generated by the implied trinomial tree are very small. Differences are most noticeable for long-term and out-of-the money call options. Using different values for the risk-free interest rate and the dividend-yield does not have much effect on the results.

The same analysis has been done for American put options. When the volatility structure defined by the matrix in chapter 4 is used, we get the results shown in table 8.5. Since both implied models give similar results, we have only listed the results of the implied trinomial tree. Again, no large difference can be found in this table. This analysis has been repeated for different kinds of volatility structures and different combinations of risk-free interest rate and dividend-yield.

t/strike	85	90	95	100	105	110	115	120	130	140
0,175	0,048641	0,174196	0,466072	1,73208	5,09479	10	15	20	30	40
	0,037434	0,150799	0,464972	1,72674	5,08808	10	15	20	30	40
0,425	0,321891	0,621381	1,33211	2,87533	5,59278	10	15	20	30	40
	0,304783	0,619806	1,32613	2,84607	5,53691	10	15	20	30	40
0,695	0,688116	1,21347	2,16391	3,80374	6,24677	10,0378	15	20	30	40
	0,678632	1,20569	2,1435	3,75498	6,13107	10,0066	15	20	30	40
0,94	1,0454	1,72401	2,84508	4,45695	6,90684	10,2706	15	20	30	40
	1,04144	1,71534	2,81303	4,38989	6,7526	10,1073	15	20	30	40
1	1,13334	1,831	2,9973	4,60833	7,03088	10,3479	15	20	30	40
	1,12757	1,82121	2,96354	4,53618	6,87227	10,1561	15	20	30	40
1,5	1,76814	2,65517	3,89054	5,58722	7,88211	10,9464	15,0708	20	30	40
	1,7643	2,63683	3,84598	5,49487	7,69916	10,6512	15	20	30	40
2	2,3582	3,3474	4,65819	6,37459	8,60696	11,5339	15,3477	20	30	40
	2,34665	3,32065	4,59824	6,25151	8,38728	11,2013	15,0344	20	30	40
3	3,27853	4,37228	5,80268	7,58246	9,78945	12,5091	15,9536	20,0919	30	40
	3,25229	4,33216	5,71778	7,41938	9,50259	12,0827	15,3954	20	30	40
4	4,02873	5,20345	6,69996	8,51261	10,7678	13,3932	16,6037	20,4291	30	40
	3,98148	5,13944	6,58142	8,31434	10,4083	12,8693	15,9186	20	30	40
5	4,6313	5,94581	7,44936	9,23448	11,5115	14,1774	17,2265	20,8229	30	40
	4,59723	5,85918	7,29957	9,00478	11,1076	13,5535	16,4285	20,0943	30	40

Table 8.5: Values of American put options.

These small differences in the results are very fortunate, since it means that the implied volatility structure derived from market values of American options can be used in an implied model, without creating large errors. This is very useful for assets, which do not have European options traded on them, but only American. With the implied volatility structure of American options one can then determine values for European options needed in the algorithm. It is possible to make an implied trinomial tree based on values of American options, but this is very slow. This is caused by the fact that the value of an option, priced by the tree constructed to a certain time, has to be calculated at every node. It can thus be shown that the algorithm will then be $O(n^4)$ instead of $O(n^2)$ for the models discussed in the previous section. Implied models, based on the instantaneous volatility function, derived in chapter 5, can not be adjusted for market values of American options.

Hedge-parameters for American options are very similar to those for European options. This is the reason that we will not show these tables here.

8.4 Barrier options

The rest of this chapter will be focused on barrier options. Barrier options were already discussed in chapter 2. Valuation formulae for barriers in case of a constant volatility were given in appendix B. Here we will compare the values of barriers generated by the implied models with the values that result from using the known analytic formula. In the last case, we use the implied volatility of the European option with the same strike and maturity as the barrier option. We also discuss a way to determine the probability of hitting the barrier given a certain volatility structure. While applying the models, we have chosen the stock price nodes for trinomial trees very carefully, as discussed in Ritchken (1995), or Cheuk and Vorst (1996). For the finite difference method, a similar approach was taken.

Problems with constant volatility

Pricing barriers with the formulae given in appendix B will give some problems. For instance, what volatility should be chosen? If one uses a constant volatility to price different barrier options, the volatility structure observed in the market is ignored. If the implied volatility of the call option underlying the barrier is chosen, there exists another problem. To see this, assume there are two up barrier options with the same time to maturity, but with a different strike. If the two standard options underlying the barriers have different implied volatilities, we see from (B.4) that the pricing of both options is based on different probabilities of hitting the barrier. Of course, there is only one probability of hitting the barrier during the lifetime of the options. A third problem comes from the fact that a knock-in barrier and a knock-out barrier call should sum to a plain vanilla call option if the barriers are equal. If choosing a volatility for pricing a knock-in option, different from the implied volatility of the underlying call option, one can not price the equivalent out barrier option with this same volatility. This would give arbitrage opportunities, since the sum of the barriers is a plain vanilla, whose price is now different from the market price. To overcome these problems, barriers can be priced with implied models.

Comparing barrier prices

Closed form formulae for barrier options in the presence of a volatility structure do not exist. This can be attributed to the fact that the symmetry is gone, and thus the reflection principle can not be used anymore. In the case of non-constant volatilities, values must thus be found numerically. However, the following parity must still hold for European styled barrier options, in order to exclude arbitrage opportunities:

$$C_{ui}(K, H_1) + C_{uo}(K, H_1) = C(K) = C_{di}(K, H_2) + C_{do}(K, H_2) \quad (8.2)$$

The results in this section are based on a trinomial tree of 1000 steps and a finite difference grid of 500x500. We will first look at up barrier options with the barrier on 140. We start by looking at the following implied volatility structure.

$$\hat{\sigma} = 0.2 + 0.001(S_0 - K) \tag{8.3}$$

This means that implied volatility is a downward sloping function of the strike, K . With this volatility function we calculate values for barrier options with different strikes and time to maturities. The tables below show the results for up-and-out barriers, up-and-in barriers, and the sum of the two. The shaded cells in the tables present the price that results from the Black-Scholes formula for barrier options, when using the implied volatility of the call with same strike and maturity. The values below them are the numerical results from the implied trinomial tree. Every third row results from using the implied finite difference method based on the instantaneous volatility.

t/strike	85	90	95	100	105	110	115	120	130	140
0,175	15,3117	10,6821	6,61296	3,48793	1,50291	0,507874	0,129381	0,023856	0,000243	0
	15,3215	10,6888	6,61778	3,4902	1,50484	0,509245	0,130019	0,024075	0,00026	0
	15,3215	10,6885	6,6155	3,48765	1,50433	0,50885	0,130348	0,024267	0,00028	0
0,425	15,3376	11,3975	7,95585	5,15067	3,04856	1,62157	0,757896	0,300846	0,020853	0
	16,1069	11,9878	8,39736	5,46861	3,27123	1,76869	0,848465	0,351617	0,029126	0
	16,1054	11,9856	8,39374	5,46628	3,26887	1,76633	0,84728	0,350423	0,028839	0
0,695	14,0444	10,7642	7,87719	5,45564	3,53631	2,1131	1,13832	0,53302	0,05355	0
	16,3408	12,5921	9,29572	6,52151	4,30742	2,64393	1,47572	0,727028	0,085373	0
	16,3428	12,5931	9,29584	6,52231	4,30841	2,64192	1,47566	0,725549	0,084712	0
0,94	12,533	9,73282	7,25969	5,16008	3,45842	2,15344	1,21797	0,602785	0,068493	0
	15,8539	12,4061	9,3593	6,75386	4,62337	2,95879	1,73205	0,898135	0,115803	0
	15,8638	12,4143	9,36367	6,75966	4,62696	2,96075	1,7356	0,898301	0,115651	0
1	12,1664	9,46798	7,08364	5,05561	3,40616	2,13448	1,21634	0,607124	0,070312	0
	15,6681	12,2906	9,30222	6,74212	4,63837	2,98618	1,76369	0,918774	0,119245	0
	15,6779	12,2994	9,30854	6,74895	4,64452	2,99063	1,76502	0,920242	0,12006	0
1,5	9,47408	7,4409	5,64401	4,10422	2,8323	1,82773	1,07821	0,55982	0,070916	0
	13,6564	10,8267	8,31396	6,13612	4,3184	2,8525	1,73009	0,928105	0,12459	0
	13,6763	10,8435	8,32709	6,14977	4,32757	2,8585	1,73466	0,930827	0,127852	0
2	7,48142	5,89121	4,48945	3,28714	2,28935	1,49449	0,893971	0,471741	0,062098	0
	11,5477	9,17629	7,06945	5,24452	3,71112	2,46924	1,50818	0,813071	0,112515	0
	11,5695	9,19587	7,08809	5,26107	3,72479	2,47792	1,51507	0,81939	0,11467	0
3	4,94891	3,89776	2,97689	2,18913	1,53465	1,01072	0,611346	0,326985	0,044529	0
	8,17268	6,48147	4,99412	3,7023	2,62471	1,74831	1,06953	0,578471	0,079776	0
	8,19526	6,50428	5,01071	3,72064	2,63713	1,75779	1,07753	0,584951	0,083871	0
4	3,49371	2,74837	2,09876	1,54482	1,0852	0,717008	0,435605	0,23428	0,032387	0
	5,89391	4,66231	3,57896	2,64757	1,87047	1,24209	0,759777	0,411603	0,053791	0
	5,91341	4,67909	3,59546	2,66415	1,88534	1,25547	0,76951	0,418351	0,06191	0
5	2,58609	2,03188	1,55073	1,14155	0,802541	0,531034	0,323334	0,174408	0,0243	0
	4,35318	3,43168	2,62774	1,9403	1,36945	0,910172	0,555736	0,296511	0,039113	0
	4,36923	3,44787	2,64327	1,95483	1,38147	0,919232	0,563589	0,30709	0,047561	0

Table 8.6: Values for the Knock-out option with barrier on 140.

Again, the differences between both implied models are very small. When comparing the analytical values with those of the implied models, we see that the differences for short-term knock-out barriers are close to zero. This can be explained by the fact that the probability of a knock-out in such a short time is almost zero. Thus, the price of the barrier is almost equal to a European option. As the time to maturity rises, so do the differences. For 5 year knock-out barriers the differences are about 70%, which is quite large. One other thing that can be noticed is that the values from the implied models are

always larger than the values from the analytic formulae, when using this volatility structure. The following table shows the results for knock in barriers. Since both implied models yield similar results, we only list those of the implied trinomial tree.

t/strike	85	90	95	100	105	110	115	120	130	140
0,175	0,00978	0,006259	0,003867	0,002296	0,001302	0,000699	0,000352	0,000163	2,37E-05	4,78E-07
	3,97E-05	3,61E-05	3,25E-05	2,89E-05	2,53E-05	2,17E-05	1,81E-05	1,44E-05	7,24E-06	4,78E-07
0,425	0,865395	0,676919	0,518823	0,388329	0,282587	0,198713	0,133837	0,08515	0,025837	0,002755
	0,096676	0,087913	0,07915	0,070387	0,061624	0,052861	0,044099	0,035337	0,017881	0,002755
0,695	3,1713	2,62335	2,13509	1,7047	1,33005	1,00867	0,7378	0,514451	0,198176	0,039434
	0,876169	0,797055	0,717942	0,638829	0,559717	0,480616	0,401553	0,322634	0,167502	0,039434
0,94	5,54637	4,69804	3,9223	3,21905	2,58792	2,02829	1,53935	1,12019	0,488065	0,131601
	2,22552	2,02543	1,82535	1,62527	1,42525	1,22537	1,02586	0,827427	0,442736	0,131601
1	6,11478	5,20095	4,36156	3,59692	2,90709	2,29195	1,75122	1,2846	0,573203	0,163397
	2,61482	2,38	2,14519	1,91041	1,6757	1,44121	1,2073	0,97485	0,525582	0,163397
1,5	10,3501	9,00484	7,73981	6,55795	5,46237	4,45643	3,54381	2,72858	1,40991	0,550308
	6,16865	5,62078	5,07316	4,52605	3,98004	3,43618	2,89654	2,36488	1,35723	0,550308
2	13,6733	12,0503	10,5063	9,04588	7,67401	6,39605	5,21797	4,14645	2,35444	1,09607
	9,60937	8,76754	7,92693	7,0885	6,2539	5,42579	4,60832	3,80812	2,30914	1,09607
3	18,393	16,4718	14,6237	12,8542	11,1694	9,57572	8,08071	6,69261	4,27598	2,41917
	15,1716	13,8882	12,6106	11,3411	10,084	8,84408	7,62846	6,44725	4,24821	2,41917
4	21,5721	19,5299	17,5539	15,6493	13,8219	12,0778	10,4242	8,8692	6,09246	3,83926
	19,1743	17,6195	16,0757	14,5466	13,0372	11,5535	10,1042	8,69907	6,07364	3,83926
5	23,8623	21,7851	19,7672	17,813	15,9276	14,1166	12,3863	10,7439	7,75719	5,24101
	22,0974	20,386	18,6902	17,0141	15,3628	13,7425	12,1601	10,623	7,7464	5,24101

Table 8.7: Values for the Knock-in option with barrier on 140.

This time the model values the barrier options lower than the analytic formulae. This should be the case from the barrier-parity given in (8.2). One other thing that can be noticed is that the largest differences (in percentages) can now be found for the short-term options. The options with a longer time to maturity do not have much difference. Further it can be seen that in the last column the differences are zero. This is because an up-and-in option with the strike greater or equal to the barrier is of course the same as a plain vanilla option. The table below shows that the sum of the knock-in and knock-out options gives good results.

t/strike	85	90	95	100	105	110	115	120	130	140
0,175	15,32148	10,68836	6,616827	3,490226	1,504212	0,508573	0,129733	0,024019	0,000267	4,78E-07
	15,32154	10,68884	6,617812	3,490229	1,504865	0,509267	0,130037	0,02409	0,000267	4,78E-07
0,425	16,203	12,07442	8,474673	5,538999	3,331147	1,820283	0,891733	0,385996	0,04669	0,002755
	16,20358	12,07571	8,47651	5,538997	3,332854	1,821551	0,892564	0,386954	0,047007	0,002755
0,695	17,2157	13,38755	10,01228	7,16034	4,86636	3,12177	1,87612	1,047471	0,251726	0,039434
	17,21697	13,38916	10,01366	7,160339	4,867137	3,124546	1,877273	1,049662	0,252875	0,039434
0,94	18,07937	14,43086	11,18199	8,37913	6,04634	4,18173	2,75732	1,722975	0,556558	0,131601
	18,07942	14,43153	11,18465	8,37913	6,04862	4,18416	2,75791	1,725562	0,558539	0,131601
1	18,28118	14,66893	11,4452	8,65253	6,31325	4,42643	2,96756	1,891724	0,643515	0,163397
	18,28292	14,6706	11,44741	8,65253	6,31407	4,42739	2,97099	1,893624	0,644827	0,163397
1,5	19,82418	16,44574	13,38382	10,66217	8,29467	6,28416	4,62202	3,2884	1,480826	0,550308
	19,82505	16,44748	13,38712	10,66217	8,29844	6,28868	4,62663	3,292985	1,48182	0,550308
2	21,15472	17,94151	14,99575	12,33302	9,96336	7,89054	6,111941	4,618191	2,416538	1,09607
	21,15707	17,94383	14,99638	12,33302	9,96502	7,89503	6,1165	4,621191	2,421655	1,09607
3	23,34191	20,36956	17,60059	15,04333	12,70405	10,58644	8,692056	7,019595	4,320509	2,41917
	23,34428	20,36967	17,60472	15,0434	12,70871	10,59239	8,69799	7,025721	4,327986	2,41917
4	25,06581	22,27827	19,65266	17,19412	14,9071	12,79481	10,85981	9,10348	6,124847	3,83926
	25,06821	22,28181	19,65466	17,19417	14,90767	12,79559	10,86398	9,110673	6,127431	3,83926
5	26,44839	23,81698	21,31793	18,95455	16,73014	14,64763	12,70963	10,91831	7,78149	5,24101
	26,45058	23,81768	21,31794	18,9544	16,73225	14,65267	12,71584	10,91951	7,785513	5,24101

Table 8.8: Sum of knock-in and knock-out should equal plain vanilla.

This same analysis is repeated, with a barrier on 110 instead of 140. The differences are a lot smaller. Only for short-term options, some differences can be detected. This is of course a result from the fact that hitting the barrier during the lifetime of the option will be almost certain as time-to-maturity increases. The differences between analytical values and the values from the implied model still have the same sign as discussed earlier. To investigate the source of the differences further, we look at the probability of hitting the barrier during the lifetime of the option. The probability that is used for analytic formulae can be found in appendix B. To determine the probability of hitting the barrier in the implied model, we use the following formula:

$$Pr\left(\max_{t \in [0, T]} S_t \geq H\right) = e^{-rT} E\left(e^{rT} I_{\{S_t \geq H, \text{ for some } t \in [0, T]\}}\right) \tag{8.4}$$

Thus, we see that we can determine the probability of hitting the barrier by valuing a derivative that pays e^{rT} if the barrier is hit and 0 else. This follows from risk-neutral valuation, discussed in chapter 4. This derivative can be seen as a rebate, which is sometimes specified for barrier options. Table 8.9 shows the results.

t/strike	85	90	95	100	105	110	115	120	130	140
0,175	0,000179 7,27E-07	0,000126 7,27E-07	8,66E-05 7,27E-07	5,78E-05 7,27E-07	3,75E-05 7,27E-07	2,35E-05 7,27E-07	1,42E-05 7,27E-07	8,2E-06 7,27E-07	2,38E-06 7,27E-07	5,48E-07 7,27E-07
0,425	0,016002 0,00179	0,013764 0,00179	0,011718 0,00179	0,009862 0,00179	0,008197 0,00179	0,00672 0,00179	0,005425 0,00179	0,004306 0,00179	0,002557 0,00179	0,001381 0,00179
0,695	0,059128 0,016382	0,053766 0,016382	0,04858 0,016382	0,043588 0,016382	0,038811 0,016382	0,034266 0,016382	0,029972 0,016382	0,025946 0,016382	0,018758 0,016382	0,012801 0,016382
0,94	0,1041 0,041944	0,096883 0,041944	0,089743 0,041944	0,082701 0,041944	0,075781 0,041944	0,069008 0,041944	0,062408 0,041944	0,056011 0,041944	0,043941 0,041944	0,033042 0,041944
1	0,114944 0,049372	0,107404 0,049372	0,099915 0,049372	0,092499 0,049372	0,085178 0,049372	0,077978 0,049372	0,070926 0,049372	0,064051 0,049372	0,050958 0,049372	0,03896 0,049372
1,5	0,196789 0,118148	0,187826 0,118148	0,178743 0,118148	0,169553 0,118148	0,160268 0,118148	0,150905 0,118148	0,141482 0,118148	0,132023 0,118148	0,113103 0,118148	0,094402 0,118148
2	0,262417 0,186384	0,253225 0,186384	0,243819 0,186384	0,2342 0,186384	0,224371 0,186384	0,214337 0,186384	0,204104 0,186384	0,193682 0,186384	0,172325 0,186384	0,150411 0,186384
3	0,357977 0,300665	0,349402 0,300665	0,340544 0,300665	0,331393 0,300665	0,321939 0,300665	0,312173 0,300665	0,302084 0,300665	0,291666 0,300665	0,269808 0,300665	0,246555 0,300665
4	0,424125 0,386812	0,416458 0,386812	0,408503 0,386812	0,400247 0,386812	0,391673 0,386812	0,382768 0,386812	0,373514 0,386812	0,363895 0,386812	0,343493 0,386812	0,32142 0,386812
5	0,473055 0,452654	0,466256 0,452654	0,459184 0,452654	0,451826 0,452654	0,444164 0,452654	0,436181 0,452654	0,42786 0,452654	0,41918 0,452654	0,400662 0,452654	0,380443 0,452654

Table 8.9: Probabilities of hitting the barrier.

In most cases, the probability of hitting the barrier is lower when the implied model is used. This partially explains the fact that out-barriers are priced higher by the implied model.

The same analysis can be repeated for a volatility function given by:

$$\hat{\sigma} = 0.2 - 0.001(S_0 - K) \tag{8.5}$$

Hence, the smile is an upward sloping function of strike. In this case, differences are again quite large but they have the opposite sign as before. In most cases, the

probabilities of hitting the barrier during the lifetime of the option are larger, when the implied model is used.

Next we consider a volatility term structure, given by the following functional form:

$$\hat{\sigma} = 0.2 + 0.02T \tag{8.6}$$

Here, T denotes the time-to-maturity of the option. Again, the same procedure is followed, which yields the following two tables when all other parameters are left unchanged.

t/strike	85	90	95	100	105	110	115	120	130	140
0,175	15,2882	10,6383	6,59369	3,54508	1,62596	0,632079	0,208339	0,058234	0,002414	0
	15,2884	10,6384	6,59505	3,54503	1,62806	0,633508	0,208753	0,058499	0,002425	0
0,425	15,422	11,4031	7,97211	5,23825	3,215	1,82746	0,947685	0,43532	0,045364	0
	15,4173	11,4007	7,96835	5,23458	3,21429	1,82762	0,947542	0,434317	0,045066	0
0,695	14,0886	10,6551	7,72535	5,33875	3,48856	2,12919	1,18946	0,586899	0,068289	0
	14,0721	10,6418	7,71435	5,32674	3,4829	2,12198	1,18635	0,584878	0,06755	0
0,94	12,3266	9,36998	6,85451	4,79569	3,18047	1,97264	1,11985	0,560745	0,066638	0
	12,3012	9,34629	6,83679	4,77672	3,16784	1,96334	1,11196	0,554461	0,064532	0
1	11,8846	9,03593	6,61503	4,6336	3,07754	1,91193	1,08716	0,545185	0,064922	0
	11,8544	9,012	6,59368	4,61259	3,06102	1,89889	1,08011	0,540962	0,063596	0
1,5	8,56874	6,4854	4,73717	3,31716	2,20566	1,37304	0,782636	0,393414	0,047001	0
	8,51634	6,44247	4,70285	3,28445	2,18565	1,35658	0,769165	0,386119	0,044917	0
2	6,13379	4,60644	3,34245	2,32751	1,54049	0,955341	0,542867	0,272224	0,032423	0
	6,06584	4,55137	3,29859	2,28918	1,51435	0,937608	0,530933	0,263804	0,030769	0
3	3,25779	2,41371	1,73072	1,19283	0,782536	0,48169	0,272034	0,135716	0,016058	0
	3,17812	2,35115	1,68189	1,15368	0,757487	0,465558	0,258695	0,130178	0,014729	0
4	1,83602	1,34775	0,95858	0,656027	0,42779	0,261989	0,147337	0,073268	0,008625	0
	1,76412	1,29297	0,917411	0,623475	0,407689	0,247352	0,139491	0,067322	0,007819	0
5	1,08997	0,795084	0,562404	0,383075	0,24879	0,151842	0,085147	0,042241	0,004968	0
	1,02986	0,74851	0,529062	0,356611	0,232441	0,141624	0,078615	0,037993	0,003498	0

Table 8.10: Values of knock-out options in the presence of a volatility term structure.

This time the differences are very small. Most of the time, the implied model gives lower prices than the analytic formula used with the appropriate implied volatility. The small difference in prices of knock-out options imply that the differences for the knock-in option should be small too. Table 8.11 shows that this is the case.

t/strike	85	90	95	100	105	110	115	120	130	140
0,175	0,004199	0,003818	0,003436	0,003055	0,002673	0,002292	0,001911	0,001529	0,000768	0,000105
	0,004259	0,003872	0,003485	0,003098	0,002712	0,002325	0,001938	0,001551	0,000779	0,000105
0,425	0,709977	0,645706	0,581435	0,517165	0,4529	0,388656	0,324501	0,26066	0,137422	0,041292
	0,715079	0,650332	0,585585	0,520838	0,456096	0,391377	0,326748	0,262437	0,138318	0,041292
0,695	3,1071	2,82734	2,54763	2,26808	1,989	1,71111	1,43589	1,16617	0,665419	0,285556
	3,12434	2,84283	2,56138	2,2801	1,9993	1,7197	1,44287	1,17162	0,668277	0,285556
0,94	5,84223	5,31964	4,79769	4,27719	3,75972	3,24799	2,74637	2,26134	1,37998	0,709614
	5,87083	5,34501	4,81985	4,29616	3,77563	3,26096	2,75653	2,2689	1,38368	0,709614
1	6,52007	5,93799	5,35688	4,77786	4,20296	3,63551	3,08063	2,54561	1,57689	0,838396
	6,55208	5,9663	5,38152	4,79886	4,22045	3,64964	3,09182	2,55418	1,58144	0,838396
1,5	11,7465	10,7228	9,70726	8,70463	7,72107	6,76433	5,84374	4,97004	3,41165	2,19139
	11,802	10,7705	9,74743	8,73734	7,74765	6,78477	5,85868	4,98139	3,41769	2,19139
2	15,9925	14,653	13,3353	12,0466	10,7951	9,58996	8,44074	7,35733	5,42713	3,87357
	16,0642	14,713	13,3843	12,0849	10,8252	9,61289	8,45756	7,36874	5,43405	3,87357
3	22,2319	20,5751	18,9667	17,4137	15,9227	14,5003	13,1521	11,8835	9,60256	7,68605
	22,3155	20,6426	19,0195	17,4528	15,9537	14,524	13,166	11,897	9,61099	7,68605
4	26,7268	25,0028	23,3414	21,7467	20,2221	18,7705	17,3942	16,095	13,7326	11,6883
	26,8037	25,0636	23,3882	21,7792	20,2489	18,788	17,4092	16,1021	13,7407	11,6883
5	30,2917	28,6195	27,0137	25,4757	24,0065	22,6066	21,2762	20,0152	17,6995	15,6535
	30,358	28,6704	27,0542	25,5022	24,0298	22,6252	21,2894	20,0232	17,7016	15,6535

Table 8.11: Values of knock-in options in the presence of a volatility term structure.

Again, the sum of the options gives the plain vanilla call option. In table 8.12, we show the probabilities of hitting the barrier during the lifetime of the option. Since the implied volatility only varies with time, the probabilities for all options with the same time-to-maturity are the same, when using the analytic formula. The first row of the table gives the probability that is used in the analytic formula; the second row results from pricing the special derivative discussed before.

T	0,175	0,425	0,695	0,94	1	1,5	2	3	4	5
Pr analytic	0,007311	0,085459	0,179311	0,248925	0,263807	0,362830	0,431430	0,520614	0,576275	0,614206
Pr implied	0,007338	0,085637	0,179704	0,249554	0,264507	0,364175	0,433521	0,524331	0,581630	0,621142

Table 8.12: Probability of hitting the barrier in the presence of a volatility term structure.

It can be seen that these probabilities do not differ much. If the sign in the volatility function given by (8.6) is changed, we come to similar conclusions. So from the analysis so far, it can be concluded that a skew has far more influence on barriers than a term structure of volatility.

As a last example, we look at the volatility matrix given in chapter 4. Again, the same method for interpolation and extrapolation is used to obtain all necessary implied volatilities. The table below shows the results for the knock-out option.

t/strike	85	90	95	100	105	110	115	120	130	140
0,175	15,2641	10,4337	5,76567	2,05143	0,321329	0,017254	0,005403	0,002378	0,000222	0
	15,2546	10,4113	5,76606	2,05139	0,322109	0,017331	0,003718	0,000889	3,19E-05	0
0,425	15,6385	11,1904	7,02727	3,62866	1,27305	0,319918	0,056253	0,025955	0,002788	0
	15,8082	11,225	7,02527	3,61973	1,26617	0,312725	0,049482	0,020125	0,000855	0
0,695	15,4403	11,6492	8,02364	4,89402	2,38561	0,821298	0,246886	0,074026	0,005929	0
	16,4766	12,1674	8,25676	4,98579	2,39608	0,810998	0,234588	0,064242	0,002161	0
0,94	14,7476	11,4793	8,33603	5,52903	3,2365	1,49626	0,584402	0,200727	0,012084	0
	17,0804	12,9698	9,27178	6,01068	3,46947	1,55401	0,596363	0,201111	0,007987	0
1	14,5275	11,3852	8,33134	5,61799	3,3659	1,64533	0,66677	0,233031	0,01432	0
	17,2174	13,1385	9,49755	6,24486	3,68424	1,74295	0,693898	0,2382	0,009898	0
1,5	12,6302	10,1469	7,79764	5,65562	3,79923	2,30019	1,23682	0,563157	0,055702	0
	17,7637	14,0183	10,5853	7,53927	4,96485	2,92665	1,6062	0,725054	0,081695	0
2	10,7186	8,7109	6,82463	5,1037	3,59356	2,32561	1,34429	0,681565	0,080753	0
	16,67	13,3086	10,2196	7,45439	5,07359	3,17132	1,8528	0,822604	0,09169	0
3	7,85494	6,42758	5,0465	3,81049	2,73797	1,8436	1,11229	0,597903	0,076692	0
	13,4208	10,761	8,36861	6,22976	4,37446	2,8162	1,69179	0,81503	0,085882	0
4	5,87728	4,78158	3,7319	2,80624	1,98604	1,3384	0,817118	0,441031	0,058455	0
	10,1782	8,13605	6,32489	4,71773	3,393	2,22937	1,3547	0,698102	0,081361	0
5	4,52423	3,59262	2,80651	2,11499	1,47804	0,970257	0,594235	0,322144	0,042224	0
	7,22057	5,75572	4,39112	3,18176	2,27209	1,53519	0,900716	0,423855	0,051243	0

Table 8.13: Values for the knock-out option when a volatility structure is used

As was the case for analysing a skew, the differences are again quite large. In most cases, the model gives higher values than the analytic formula. The implied model gives smaller values for short-term barriers with a high strike. Table 8.14 shows the results for knock-in options. This table shows some very large differences for short-term barriers with low strikes. It seems that the model gives a much smaller probability of hitting the barrier. To investigate this further, we can look at the probability of hitting the barrier, which is listed in table 8.15.

t/strike	85	90	95	100	105	110	115	120	130	140
0,175	0,001281	8,99E-05	8,14E-08	6,26E-11	1,55E-13	0	6,88E-10	3,47E-07	2,07E-05	7,65E-05
	5,87E-05	5,33E-05	4,8E-05	4,27E-05	3,74E-05	3,2E-05	2,67E-05	2,14E-05	1,07E-05	1,55E-06
0,425	0,200695	0,047699	0,009775	0,001858	0,000112	2,54E-05	9,95E-06	0,000166	0,000896	0,001176
	0,0148	0,013464	0,012127	0,010791	0,009454	0,008118	0,006782	0,005453	0,002839	0,001176
0,695	1,07566	0,54781	0,258948	0,115636	0,029066	0,004754	0,002176	0,00204	0,002757	0,002947
	0,032671	0,029735	0,026799	0,023863	0,020928	0,017993	0,01506	0,012135	0,006551	0,002946
0,94	2,39493	1,54623	0,986128	0,527148	0,271684	0,087977	0,039163	0,023109	0,00844	0,004998
	0,062182	0,056613	0,051043	0,045473	0,039904	0,034337	0,028777	0,023244	0,012666	0,004998
1	2,7682	1,82334	1,2294	0,683736	0,367687	0,139038	0,060661	0,033318	0,011147	0,005979
	0,077728	0,070764	0,063799	0,056835	0,049872	0,04291	0,035958	0,029037	0,015735	0,005979
1,5	5,81312	4,48997	3,34398	2,3803	1,60011	0,999057	0,680542	0,413831	0,158826	0,03216
	0,679413	0,618345	0,557277	0,496211	0,435151	0,374109	0,313149	0,252368	0,13358	0,032158
2	8,78459	7,17703	5,72082	4,4252	3,29818	2,40794	1,82338	1,20048	0,592	0,194748
	2,8334	2,58024	2,3271	2,07397	1,82089	1,56798	1,31552	1,06388	0,582304	0,194748
3	13,4018	11,484	9,7892	8,20463	6,73799	5,39727	4,33752	3,31622	1,93365	1,01878
	7,83546	7,15137	6,46771	5,78483	5,10374	4,42646	3,75951	3,10542	1,9275	1,01878
4	16,828	14,8145	12,9943	11,2582	9,70819	8,15484	6,78973	5,5259	3,52517	2,13184
	12,5265	11,4625	10,402	9,34623	8,30089	7,26501	6,25481	5,27463	3,50695	2,13184
5	19,3679	17,4654	15,5217	13,6507	12,0492	10,5176	8,97699	7,53046	5,2497	3,40811
	16,6718	15,3021	13,9374	12,5834	11,2575	9,95455	8,67186	7,4355	5,24279	3,40811

Table 8.14: Values for the Knock-in option when a volatility structure is used

t/strike	85	90	95	100	105	110	115	120	130	140
0,175	2,35E-05	1,81E-06	1,82E-09	1,58E-12	5,16E-15	1,11E-16	2,77E-11	1,75E-08	2,08E-06	5,78E-05
	9,79E-07	9,79E-07	9,79E-07	9,79E-07	9,79E-07	9,79E-07	9,79E-07	9,79E-07	9,79E-07	9,79E-07
0,425	0,003715	0,000971	0,000221	4,73E-05	3,25E-06	8,61E-07	4,05E-07	8,45E-06	9,03E-05	0,000661
	0,000274	0,000274	0,000274	0,000274	0,000274	0,000274	0,000274	0,000274	0,000274	0,000274
0,695	0,0201	0,011262	0,005915	0,002972	0,000854	0,000163	8,95E-05	0,000105	0,000279	0,001481
	0,000609	0,000609	0,000609	0,000609	0,000609	0,000609	0,000609	0,000609	0,000609	0,000609
0,94	0,045099	0,032026	0,022687	0,013642	0,008032	0,003035	0,001619	0,001191	0,000853	0,002351
	0,00117	0,00117	0,00117	0,00117	0,00117	0,00117	0,00117	0,00117	0,00117	0,00117
1	0,052222	0,037831	0,028329	0,017721	0,010886	0,004802	0,002511	0,001719	0,001126	0,002743
	0,001469	0,001469	0,001469	0,001469	0,001469	0,001469	0,001469	0,001469	0,001469	0,001469
1,5	0,111218	0,094402	0,078031	0,062401	0,047859	0,034785	0,028298	0,021356	0,015412	0,011266
	0,013263	0,013263	0,013263	0,013263	0,013263	0,013263	0,013263	0,013263	0,013263	0,013263
2	0,170155	0,152622	0,134858	0,117019	0,09931	0,084126	0,075665	0,061403	0,053651	0,046256
	0,056151	0,056151	0,056151	0,056151	0,056151	0,056151	0,056151	0,056151	0,056151	0,056151
3	0,26527	0,248944	0,234402	0,21936	0,203835	0,187855	0,176972	0,163141	0,151924	0,149102
	0,159338	0,159338	0,159338	0,159338	0,159338	0,159338	0,159338	0,159338	0,159338	0,159338
4	0,339217	0,325975	0,314451	0,302464	0,292529	0,279667	0,269014	0,258034	0,243842	0,23802
	0,261038	0,261038	0,261038	0,261038	0,261038	0,261038	0,261038	0,261038	0,261038	0,261038
5	0,39676	0,388747	0,378319	0,367411	0,360623	0,353647	0,344039	0,334068	0,323719	0,312976
	0,355376	0,355376	0,355376	0,355376	0,355376	0,355376	0,355376	0,355376	0,355376	0,355376

Table 8.15: Probabilities of hitting the barrier when a volatility structure is used

Table 8.15 confirms that there are indeed some very large differences in the probabilities. For the options with low strikes, these differences are very large (in percentages). This partially explains the differences in prices for the knock-in barrier options. Intuitively it is clear that for these options the probability of hitting the barrier is the most important factor. When the underlying asset reaches the barrier at 140, the barrier knocks in and is immediately deep in-the-money. So when it is knocked in, it is almost certain that the option will be exercised at maturity. This can also be seen in the following figure:

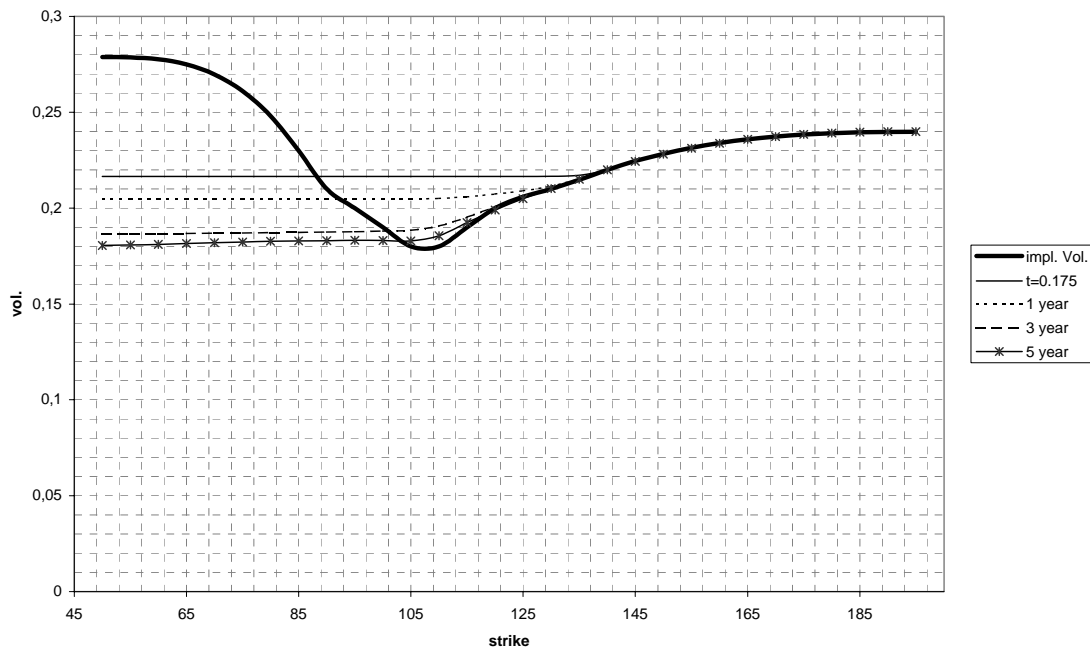


Figure 8.1: Plot of implied volatilities of knock-in barriers

The thick line in figure 8.1 shows the implied volatility of European options. This is assumed constant for all maturities. With this implied volatility, an implied trinomial tree was built, with which knock-in barriers were priced. From the resulting values, implied barrier volatilities were calculated. This volatility makes the result from applying the analytic formula equal to the value given by the implied trinomial tree. This implied barrier volatility was calculated for different maturities. For high strikes, these implied volatilities are equal to the implied volatility of European options. This follows from the fact that knock-in barrier options, with a strike higher than the barrier, are equivalent to European options. When strikes get lower, the implied barrier volatility seems constant. Calculating the probability of hitting the barrier with the analytic formula in appendix B, with this volatility, gives the same value as the special derivative priced with the implied trinomial tree. This shows that the probability of hitting the barrier is the most important factor when pricing these options with a low strike. When plotting the implied barrier volatility for down-and-out barriers, such a pattern can be seen for put options with a high strike.

Hedge parameters for barriers

Next, we investigate the influence of using an implied model on the hedge parameters. In this section, we only look at the volatility structure. First the delta is determined and compared with that of the analytic formulae. The next tables show the delta for knock-out and knock-in options, respectively.

t/strike	85	90	95	100	105	110	115	120	130	140
0,175	0,977486	0,938412	0,839962	0,536064	0,14837	0,012407	0,003561	0,00143	0,000128	0
	0,971666	0,91549	0,791511	0,489147	0,127894	0,010671	0,002617	0,000676	2,69E-05	0
0,425	0,870816	0,852514	0,747114	0,549612	0,293705	0,102632	0,023494	0,010437	0,001115	0
	0,878022	0,797072	0,662917	0,46024	0,23446	0,079822	0,018302	0,008278	0,000399	0
0,695	0,685199	0,699084	0,646025	0,526053	0,361553	0,179214	0,068498	0,023595	0,002062	0
	0,808386	0,722607	0,602706	0,446698	0,277827	0,13018	0,048821	0,016707	0,000754	0
0,94	0,512666	0,538149	0,512989	0,455662	0,350772	0,226693	0,113533	0,046539	0,003554	0
	0,760367	0,675701	0,565272	0,437709	0,299299	0,170625	0,082838	0,033868	0,001862	0
1	0,473955	0,503875	0,479847	0,433732	0,341153	0,22946	0,120365	0,050824	0,004018	0
	0,748467	0,665596	0,557123	0,434493	0,302078	0,178046	0,08901	0,037108	0,002122	0
1,5	0,244785	0,272533	0,281116	0,268399	0,234635	0,183751	0,118791	0,065652	0,008234	0
	0,621382	0,551747	0,469622	0,377616	0,281353	0,18957	0,11529	0,058377	0,007641	0
2	0,109707	0,135533	0,1495	0,150658	0,13913	0,113804	0,077352	0,048435	0,00685	0
	0,431695	0,383209	0,326962	0,264938	0,200452	0,138929	0,086764	0,042264	0,005155	0
3	-0,004841	0,01659	0,030031	0,037207	0,038564	0,035019	0,025811	0,017018	0,002637	0
	0,191307	0,172243	0,148107	0,120984	0,092629	0,065119	0,041176	0,020961	0,002322	0
4	-0,041742	-0,024225	-0,011261	-0,002173	0,002702	0,005349	0,005267	0,00398	0,000749	0
	0,067551	0,063829	0,056706	0,047601	0,037132	0,026669	0,017279	0,009408	0,001176	0
5	-0,051349	-0,036481	-0,02446	-0,01512	-0,008731	-0,004495	-0,001814	-0,000455	2,33E-05	0
	0,007768	0,010256	0,011491	0,011352	0,009474	0,007044	0,004561	0,002341	0,0003	0

Table 8.16: Delta for knock-out options

For short-term out barriers differences are very small, which can be expected since the probability of knocking out is small. Thus, these options behave like standard European call options. The differences start to get more interesting as the time-to-maturity increases. The next table shows the values for delta for knock-in options:

t/strike	85	90	95	100	105	110	115	120	130	140
0,175	0,000716	6,35E-05	9,03E-08	1,14E-10	-1,77E-15	0	9,26E-10	3,39E-07	1,45E-05	4,08E-05
	5,39E-05	4,9E-05	4,41E-05	3,92E-05	3,43E-05	2,94E-05	2,45E-05	1,96E-05	9,85E-06	1,44E-06
0,425	0,055494	0,016799	0,004269	0,000977	7,62E-05	1,93E-05	8E-06	0,000104	0,000438	0,000469
	0,008256	0,00751	0,006765	0,00602	0,005274	0,004529	0,003784	0,003044	0,00159	0,000669
0,695	0,199706	0,119295	0,065751	0,033882	0,010599	0,002192	0,00108	0,000994	0,001187	0,001052
	0,015544	0,014149	0,012754	0,011359	0,009964	0,00857	0,007177	0,005788	0,003153	0,001482
0,94	0,343176	0,250537	0,178615	0,110508	0,065119	0,026007	0,013009	0,008094	0,00313	0,001672
	0,024341	0,022166	0,019992	0,017818	0,015644	0,013471	0,011303	0,009148	0,005076	0,002209
1	0,375687	0,279548	0,208141	0,133682	0,08203	0,037542	0,018663	0,010992	0,003968	0,001952
	0,02804	0,025537	0,023033	0,020529	0,018026	0,015524	0,013027	0,010546	0,005842	0,002495
1,5	0,567183	0,477796	0,390619	0,307454	0,230443	0,161963	0,118468	0,078867	0,033692	0,008036
	0,108509	0,098808	0,089107	0,079406	0,069708	0,060019	0,050361	0,040766	0,022306	0,006789
2	0,674962	0,593441	0,511604	0,430406	0,351101	0,279145	0,222983	0,161738	0,086601	0,033092
	0,266497	0,242846	0,219197	0,195554	0,171926	0,148337	0,124844	0,101491	0,057384	0,021911
3	0,753022	0,685347	0,617421	0,548761	0,479762	0,410957	0,347646	0,284258	0,181892	0,106732
	0,468831	0,428466	0,388149	0,347911	0,307844	0,268104	0,229173	0,191214	0,123846	0,07156
4	0,762991	0,705872	0,647539	0,588419	0,529479	0,469727	0,411337	0,354002	0,251018	0,169492
	0,568582	0,521555	0,474778	0,428322	0,382541	0,337355	0,293576	0,251398	0,176256	0,116894
5	0,750558	0,700402	0,650065	0,598825	0,547274	0,496203	0,445047	0,394325	0,302331	0,220937
	0,611679	0,563664	0,515923	0,468739	0,422937	0,378198	0,334363	0,292208	0,218239	0,155096

Table 8.17: Delta for knock-in options

This table shows large differences on the same places as in table 8.14, where the prices were given. Adding all values of table 8.16 to the corresponding values of table 8.17 will result in a table that is almost equal to table 8.1. This should be the case from the barrier parity given by (8.2).

The following table shows the results for the gamma of the barrier options.

t/strike	85	90	95	100	105	110	115	120	130	140
0,175	0,004809	0,016059	0,042718	0,083631	0,054154	0,007918	0,002126	0,000786	6,87E-05	0
	0,010809	0,030129	0,060216	0,080812	0,040174	0,005514	0,001577	0,000449	2,05E-05	0
0,425	-0,002963	0,014182	0,032329	0,047386	0,048079	0,026533	0,008488	0,003688	0,000396	0
	0,019745	0,03325	0,045595	0,048578	0,037699	0,017996	0,005878	0,00293	0,000159	0
0,695	-0,018692	-0,003342	0,012748	0,02597	0,034426	0,029248	0,015458	0,006375	0,000622	0
	0,018552	0,02708	0,033418	0,034761	0,03047	0,020015	0,009702	0,004068	0,000237	0
0,94	-0,026346	-0,015247	-0,003339	0,009239	0,017667	0,022031	0,016184	0,008477	0,000877	0
	0,014751	0,021182	0,025502	0,027116	0,02434	0,018829	0,011638	0,005698	0,000422	0
1	-0,027269	-0,016961	-0,006094	0,005873	0,014424	0,019371	0,015442	0,008535	0,000936	0
	0,013534	0,019657	0,023631	0,025334	0,023057	0,018158	0,011591	0,005819	0,000441	0
1,5	-0,027351	-0,021807	-0,015395	-0,008587	-0,002182	0,002777	0,004166	0,00387	0,000771	0
	-0,001031	0,00416	0,008183	0,01064	0,011229	0,010103	0,007431	0,004491	0,000731	0
2	-0,0226	-0,019232	-0,015361	-0,011194	-0,007085	-0,00353	-0,001302	0,000129	0,000142	0
	-0,013942	-0,008804	-0,004457	-0,001115	0,001088	0,002067	0,001834	0,00125	0,000207	0
3	-0,014138	-0,012472	-0,01042	-0,008295	-0,006217	-0,004285	-0,002601	-0,001377	-0,000168	0
	-0,019031	-0,014709	-0,010918	-0,007654	-0,004997	-0,002927	-0,001623	-0,000712	-6,33E-05	0
4	-0,008787	-0,007732	-0,006457	-0,005173	-0,003859	-0,002747	-0,001747	-0,000981	-0,000136	0
	-0,016078	-0,012785	-0,009854	-0,007263	-0,005163	-0,003345	-0,001995	-0,001006	-0,000114	0
5	-0,005649	-0,004787	-0,004016	-0,003243	-0,002382	-0,001634	-0,001057	-0,0006	-8,37E-05	0
	-0,011264	-0,009001	-0,006878	-0,004988	-0,003559	-0,002401	-0,00141	-0,000649	-7,52E-05	0

Table 8.18: Gamma for knock-out options

This table exhibits differences in both sign and magnitude. For the knock-in options the results are shown in the table below:

t/strike	85	90	95	100	105	110	115	120	130	140
0,175	0,000374	4,25E-05	1,03E-07	1,1E-08	3,34E-16	0	-4,01E-08	3,13E-07	9,58E-06	2,03E-05
	4,69E-05	4,26E-05	3,84E-05	3,41E-05	2,99E-05	2,56E-05	2,13E-05	1,71E-05	8,58E-06	1,3E-06
0,425	0,013395	0,00531	0,001708	0,000477	4,91E-05	1,39E-05	6,16E-06	6,12E-05	0,000198	0,000171
	0,003984	0,003624	0,003264	0,002905	0,002545	0,002186	0,001827	0,00147	0,000772	0,000331
0,695	0,030366	0,021872	0,014385	0,008716	0,003477	0,000929	0,000495	0,000447	0,000467	0,000341
	0,006527	0,005942	0,005357	0,004772	0,004187	0,003602	0,003019	0,002437	0,001341	0,000656
0,94	0,038056	0,032293	0,026321	0,019349	0,013317	0,006749	0,003845	0,002537	0,001046	0,000504
	0,008897	0,008104	0,007312	0,006519	0,005726	0,004934	0,004144	0,003361	0,001897	0,00089
1	0,038918	0,033668	0,028276	0,021559	0,015437	0,008792	0,005063	0,003224	0,001267	0,000573
	0,009715	0,00885	0,007986	0,007121	0,006256	0,005392	0,004531	0,003677	0,002078	0,00097
1,5	0,038152	0,036066	0,033295	0,029798	0,025598	0,020808	0,016598	0,01232	0,006002	0,001752
	0,021105	0,019231	0,017358	0,015485	0,013614	0,011745	0,009889	0,008055	0,004603	0,001761
2	0,032451	0,031666	0,030448	0,028727	0,026444	0,023524	0,020174	0,016577	0,009963	0,00465
	0,031188	0,028453	0,025719	0,022988	0,020261	0,017545	0,014854	0,012193	0,007277	0,003318
3	0,022418	0,022471	0,022102	0,021531	0,020726	0,019652	0,018011	0,016299	0,01215	0,008418
	0,032705	0,029975	0,027252	0,024541	0,021851	0,019198	0,016627	0,014145	0,009839	0,006439
4	0,015875	0,016073	0,016007	0,015853	0,015433	0,015069	0,014441	0,013701	0,011695	0,009435
	0,027398	0,02529	0,023205	0,021148	0,019144	0,017184	0,015317	0,013545	0,010452	0,007901
5	0,011818	0,01189	0,012067	0,012203	0,012039	0,011844	0,011711	0,011507	0,01058	0,009396
	0,020774	0,019379	0,018003	0,016659	0,015392	0,014177	0,013	0,011885	0,009953	0,008184

Table 8.19: Gamma for knock-in options

Differences in table 8.19 are most noticeable for short-term in-the-money barriers. Again, these tables can be added to yield the table for gamma of European options.

As a final example we look at the risk involved in changes of implied volatility. Since we have an entire volatility structure, it is not clear how vega should be determined. As described earlier, one can lift the entire volatility structure with a constant value and then determine the change of the barrier values resulting from this lift. For standard European options, this approach must yield the same results as in the analytical case when using the appropriate implied volatility. For barrier options this is not necessarily the case.

Another way to determine the risk involved in changes of implied volatility is to look at changes of option prices when a small part of the volatility structure is changed. To achieve this, we can add a function to the volatility structure. For the one-dimensional case, one can choose the following function.

$$f(x, x_0) = I - e^{-\left(\frac{dx}{x-x_0}\right)^a} \tag{8.7}$$

Here, x_0 denotes the centre of the area that one wants to change. When $x = x_0$ the function should be set to I . dx is a measure of the width of the area that one wants to lift. The even integer $a > 0$, determines how this function behaves at the boundaries. When a is chosen large, the function value jumps from 0 to I when the boundary is crossed. When it is chosen small, the transition is smoother. A smooth transition is preferred for implied methods that use the instantaneous volatility. Since, to determine the instantaneous volatility, partial derivatives of the implied volatility structure are needed. The following figure gives a plot of this function when $dx = 1$, $x_0 = 5$ and $a = 4$.

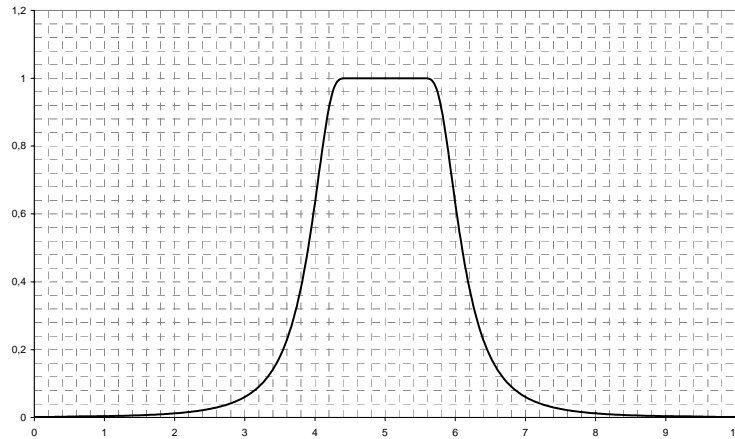


Figure 8.2: Plot of function (8.7)

This idea can easily be extended to multiple dimensions, by simply multiplying more of these functions. By adding this function to the volatility structure, we can determine the sensitivity of the option price when a part of the structure changes. This approach was taken for a change in the area around every implied volatility in the matrix. We can then determine a matrix for vega for every option. The elements of this matrix are defined by the following formula:

$$\frac{\partial V}{\partial \hat{\sigma}_{i,j}} \equiv \frac{V(\hat{\sigma}(T, K) + hf_1(T, T_i)f_2(K, K_j)) - V(\hat{\sigma}(T, K) - hf_1(T, T_i)f_2(K, K_j))}{2h} \quad (8.8)$$

where $V(\dots)$ denotes the value of the derivative, given a certain volatility structure. T_i and K_j denote the i -th maturity and j -th strike of the volatility matrix, respectively. $\hat{\sigma}(T, K)$ denotes the implied volatility structure. f_1 and f_2 are defined by (8.7). As an example, we illustrate this approach for a five-year at-the-money barrier option, with the barrier on 140. We investigate both the knock-in and the knock-out barrier. We set dx for f_1 equal to 1 and for f_2 equal to 0.2. In both functions a is set to 4.

t/strike	85	90	95	100	105	110	115	120	130	140
1,5	0	0	0	0	0	0	0	0	0	0
	0	0	0	0	0	0	0	0	0,160947	0,16859
2	0	0	0	0	0	0	0	0	0	0
	0	0	0	0	0	0	-0,111217	-0,161227	0,548254	0,420302
3	0	0	0	0	0	0	0	0	0	0
	0	0	0	-0,203484	-0,514546	-0,878553	-1,09442	-1,06397	2,23213	1,91604
4	0	0	0	0	0	0	0	0	0	0
	0,122671	0,141703	0	-0,718379	-2,22331	-4,484	-6,47091	-6,54699	7,25098	8,9083
5	-0,369683	-1,82546	-19,0455	-30,1296	-19,0455	-1,82546	-0,369683	-0,117464	0	0
	0,941518	4,4387	41,286	63,686	38,5991	0,972253	-6,94497	-26,1934	-132,105	-15,1739

Table 8.20: Vega for the Knock-out option

t/strike	85	90	95	100	105	110	115	120	130	140
1,5	0	0	0	0	0	0	0	0	0	0
	0	0	0	0	0	0	0	0	-0,160946	-0,16859
2	0	0	0	0	0	0	0	0	0	0
	0	0	0	0	0	0	0,111234	0,161233	-0,548253	-0,420302
3	0	0	0	0	0	0	0	0	0	0
	0	0	0	0,210383	0,518907	0,878971	1,09451	1,064	-2,23212	-1,91604
4	0	0	0,100169	0,158464	0,100169	0	0	0	0	0
	-0,121318	-0,135021	0	0,828674	2,29303	4,49068	6,47226	6,54742	-7,2509	-8,90827
5	1,21617	6,00534	62,6554	99,1194	62,6554	6,00534	1,21617	0,38643	0	0
	0	-0,258815	2,32389	5,30389	5,01079	3,20763	7,79146	26,4624	132,158	15,1907

Table 8.21: Vega for the Knock-in option

Since for short maturities, the values were all close to zero, they are not listed here. In both tables, small values are set to 0. Adding both tables shows again that the results from the analytical formulae are the same as those from the implied model. This table shows some interesting results. It can be seen that a change in the volatility structure can have a large impact on the prices of the two barriers. Especially for implied volatilities near the barrier, this impact is large. When the short-term implied volatilities change, there will be no relevant change in the price of the two barriers. It may also be interesting to perform this analysis on the instantaneous volatility structure.

9

Conclusions

9.1 Introduction

The purpose of this thesis has been to analyse implied models. After a thorough discussion on implied models, the performance of these models was considered. This was followed by an application of the models, on both American and barrier options. The following section discusses the main conclusions that were found during this research project. The last section gives some suggestions for further research.

9.2 Conclusions

After the introduction of the famous Black and Scholes model in 1973, empirical evidence, e.g. Rubinstein (1985), has shown that implied volatilities vary across different strikes and time-to-maturities. To improve the Black-Scholes formulae, different kinds of stochastic processes for the underlying asset were suggested. The research presented in this thesis has focussed on the deterministic volatility models. The stochastic process used is a simple extension of the geometric Brownian motion, by allowing for a deterministic function for the instantaneous volatility. It was shown how this volatility function can be derived from market values of European options. After a discussion of different ways to construct implied models, we have looked at their performance. This has shown that the implied binomial model has a very poor performance, when trying to fit a given volatility structure. Implied trinomial trees do a very good job at fitting a volatility structure. The best results are obtained when negative transition probabilities are adjusted such that the local volatility is optimised. When the number of steps used in the tree gets large, one might consider using a continuous approach. This can save a tremendous amount of storage capacity, since the tree does not have to be constructed forward. The performance of implied finite difference methods is also very good. For a small number of steps, the method proposed by Andersen and Brotherton-Ratcliffe (1998) performs best. For grids greater than 100×100 , there is no clear winner.

When applying the models to American options, we found no large differences compared to prices generated by standard models. This is an interesting result, since it means that one can use the volatility structure of American options as input for implied models. In this case, the American options are not priced correctly, but the differences are not very large either. The implied models that fit option prices directly can be adjusted to fit American options, but such a model will become very slow. For implied methods that use the instantaneous volatility, it is not clear how to adjust them when only American

options are observed in the market. In practice, it often happens that an asset has only American options traded on it, so this result can be used in those cases.

The models have also been applied to barrier options. It was shown that a skew or smile in the volatility can have a large impact on barrier prices. A term structure of volatility is much less relevant. One cause of this is the probability of hitting the barrier. Chapter 8 has shown how this probability can be determined for implied models, using a special derivative.

9.3 Further research

This thesis has mainly focussed on different implied models and their performance. Applications to both American and barrier options were presented. It will be interesting to investigate the impact of implied models on all other kinds of derivatives, such as lookbacks. When options get more complex, the implied Monte Carlo simulation might be used. For simple options this method is far too slow compared to the other models.

More research can also be done on the greeks. Derman (1999) has introduced the terms, sticky-strike, sticky-delta and sticky-implied tree, depending on what parameter is kept constant, or sticky, while defining the volatility structure. In chapter 8 we have assumed a sticky-strike situation to determine the hedge-parameters analytically. The greeks determined from the implied models assume a sticky-implied tree situation. It will also be interesting to look at the sticky-delta rule, where the delta is sticky. Further, there are many other ways to measure the risk involved in changes of the volatility structure. It might be interesting to investigate what happens when the volatility structure becomes more skewed. The impact of a change of only short-term volatilities might also be considered, since in practice these volatilities show more variation than the long-term volatilities.

Another interesting topic to investigate is implied models that allow for stochastic volatility, or jumps in the underlying asset. This thesis has presented a simple implied model that allows for stochastic volatility. As an example it was discussed how the Heston model can be incorporated by choosing the transition probabilities carefully. Britten-Jones and Neuberger (2000) show how other stochastic volatility models can be incorporated. Their model is a discrete version of the model described in Derman and Kani (1998). An implied model that allows for jumps is discussed in Andersen and Andreasen (1999). It will be interesting to investigate the result of such methods on the prices of exotic options and their greeks.

Appendix A: Stochastic calculus

Some definitions

The stochastic processes used in this thesis are based on the Wiener process. A stochastic process $\{W_t; t \geq 0\}$ is called a Wiener process if:

1. $W_{t_1}, W_{t_2} - W_{t_1}, \dots, W_{t_k} - W_{t_{k-1}}$ are independent for all $0 \leq t_1 < t_2 \dots < t_k$
2. $W_{t+s} - W_s \sim N(0, t) \quad \forall s, t \geq 0$ (A.1)
3. $t \rightarrow W_t$ is continuous with probability 1

A stochastic process $X = \{X_t; t \geq 0\}$ is called an Itô process if it can be written in the following form:

$$dX = a(X, t)dt + b(X, t)dW \quad (\text{A.2})$$

where W is a Wiener process. In the special case where $a(\dots)$ and $b(\dots)$ are constant, the process is called a generalized Wiener process.

Itô's lemma

Suppose that the stochastic variable X follows an Itô process as defined in (A.2). Let g be a twice continuously differentiable function of X and t . Itô's lemma states that a variable $y = g(t, X)$ follows the process:

$$dy = \frac{\partial g}{\partial X} dX + \frac{\partial g}{\partial t} dt + \frac{1}{2} \frac{\partial^2 g}{\partial X^2} b^2(X, t) dt \quad (\text{A.3})$$

Intuitively this can be seen by looking at the Taylor expansion and using $dWdW = dt$. This equation can be easily extended to the case of more stochastic processes, when using $dW_1 dW_2 = \rho dt$, where W_1 and W_2 are both Wiener processes with correlation ρ .

More on stochastic differential equations can be found in Øksendal (1998).

Appendix B: Pricing barrier options

When it is assumed that the underlying asset has a constant volatility, formulae for barrier options can be derived using risk neutral valuation. The formulae for barriers can be found in Hull (1997) or Rich (1994). For call options, they are given below:

$$Cdi = Se^{-qT} \left(\frac{H}{S}\right)^{2\lambda} N(y) - Ke^{-rT} \left(\frac{H}{S}\right)^{2\lambda-2} N(y - \sigma\sqrt{T}) \quad \text{if } H \leq K \quad (\text{B.1})$$

$$\begin{aligned} Cdo = SN(x_1)e^{-qT} - Ke^{-rT} N(x_1 - \sigma\sqrt{T}) - Se^{-qT} \left(\frac{H}{S}\right)^{2\lambda} N(y_1) & \quad \text{if } H \geq K \\ + Ke^{-rT} \left(\frac{H}{S}\right)^{2\lambda-2} N(y_1 - \sigma\sqrt{T}) & \end{aligned} \quad (\text{B.2})$$

$$\begin{aligned} Cui = SN(x_1)e^{-qT} - Ke^{-rT} N(x_1 - \sigma\sqrt{T}) - Se^{-qT} \left(\frac{H}{S}\right)^{2\lambda} [N(-y) - N(-y_1)] \\ + Ke^{-rT} \left(\frac{H}{S}\right)^{2\lambda-2} [N(-y + \sigma\sqrt{T}) - N(-y_1 + \sigma\sqrt{T})] & \quad \text{if } H > K \end{aligned} \quad (\text{B.3})$$

Where we have used:

$$\begin{aligned} \lambda = \frac{r - q + \frac{1}{2}\sigma^2}{\sigma^2} & \quad x_1 = \frac{\ln\left(\frac{S}{H}\right)}{\sigma\sqrt{T}} + \lambda\sigma\sqrt{T} \\ y = \frac{\ln\left(\frac{H^2}{SX}\right)}{\sigma\sqrt{T}} + \lambda\sigma\sqrt{T} & \quad y_1 = \frac{\ln\left(\frac{H}{S}\right)}{\sigma\sqrt{T}} + \lambda\sigma\sqrt{T} \end{aligned}$$

The remaining values follow from the Knock-out and Knock-in parity. The values of up options with the strike higher than the barrier, are not given here, since these are trivial cases. Formulae for put barrier options can be found in Hull (1997). Rich (1994) shows that the probability of hitting the barrier during the lifetime of the option is given by:

$$Pr(S_t = H, \text{ for some } t \in [0, T]) = 1 - N(\phi(x_1 - \sigma\sqrt{T})) + \left(\frac{H}{S}\right)^{2\lambda-2} N(\phi(y_1 - \sigma\sqrt{T})) \quad (\text{B.4})$$

Where $\phi = 1$ for down barrier options and $\phi = -1$ for up barrier options.

Appendix C: Splines

This appendix will describe how splines can be used. First we take a look at splines of degree 1, or linear interpolation. After that cubic splines will be described for interpolation as well as extrapolation. Finally a method is introduced to use splines in two dimensions.

Linear interpolation

A spline is a function that consists of polynomial pieces joined together, with certain smoothness conditions. Assume we have a table with the following function values:

x	x_0	x_1	x_n
y	y_0	y_1	y_n

Where we assume, with no loss of generality, that the x values are arranged such that $x_0 < x_1 < \dots < x_n$. Further assume the following function:

$$S(x) = \begin{cases} S_0(x) & x \in [x_0, x_1] \\ S_1(x) & x \in [x_1, x_2] \\ \vdots & \vdots \\ S_{n-1}(x) & x \in [x_{n-1}, x_n] \end{cases} \tag{C.1}$$

If the functions are polynomial of the first degree, we have:

$$S_i(x) = a_i x + b_i \tag{C.2}$$

Now if $S(x)$ is continuous, we call it a spline of the first degree. This can be easily generalised to a spline of degree k . Equation (C.1) stays still valid and equation (C.2) becomes:

$$S_i(x) = a_{ki} x^k + a_{k-1i} x^{k-1} + \dots + a_{1i} x + a_{0i} \tag{C.3}$$

If the function $S(x)$ is continuous and the first $k-1$ derivatives are continuous on the interval $[x_0, x_n]$, then $S(x)$ will be called a spline of degree k . When we take a look at the first degree spline we can choose:

$$S_i(x) = y_i + \frac{y_{i+1} - y_i}{x_{i+1} - x_i}(x - x_i) \tag{C.4}$$

Now it can be seen that $S(x_i) = y_i$ and $S(x)$ is continuous on the interval $[x_0, x_n]$.

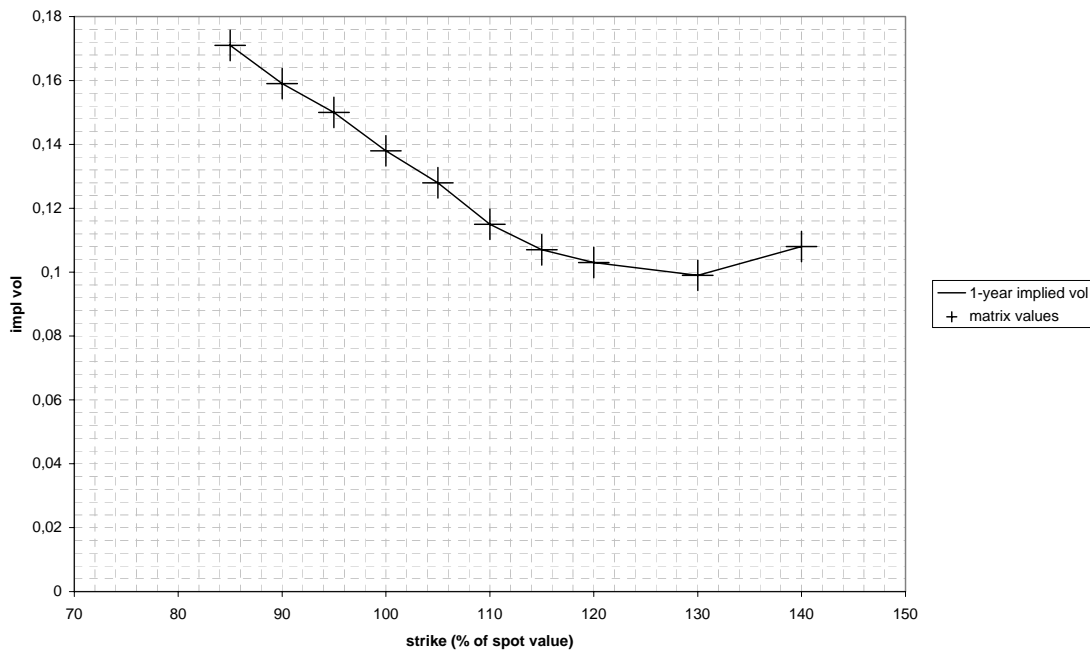


Figure C.1: Fitting a first-degree spline for 1-year implied volatilities.

In Figure C.1 the graph of the first degree spline is depicted for the 5-th row of the volatility matrix given in chapter 4, table 4.1, corresponding to options with a one-year time to maturity. This method is easy to extent to two dimensions, in which case it can be used on a volatility matrix. However, in order to have an instantaneous volatility function that is well behaved, we need an interpolation method that creates a function with continuous first and second order derivatives. Cubic splines, or splines of the third degree have enough parameters to do this.

Cubic splines

As discussed above a cubic spline is a function, S , that can go through the points (x_i, y_i) in such a way that $S(x)$ $S'(x)$ and $S''(x)$ are continuous on the interval $[x_0, x_n]$. The

coefficients of the functions $S_i(x)$ should be chosen such that this holds. Since there are n subintervals, we have $4n$ coefficients available. Since at each interval the function has to go to the two points at the beginning and end of the interval. This will give $2n$ restrictions. Further we have $2(n-1)$ restrictions in order to make the first and second order derivatives of S continuous. So there are 2 degrees of freedom left. One way to use these is to impose a last restriction:

$$S''(x_0) = S''(x_n) = 0 \quad (\text{C.5})$$

The resulting spline is then called a natural cubic spline. Now in order to determine the coefficients we start by looking at the second derivative. First assume that the values of the derivatives at x_0, x_1, \dots, x_n are denoted by z_0, z_1, \dots, z_n . From (C.5) we have $z_0 = z_n = 0$. Since the second derivative has to be continuous and of first degree (since S is of third degree), we can write $S_i''(x)$ as:

$$S_i''(x) = \frac{z_{i+1}}{h_i}(x - x_i) + \frac{z_i}{h_i}(x_{i+1} - x) \quad (\text{C.6})$$

where $h_i = x_{i+1} - x_i$. This function can now be integrated twice to yield S_i :

$$S_i(x) = \frac{z_{i+1}}{6h_i}(x - x_i)^3 + \frac{z_i}{6h_i}(x_{i+1} - x)^3 + C(x - x_i) + D(x_{i+1} - x) \quad (\text{C.7})$$

With the conditions $S_i(x_i) = y_i$ and $S_i(x_{i+1}) = y_{i+1}$ we can solve for S_i :

$$S_i(x) = \frac{z_{i+1}}{6h_i}(x - x_i)^3 + \frac{z_i}{6h_i}(x_{i+1} - x)^3 + \left(\frac{y_{i+1}}{h_i} - \frac{h_i}{6} z_{i+1} \right) (x - x_i) + \left(\frac{y_i}{h_i} - \frac{h_i}{6} z_i \right) (x_{i+1} - x) \quad (\text{C.8})$$

Now all that is left is to determine the z_i 's. The only restriction that we have not used so far is the continuity of the first derivative. From (C.8) the first derivative follows:

$$S_i'(x) = \frac{z_{i+1}}{2h_i}(x - x_i)^2 - \frac{z_i}{2h_i}(x_{i+1} - x)^2 + \frac{y_{i+1}}{h_i} - \frac{h_i}{6} z_{i+1} - \frac{y_i}{h_i} + \frac{h_i}{6} z_i \quad (\text{C.9})$$

So we have:

$$S_i'(x_i) = -\frac{h_i}{6} z_{i+1} - \frac{h_i}{3} z_i + b_i \quad (\text{C.10})$$

with:

$$b_i = \frac{1}{h_i}(y_{i+1} - y_i)$$

and we have:

$$S_{i-1}'(x_i) = \frac{h_{i-1}}{6} z_{i-1} + \frac{h_{i-1}}{3} z_i + b_{i-1} \quad (\text{C.11})$$

Extrapolation

As has already been mentioned, implied numerical methods need volatilities at combinations of K and T that lie far outside the boundaries of an average volatility matrix. Most of the time such volatilities can not be observed in the market, since those options are not traded. This is why we need extrapolation methods. One easy way of doing this, is to use the implied volatility at the boundary of the matrix and use this value for (K, T) values outside the boundaries. However, doing this will give a discontinuity in the first derivative of the implied volatility function w.r.t. the strike. One way to overcome this, is to choose values for the strike, outside the boundaries where the implied volatility must be converged to some constant value. In the example for a 1 year time to maturity we can set $x_0 = 70$ and $x_n = 180$. The closer x_0 and x_n are chosen by the boundary, the faster the spline will be converged. Further we can take x_1, x_2, \dots, x_{n-1} and the corresponding y_i to be the values found in the volatility matrix for one year options. Now y_0 and y_n should be chosen in such that $S''(x_0) = S'(x_0) = 0 = S'(x_n) = S''(x_n)$ for some cubic spline function S . Then from (C.10) we have:

$$S'_0(x_0) = -\frac{h_0}{6}z_1 + b_0 = 0 \quad (\text{C.14})$$

so:

$$\frac{h_0}{6}z_1 + \frac{1}{h_0}y_0 = \frac{1}{h_0}y_1 \quad (\text{C.15})$$

similarly, we find from (C.11) that:

$$\frac{h_{n-1}}{6}z_{n-1} + \frac{1}{h_{n-1}}y_n = \frac{1}{h_{n-1}}y_{n-1} \quad (\text{C.16})$$

where we have used the fact that $z_0 = z_n = 0$. Substituting $i=1$ and $i=n$ in (C.12) will give the following two equations:

$$-\frac{6}{h_0}y_0 + u_1z_1 + h_1z_2 = 6b_1 - \frac{6}{h_0}y_1 \quad (\text{C.17})$$

$$h_{n-2}z_{n-2} + u_{n-1}z_{n-1} - \frac{6}{h_{n-1}}y_n = -\frac{6}{h_{n-1}}y_{n-1} - 6b_{n-2} \quad (\text{C.18})$$

Using these restrictions, we can write (C.13) as:

Using splines for two dimensions

Since the implied volatility depends on both T and K , we actually need a two dimensional interpolation technique. One easy way of doing this, is to use a one dimensional spline two times. Consider a combination (K, T) where we want to find an implied volatility for. Now one can determine a spline in the T -direction for all columns of the volatility matrix. When these splines are determined, one can evaluate all the splines at T . Now a table with values $(K_i, \hat{\sigma}(K_i, T))$ is found, where $\hat{\sigma}(K_i, T)$ denote the implied volatilities found with splines in the T -direction and the K_i are the strikes found in the volatility matrix. These combinations of $(K_i, \hat{\sigma}(K_i, T))$ can now again be used to determine a spline in the K -direction. With this spline, the function value at K can be computed, giving a value for the implied volatility for an option with strike K and time to maturity T . With these splines we can determine the implied volatility for all combinations of (K, T) needed for numerical methods.

Appendix D: Instantaneous volatility function

We want to write the instantaneous volatility function, given by:

$$\sigma^2(K, T) = 2 \frac{\frac{\partial C}{\partial T} + qC + K(r - q) \frac{\partial C}{\partial K}}{K^2 \left(\frac{\partial^2 C}{\partial K^2} \right)}, \quad (\text{D.1})$$

in terms of implied volatilities. We first start with the terms found in the numerator:

$$\frac{\partial C}{\partial T} = \left(\frac{SN'(d_+) \hat{\sigma} e^{-qT}}{2\sqrt{T}} - qSN(d_+) e^{-qT} + rKe^{-rT} N(d_-) \right) + Se^{-qT} \sqrt{T} N'(d_+) \frac{\partial \hat{\sigma}}{\partial T} \quad (\text{D.2})$$

Where d_{\pm} are given by:

$$d_{\pm} = \frac{\ln \frac{S}{K} + (r - q)T}{\hat{\sigma} \sqrt{T}} \pm \frac{1}{2} \hat{\sigma} \sqrt{T} \quad (\text{D.3})$$

The first term of formula (D.2) is the theta in the Black-Scholes world, the second term follows from applying the chain-rule. The chain rule needs to be applied since we now assume that the implied volatility depends on T . The second term in the numerator of (D.1) is qC and can be written as:

$$qC = qSe^{-qT} N(d_+) - qKe^{-rT} N(d_-) \quad (\text{D.4})$$

Further we can write the derivative in the last term of the numerator of (D.1) as:

$$\frac{\partial C}{\partial K} = -e^{-rT} N(d_-) + Se^{-qT} \sqrt{T} N'(d_+) \frac{\partial \hat{\sigma}}{\partial K} \quad (\text{D.5})$$

Now using (D.3)-(D.5), to find the numerator in (D.1), multiplied by the factor 2 of (D.1), we see that a lot of terms cancel each other out. The numerator can then be written as:

$$2 \left(\frac{SN'(d_+) \hat{\sigma} e^{-qT}}{2\sqrt{T}} + S\sqrt{T} N'(d_+) e^{-qT} \frac{\partial \hat{\sigma}}{\partial T} + (r - q)K \left(S\sqrt{T} N'(d_+) e^{-qT} \frac{\partial \hat{\sigma}}{\partial K} \right) \right) = \quad (\text{D.6})$$

$$SN'(d_+) e^{-qT} \sqrt{T} \left(\frac{\hat{\sigma}}{T} + 2 \frac{\partial \hat{\sigma}}{\partial T} + 2(r - q)K \frac{\partial \hat{\sigma}}{\partial K} \right)$$

Next, we take a look at the denominator of (D.1). Therefore we require the second derivative of the call option formula, w.r.t. the strike. This second derivative can be found by taking the derivative of (D.5) w.r.t. K :

$$\frac{\partial^2 C}{\partial K^2} = -e^{-rT} N'(d_-) \frac{\partial d_-}{\partial K} + Se^{-qT} \sqrt{T} N''(d_+) \frac{\partial d_+}{\partial K} \frac{\partial \hat{\sigma}}{\partial K} + Se^{-qT} \sqrt{T} N'(d_+) \frac{\partial^2 \hat{\sigma}}{\partial K^2} \quad (\text{D.7})$$

now, from (D.3) it follows that:

$$\frac{\partial d_{\pm}}{\partial K} = -\frac{1}{K \hat{\sigma} \sqrt{T}} + \left(-\frac{1}{\hat{\sigma}^2} \frac{\ln \frac{S}{K} + (r-q)T}{\sqrt{T}} \pm \frac{1}{2} \sqrt{T} \right) \frac{\partial \hat{\sigma}}{\partial K} = -\frac{1}{K \hat{\sigma} \sqrt{T}} - \frac{1}{\hat{\sigma}} d_{\mp} \frac{\partial \hat{\sigma}}{\partial K} \quad (\text{D.8})$$

In the last term of the right-hand-side, d_- should be used when taking the derivative of d_+ w.r.t. K and d_+ should be used when taking the derivative of d_- . Now equation (D.7) can be rewritten. Therefore some formulae are useful. First we have:

$$N'(x) = \frac{1}{\sqrt{2\pi}} e^{-\frac{1}{2}x^2},$$

It can easily be seen that:

$$N''(x) = -xN'(x)$$

Further, from (D.3) it follows that one can take $d_{\pm} = a \pm b$, so $d_+^2 = d_-^2 + 4ab$, where a and b are the first and second term of (D.3), respectively. Using this yields:

$$d_+^2 = d_-^2 + 2 \left(\ln \frac{S}{K} + (r-q)T \right)$$

So with these two relations, $N''(d_+)$ and $N'(d_-)$ can both be written in terms of $N'(d_+)$. After some manipulations the denominator of (D.1) can eventually be written as:

$$\begin{aligned} K^2 Se^{-qT} N'(d_+) \sqrt{T} \left(\frac{1}{\hat{\sigma}} \left\{ \frac{1}{K^2 T} + \frac{2d_+}{K \sqrt{T}} \frac{\partial \hat{\sigma}}{\partial K} + d_+ d_- \left(\frac{\partial \hat{\sigma}}{\partial K} \right)^2 \right\} + \frac{\partial^2 \hat{\sigma}}{\partial K^2} \right) = \\ K^2 Se^{-qT} N'(d_+) \sqrt{T} \left(\frac{\partial^2 \hat{\sigma}}{\partial K^2} - d_+ \sqrt{T} \left(\frac{\partial \hat{\sigma}}{\partial K} \right)^2 + \frac{1}{\hat{\sigma}} \left(\frac{1}{K \sqrt{T}} + d_+ \frac{\partial \hat{\sigma}}{\partial K} \right)^2 \right) \end{aligned} \quad (\text{D.9})$$

Now combining formulae (D.6) and (D.9) gives the formula for the instantaneous volatility, expressed in terms of the implied volatility function:

$$\sigma^2(K, T) = \frac{2 \frac{\partial \hat{\sigma}}{\partial T} + \frac{\hat{\sigma}}{T} + 2K(r - q) \frac{\partial \hat{\sigma}}{\partial K}}{K^2 \left(\frac{\partial^2 \hat{\sigma}}{\partial K^2} - d_+ \sqrt{T} \left(\frac{\partial \hat{\sigma}}{\partial K} \right)^2 + \frac{1}{\hat{\sigma}} \left(\frac{1}{K\sqrt{T}} + d_+ \frac{\partial \hat{\sigma}}{\partial K} \right)^2 \right)} \quad (\text{D.10})$$

Andersen and Brotherton-Ratcliffe (1998) show that this is non-negative in the absence of arbitrage opportunities.

Appendix E: Successive over-relaxation (SOR)

Assume we have the following equation:

$$\mathbf{M}\mathbf{v} = \mathbf{q} \quad (\text{E.1})$$

Where \mathbf{M} is a $(n \times n)$ -matrix and \mathbf{q} and \mathbf{v} are vectors of size n . \mathbf{v} is unknown. Now it is easy to see that the system of equations can also be written as:

$$\begin{aligned} M_{11}v_1 + M_{12}v_2 + \dots + M_{1n}v_n &= q_1 \\ M_{21}v_1 + M_{22}v_2 + \dots + M_{2n}v_n &= q_2 \\ &\vdots \\ M_{n1}v_1 + M_{n2}v_2 + \dots + M_{nn}v_n &= q_n \end{aligned} \quad (\text{E.2})$$

Which can also be transformed to:

$$\begin{aligned} v_1 &= \frac{1}{M_{11}}(q_1 - (M_{12}v_2 + M_{13}v_3 + \dots + M_{1n}v_n)) \\ v_2 &= \frac{1}{M_{22}}(q_2 - (M_{21}v_1 + M_{23}v_3 + \dots + M_{2n}v_n)) \\ &\vdots \\ v_n &= \frac{1}{M_{nn}}(q_n - (M_{n1}v_1 + M_{n2}v_2 + \dots + M_{n,n-1}v_{n-1})) \end{aligned} \quad (\text{E.3})$$

From the last set of equations, one can easily derive an iterative procedure that solves for the v_i 's. This leads to the method of successive over-relaxation:

$$v_i^{k+1} = v_i^k + \frac{\omega}{M_{ii}} \left(q_i - \sum_{j=1}^{i-1} M_{ij}v_j^{k+1} - \sum_{j=i+1}^n M_{ij}v_j^k \right) \quad (\text{E.4})$$

Where ω is the acceleration or over-relaxation parameter, which must lie between 1 and 2. This parameter can be used to speed up convergence since in most cases the iterative procedure converges from one side. If ω is chosen to be 1, (E.4) is called the Gauss-Seidel Method. In this iterative procedure we must start updating the v_i 's from low to high after some starting value v^0 is chosen. As soon as one value for v_i is updated, it will be used to determine the remaining values for v . With (E.4) one can now

approximate the solution in an iterative way, until some criteria is satisfied. For instance, the procedure can stop when:

$$\sum_{i=1}^n (v_i^{k+1} - v_i^k)^2 \leq tol, \quad (\text{E.5})$$

for some small value for tol , which should depend on n .

It is a lot faster to solve the system (E.1) exactly, with only $2n$ steps. However the SOR method can easily be adjusted to incorporate restrictions on v . For instance, when the v_i 's represent the values of an American option at some time-step in a finite difference scheme, they have to satisfy the restriction that comes from the possibility to exercise the option before maturity. This restriction can be incorporated by replacing (E.4) with:

$$v_i^{k+1} = \max \left\{ v_i^k + \frac{\omega}{M_{ii}} \left(q_i - \sum_{j=1}^{i-1} M_{ij} v_j^{k+1} - \sum_{j=i}^n M_{ij} v_j^k \right), \text{Payoff}_i \right\} \quad (\text{E.6})$$

Where Payoff_i is the payoff of the American option when the option is exercised early at node i in the grid. This method is called projected SOR.

Appendix F: Stability of finite difference

To check the stability of the finite difference method, the Von Neumann stability criterion can be used. The finite difference equation is given by:

$$\begin{aligned}
H_{k-1,j} \left(-\frac{1}{2} \alpha (1 - \Theta) (\hat{v}_{k,j} - \Delta_x \hat{b}_{k,j}) \right) + H_{k,j} (1 + \alpha (1 - \Theta) \hat{v}_{k,j}) + \\
H_{k+1,j} \left(-\frac{1}{2} \alpha (1 - \Theta) (\hat{v}_{k,j} + \Delta_x \hat{b}_{k,j}) \right) = H_{k-1,j+1} \left(\frac{1}{2} \alpha \Theta (\hat{v}_{k,j} - \Delta_x \hat{b}_{k,j}) \right) + \\
H_{k,j+1} (1 - \alpha \Theta \hat{v}_{k,j}) + H_{k+1,j} \left(\frac{1}{2} \alpha \Theta (\hat{v}_{k,j} + \Delta_x \hat{b}_{k,j}) \right)
\end{aligned} \tag{F.1}$$

In the above equation interest rates are ignored. This can be justified, because a non-zero interest rate will cause better stability properties. Now assume that the finite difference scheme has a harmonic eigensolution of the following form:

$$H_{k,j} = \xi^{M+1-j} e^{ik\omega\Delta_x} \tag{F.2}$$

Where i is the imaginary unit, $i = \sqrt{-1}$. ξ is called the amplification factor, which is a complex number and ω is known as the wave number. Now this relation can be inserted into (F.1). After dividing both sides by $\xi^{M-j} e^{ik\omega\Delta_x}$, this yields:

$$\begin{aligned}
\xi e^{-i\omega\Delta_x} \left(-\frac{1}{2} \alpha (1 - \Theta) (\hat{v}_{k,j} - \Delta_x \hat{b}_{k,j}) \right) + \xi (1 + \alpha (1 - \Theta) \hat{v}_{k,j}) + \\
\xi e^{i\omega\Delta_x} \left(-\frac{1}{2} \alpha (1 - \Theta) (\hat{v}_{k,j} + \Delta_x \hat{b}_{k,j}) \right) = e^{-i\omega\Delta_x} \left(\frac{1}{2} \alpha \Theta (\hat{v}_{k,j} - \Delta_x \hat{b}_{k,j}) \right) + \\
(1 - \alpha \Theta \hat{v}_{k,j}) + e^{i\omega\Delta_x} \left(\frac{1}{2} \alpha \Theta (\hat{v}_{k,j} + \Delta_x \hat{b}_{k,j}) \right)
\end{aligned} \tag{F.3}$$

Now since we have:

$$e^{i\varphi} = \cos(\varphi) + i \sin(\varphi), \tag{F.4}$$

(F.3) can be rewritten and solved for ξ :

$$\xi = \frac{1 - \alpha \Theta \hat{v}_{k,j} (1 - \cos(\omega \Delta_x)) + i \alpha \Theta \Delta_x \hat{b}_{k,j} \sin(\omega \Delta_x)}{1 + \alpha (1 - \Theta) \hat{v}_{k,j} (1 - \cos(\omega \Delta_x)) - i \alpha (1 - \Theta) \Delta_x \hat{b}_{k,j} \sin(\omega \Delta_x)} \tag{F.5}$$

The Von Neumann criterion states that in order to have stability, the modulus of the amplification factor, ξ , should be less than, or equal to one, independent of the wave number, ω . Now since the modulus of a fraction of two complex numbers equals the fraction of moduli, we have:

$$|\xi|^2 = \frac{(1 - \alpha\Theta \hat{v}_{k,j}(1 - \cos(\omega\Delta_x)))^2 + (\alpha\Theta\Delta_x \hat{b}_{k,j} \sin(\omega\Delta_x))^2}{(1 + \alpha(1 - \Theta)\hat{v}_{k,j}(1 - \cos(\omega\Delta_x)))^2 + (\alpha(1 - \Theta)\Delta_x \hat{b}_{k,j} \sin(\omega\Delta_x))^2} \equiv \frac{num}{den} \quad (\text{F.6})$$

We want this to be between zero and one, for all ω . Since both the numerator and denominator are positive, it is only necessary to check $|\xi|^2 \leq 1$. This is of course equivalent to $den - num \geq 0$. Dropping subscripts for both \hat{v} and \hat{b} , we have after some manipulations:

$$2\hat{v}(1 - \cos(\omega\Delta_x)) + (1 - 2\Theta)\alpha(\hat{v}^2(1 - \cos(\omega\Delta_x))^2 + \Delta_x^2 \hat{b}^2 (\sin(\omega\Delta_x))^2) \geq 0 \quad (\text{F.7})$$

Since $\sin^2(x) = 1 - \cos^2(x)$. We have, after dividing by $1 - \cos(\omega\Delta_x)$:

$$2\hat{v} + (1 - 2\Theta)\alpha(\hat{v}^2(1 - \cos(\omega\Delta_x)) + \Delta_x^2 \hat{b}^2 (1 + \cos(\omega\Delta_x))) \geq 0 \quad (\text{F.8})$$

Now this can be solved for Θ :

$$0 \leq \Theta \leq \frac{1}{2} \left(1 + \frac{\frac{2}{\alpha} \hat{v}}{\hat{v}^2 + \hat{b}^2 \Delta_x^2 + (\hat{b}^2 \Delta_x^2 - \hat{v}^2) \cos(\omega\Delta_x)} \right) \quad (\text{F.9})$$

Now it is easily seen that

$$(\hat{b}^2 \Delta_x^2 - \hat{v}^2) \cos(\omega\Delta_x) \leq |\hat{b}^2 \Delta_x^2 - \hat{v}^2| \quad (\text{F.10})$$

so the restriction $|\xi|^2 \leq 1$ is still satisfied if:

$$0 \leq \Theta \leq \frac{1}{2} \left(1 + \frac{\frac{2}{\alpha} \hat{v}}{\hat{v}^2 + \hat{b}^2 \Delta_x^2 + |\hat{b}^2 \Delta_x^2 - \hat{v}^2|} \right) \quad (\text{F.11})$$

Since the term on the right-hand-side is always greater than, or equal to $\frac{1}{2}$, it can be concluded that the system is unconditionally stable for all $0 \leq \Theta \leq \frac{1}{2}$. Thus the implicit finite difference method and the Crank-Nicholson method are both unconditionally stable.

References

- Andersen, L. and J. Andreasen (1999a), "Jump diffusion processes: volatility smile fitting and numerical methods for pricing," Working paper, General Re Financial Products, www.ssrn.com.
- Andersen, L. and J. Andreasen (1999b), "Jumping smiles," *Risk* 12, No. 11, pp. 65-68.
- Andersen, L. and R. Brotherton-Ratcliffe (1997), "The equity option volatility smile: an implicit finite-difference approach," *Journal of computational finance* 1, No. 2, pp. 5-37.
- Barle, S. and N. Cakici (1998), "How to grow a smiling tree," *Journal of financial engineering* 7, No. 2, pp. 127-146.
- Black, F. and M. Scholes (1973), "Pricing of options and corporate liabilities," *Journal of political economy* 81, pp. 637-659.
- Breeden, D. and R. Litzenberger (1978), "Prices of state-contingent claims implicit in option prices," *Journal of business* 51, pp. 621-651.
- Britten-Jones, M. and A. Neuberger (2000), "Option prices, implied price processes, and stochastic volatility," *Journal of finance*, forthcoming april issue.
- Cheney, W. and D. Kincaid (1994), "Numerical mathematics and computing," 3rd ed. Brooks/Cole publishing company.
- Cheuk, T. and A. Vorst (1996), "Complex barrier options," *Journal of derivatives*, fall, pp. 8-22.
- Cox, J., S. Ross and M. Rubinstein (1979), "Option pricing: a simplified approach," *Journal of finance* 34, pp. 229-264.
- Derman, E. and I. Kani (1994), "Riding on a smile," *Risk* 7, No. 2, pp. 32-39.
- Derman, E., I. Kani and N. Chriss (1996), "Implied trinomial trees of the volatility smile," *Journal of derivatives*, summer, pp. 7-22.
- Derman, E. and I. Kani (1998), "Stochastic implied trees: arbitrage pricing with stochastic term and strike structure of volatility," *International journal of theoretical and applied finance*, 1, pp 7-22.

- Derman, E. (1999), "Regimes of volatility," *Risk* 12, No. 4, pp 55-60.
- Dupire, B. (1994), "Pricing with a smile," *Risk* 7, No. 1, pp. 18-20.
- Harrison, J. and S. Pliska (1981), "Martingales and stochastic integrals in the theory of continuous trading," *Stochastic processes and their applications* 11, pp. 215-260.
- Heston, S. (1993), "A closed-form solution for options on assets with stochastic volatilities with applications to bond and currency options," *The review of financial studies* 6, No. 2, pp. 327-343.
- Hull, J. and A. White (1987), "The pricing of options on assets with stochastic volatilities," *Journal of finance* 17, No. 2, pp 281-300.
- Hull, J. (1997), "Options, futures and other derivatives," 3rd ed. Prentice Hall International.
- Merton, R. (1976), "Option pricing when underlying stock returns are discontinuous," *Journal of financial economics* 3, pp. 124-144.
- Øksendal, B. (1998), "Stochastic differential equations: An introduction with applications," 5th ed. Springer, Berlin Heidelberg New York.
- Pelsser, A. and A. Vorst (1994), "The binomial model and the greeks," *Journal of derivatives*, spring, pp. 45-49.
- Press, W., S. Teukolsky, W. Vetterling and B. Flannery (1992), "Numerical recipes in C: The art of scientific computing," 2nd ed. Cambridge University Press.
- Rich, D. (1994), "The mathematical foundations of barrier option-pricing theory," *Advances in futures and options research* 7, pp. 267-311.
- Ritchken, P. (1995), "On pricing barrier options," *Journal of derivatives*, winter, pp. 19-28.
- Rubinstein, M. (1985), "Non-parametric tests of alternative option pricing models using all reported trades and quotes on the 30 most active CBOE option classes from august 23, 1976 through august 31, 1978," *Journal of finance* 40, pp. 455-480.
- Rubinstein, M. (1994), "Implied binomial trees," *Journal of finance* 49, No. 3, pp. 771-818.
- Scott (1987), "Option pricing when the variance changes randomly," *Journal of financial and quantitative analysis* 22, pp. 419-438.

Wiggins, J. (1987), "Option values under stochastic volatility: theory and empirical estimates," *Journal of financial economics* 19, pp. 351-372.

Wilmott, P. (1998), "Derivatives; the theory and practice of financial engineering." John Wiley and Sons, Chichester.

